AFIT/GNE/PH/82-5

Accession For		
NTIS GRA&I		X
DTIC TAB		☐
Unannounced		☐
Justification		
By		
Distribution/		
Availability Codes		
Dist	Avail and/or Special	
A		

DTIC COPY INSPECTED 2

ONE DIMENSIONAL ANALYSIS

OF INERTIALLY CONFINED PLASMAS

THESIS

David A. DeBruyne
AFIT/GNE/PH/82-5   Captain   USMC

ONE DIMENSIONAL ANALYSIS

OF INERTIALLY CONFINED PLASMAS

THESIS

Presented to the Faculty of the School of Engineering

of the Air Force Institute of Technology

Air University

in Partial Fulfillment of the

Requirements for the Degree of

Master of Science

by

David A. DeBruyne

Capt   USMC

Graduate Nuclear Engineering

March 1982

Preface

This report is the culmination of my efforts to
understand selected physical phenomena inherent in a
thermonuclear plasma. An incomplete computer simulation
of inertially confined fusion, program MOXNEX, is the
central vehicle in the study. It is hoped that the modest
development and documentation contained here may contribute
to the understanding of others participating in programs
in Nuclear Engineering and Physics at the Air Force
Institute of Technology.

I would like to thank Doctor George Nickel, not only
for originating the project, but for extending it for
further study. I would like to thank Major Michael Stamm
and especially my advisor, Lieutenant Colonel William Bailey,
for patient consultation, advice, guidance and leadership.
I would also like to thank Ms. Sharon Gabriel for manuscript
preparation. I thank Miss Patricia Horton for patience,
understanding and support. Finally, and most importantly,
I would like to thank my parents, Joseph and Florence
DeBruyne, for continued faith and encouragement in this and
other endeavors.

David A. DeBruyne

ii

Contents

Contents (Cont'd)

Contents (Cont'd)

List of Figures

List of Figures (Cont'd)

List of Tables

List of Notation

Symbol	Definition or Description
a	acceleration
b	impact parameter
c	speed of light
$c_{\nu j}$	specific heat
D	deuterium
e	electron species subscript
	electronic charge unit
E_e	electron kinetic energy
E	photon energy
h	Planck's constant
He	Helium
i	ion species subscript
k	Boltzmann's constant
m_e	electron mass
m_i	ion mass
n	neutron
N_a	Avagadro's number

n_j	number density of species j
N_j	pure number of species j
p_j	momentum of species j
P_j	power resulting from process j pressure due to species j
Q	heat
r	radial distance radiation subscript
r_o	classical electron radius
RR_j	reaction rate density for process j
t	time
T	tritium
T_j	temperature of species j
V_j	volume of cell j
z	net electronic charge
z_j	atomic number of species j
α	fine structure constant
β	bremsstrahlung subscript

$I\beta$	inverse bremsstrahlung subscript
γ	ratio of radiation temperature to electron temperature
Δ	finite difference
ξ	ratio of photon energy to kinetic electron temperature
Θ	angular measure
λ_j	mean free path of particle j
Λ_{jk}	argument of the Coulomb logarithm for species j and k
ν	photon frequency photon subscript
π	pi = 3.1459....
ρ_j	density of species j
σ_j	cross section of interaction j
σ_T	Thomson cross section
τ	plasma confinement time
ϕ	angular measure
ψ	angular measure

∇ vector differential operator

*   multiplication

AFIT/GNE/PH/82-5

Abstract

Energy transfer processes in a thermonuclear plasma
including Coulombic phenomena, bremsstrahlung, and Compton
scatter are critically reviewed. These processes are
incorporated in a three temperature, inertially confined
fusion computer simulation which uses a one dimensional,
spherical, Lagrangian hydrodynamics scheme. The computer
code, still in the validation phase, uses separate subroutines to
model hydrodynamics, thermonuclear burn, neutron heating, alpha par-
ticle heating, and energy transfer processes in CGS units.

ONE DIMENSIONAL ANALYSIS
OF INERTIALLY CONFINED PLASMAS

I. Introduction

Background

The scarcity of energy resources is a growing national
concern. Nuclear energy has helped to ensure an independent
and balanced energy supply system since the early 1960's
through the use of fission reactors. An energy source yet
to contribute to civil energy reserves is nuclear fusion.

Nuclear fission is the exothermic breakup of certain
heavy elements into lighter components and is the driving
mechanism for the nuclear reactors in service today. Nuclear
fusion is the exothermic combination of certain light nuclei
into a heavier nucleus. Two concepts show promise in
exploiting nuclear fusion as an energy resource. Magnetic
fusion uses a magnetic field to confine a thermonuclear
plasma. Inertial confinement fusion bombards a fuel pellet
with a concentrated energy pulse creating a thermonuclear
plasma by the resulting compression and heating. Both con-
cepts warrant further study.

Three technologies are being researched to supply the
concentrated energy pulse for an inertial confinement
scheme, namely: electron beams, ion beams, and laser beams.
These energy sources, known as drivers, couple energy into

1

a fuel target only micrometers in diameter. The surface layer of the target absorbs much more energy than the target interior. As a result, the outer layer vaporizes and expands outward extremely rapidly. This outward pressure must be balanced by inward pressure which is manifest in a shock wave. The shock wave compresses the fuel and the compression action raises the temperature. The resulting thermonuclear burn will free large amounts of energy. In fact, this is a nuclear explosion; it is a miniature nuclear bomb. Very careful design of the target using sophisticated physics optimizes the pellet compression and attains a maximum yield from the fuel mixture (see figure 1).

The U.S. government has identified nuclear fusion as an inexhaustible energy source and sees its commercial use by 2020 (Ref 19:133-138). In view of the continuing need for energy, the government has budgeted $593.7 million dollars for fiscal year 1981 (including Reagan cuts) and $650.3 million dollars for fiscal year 1982 for fusion energy research. Of these totals, inertial confinement fusion will account for $199.6 million and $190.2 million for operating, capital equipment, and construction for fiscal years 1981 and 1982, respectively (Ref 20:55-57).

During the Winter Quarter 1980 at the Air Force Institute of Technology, Dr. George H. Nickel, assisted by class members, developed the computer code MOXNEX to model inertially confined fusion in DT microspheres while instructing a graduate class in

2

a fuel target only micrometers in diameter. The surface
layer of the target absorbs much more energy than the
target interior. As a result, the outer layer vaporizes
and expands outward extremely rapidly. This outward pres-
sure must be balanced by inward pressure which is manifest
in a shock wave. The shock wave compresses the fuel and
the compression action raises the temperature. The result-
ing thermonuclear burn will free large amounts of energy.
In fact, this is a nuclear explosion; it is a miniature
nuclear bomb. Very careful design of the target using
sophisticated physics optimizes the pellet compression and
attains a maximum yield from the fuel mixture (see figure 1).

The U.S. government has identified nuclear fusion as
an inexhaustible energy source and sees its commercial use
by 2020 (Ref 19:133-138). In view of the continuing need
for energy, the government has budgeted $593.7 million
dollars for fiscal year 1981 (including Reagan cuts) and
$650.3 million dollars for fiscal year 1982 for fusion energy
research. Of these totals, inertial confinement fusion will
account for $199.6 million and $190.2 million for operating,
capital equipment, and construction for fiscal years 1981
and 1982, respectively (Ref 20:55-57).

During the Winter Quarter 1980 at the Air Force Institute
of Technology, Dr. George H. Nickel, assisted by class members,
developed the computer code MOXNEX to model inertially confined
fusion in DT microspheres while instructing a graduate class in

2

FUEL PELLET
CONSTRUCTION

FUEL
ABLATOR
PUSHER
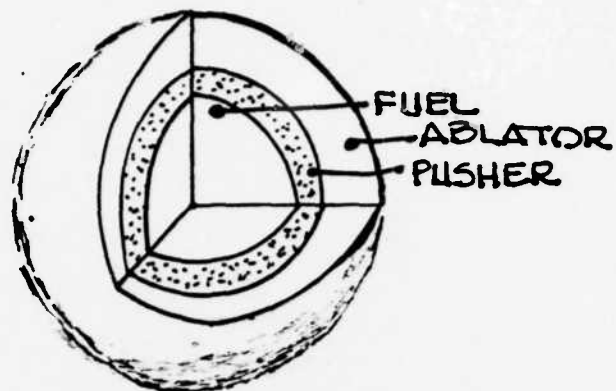
FUEL PELLET
RECEIVES
ENERGY
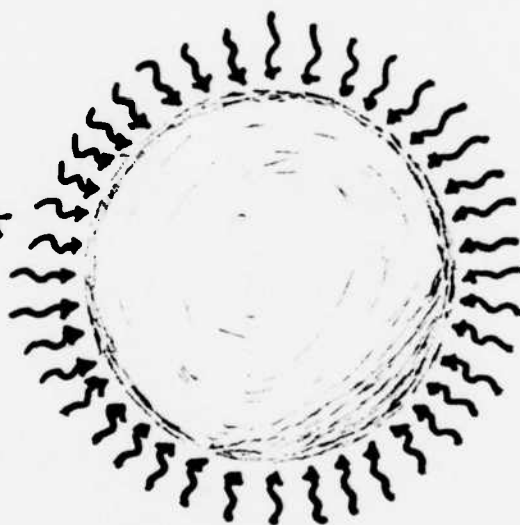
ABLATOR
VAPORIZES,
EXPANDS,
CREATING
COMPRESSING
SHOCK
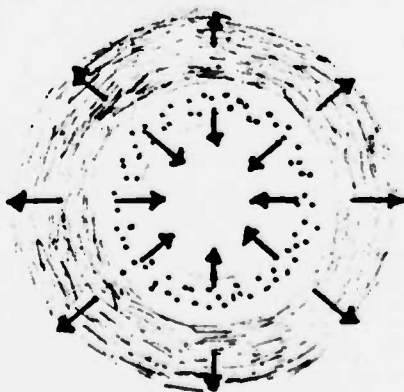
FIGURE 1: FUEL PELLET

nuclear fusion. The project was founded primarily on two prior studies, one completed by Keith A. Brueckner and Siebe Jorna at KMS Fusion in 1974 (Ref 4), and the other done by a team headed by Gary S. Fraley at Los Alamos Scientific Laboratory, also in 1974 (Ref 9). Prior to his retirement from the Air Force and subsequent assumption of a position at the Los Alamos National Laboratory, Dr. Nickel entrusted the code to Dr. William F. Bailey for further study and development.

Goals and Discussion

The goals of this project are to develop a computer code, MOXNEX, to model an inertially confined fusion plasma, validate the code, and prepare the code for further studies in Nuclear Engineering and Physics at the Air Force Institute of Technology. Though the code has yet to model fusion, progress has been made toward all three goals.

As previously mentioned, Reference 9, published in The Physics of Fluids, was a major source for initial code development. Upon critical examination, however, inconsistencies became apparent in the equations of Reference 9 in the area of radiation-electron energy transfer. These are mentioned in the text and appendices. Dr. Nickel's efforts to resolve these inconsistencies through communication with the authors were unfruitful. Development of consistent formulation, then, was necessary. The development of the radiation-electron

4

energy transfer equations is one of the major topics of
this report.

Additionally, simplifications were included in the
coding to expedite code construction. One such simplifi-
cation was the bremsstrahlung Gaunt factor being set equal
to 1. A complicated integral was evaluated numerically
and the resulting values were fit with an exponential
function.

Validation is required to enable its use as a vehicle
for further study. Confidence in the MOXNEX code will allow
its application to numerous areas of education and research.
Code hydrodynamics were examined to provide some portion of
this confidence.

Finally, code documentation is necessary to provide
user utility. Under Dr. Nickel's tutelage, each member of
the Fusion Engineering and Devices class, taught during the
Winter Quarter of 1980, contributed to the construction of
the MOXNEX code. Because of the diversity of the originators,
the code is somewhat disjointed and is not strongly supported.
Notes from each of the class members and from Dr. Nickel
are assimilated and presented in this report.

The presence of an inertial fusion code at the Air
Force Institute of Technology provides Physics Department
programs with a valuable tool. Classes in nuclear engineer-
ing, engineering physics and electro-optics may easily find
uses for the MOXNEX code and its results. Classes in

5

nuclear explosives, fusion engineering, plasma physics
laser studies, and others may be directly supported by
code use.

Additionally, further code development might also be
undertaken as design study or thesis projects. Extension of
the code to include driver input would make study of laser-
plasma coupling possible.

With this in mind, much work is required for completion
of the MOXNEX code. It is hoped that it can be a valuable
vehicle for the Department of Physics at the Air Force
Institute of Technology.

Scope

This analysis is concerned with the thermonuclear
burn and related hydrodynamic and energy transfer processes,
code validation, and documentation of the coding. Mechanisms
for the initial delivery of energy were not to be considered,
nor was the coupling of energy to the plasma investigated.

Code Synopsis with Assumptions

The three temperature MOXNEX code models inertially
confined fusion in deuterium-tritium microspheres using
separate ion, electron, and radiation temperatures. The ions
and electrons are modelled by a Maxwellian energy distribution
and the photons are modelled by a Planckian distribution.
The program is written in Fortran V using the central program

6

to call each of seven primary subroutines. A general
flowchart is seen in Figure 2. The subroutines, tasks
performed, and assumptions are discussed briefly in the
following paragraphs. Constant temperatures and number
densities are assumed at the time of each subroutine call.
Appendix A is a program listing and Appendix B is a glossary
of variables.

1.   Subroutine GDATA. This subroutine sets initial
conditions by initializing variables and is called one
time prior to execution of physical processes. Energy is
deposited in the microsphere by initializing ion, electron,
and radiation temperatures to selected levels at selected
cell locations. Compression is also set as an initial
condition by specifying an initial density.

2.   Subroutine HYDRO. Subroutine HYDRO is a one-
dimensional spherical Lagrangian hydrodynamics code. It
accounts for the hydrodynamics of the cells and the change
in temperatures due to PdV work.

Assumptions in HYDRO include (1) all materials in
the microsphere are an ideal gas, (2) pseudo-viscous pressure is
due only to the ions, (3) electron degeneracy occurs only
in the deuterium-tritium fuel regions and can be approxi-
mated with an effective temperature to account for additional
pressure, (4) total system PdV work changes can be divided
between the electron, ion, and radiation species   based on
the pressure of each component. Viscous pressure is set

7
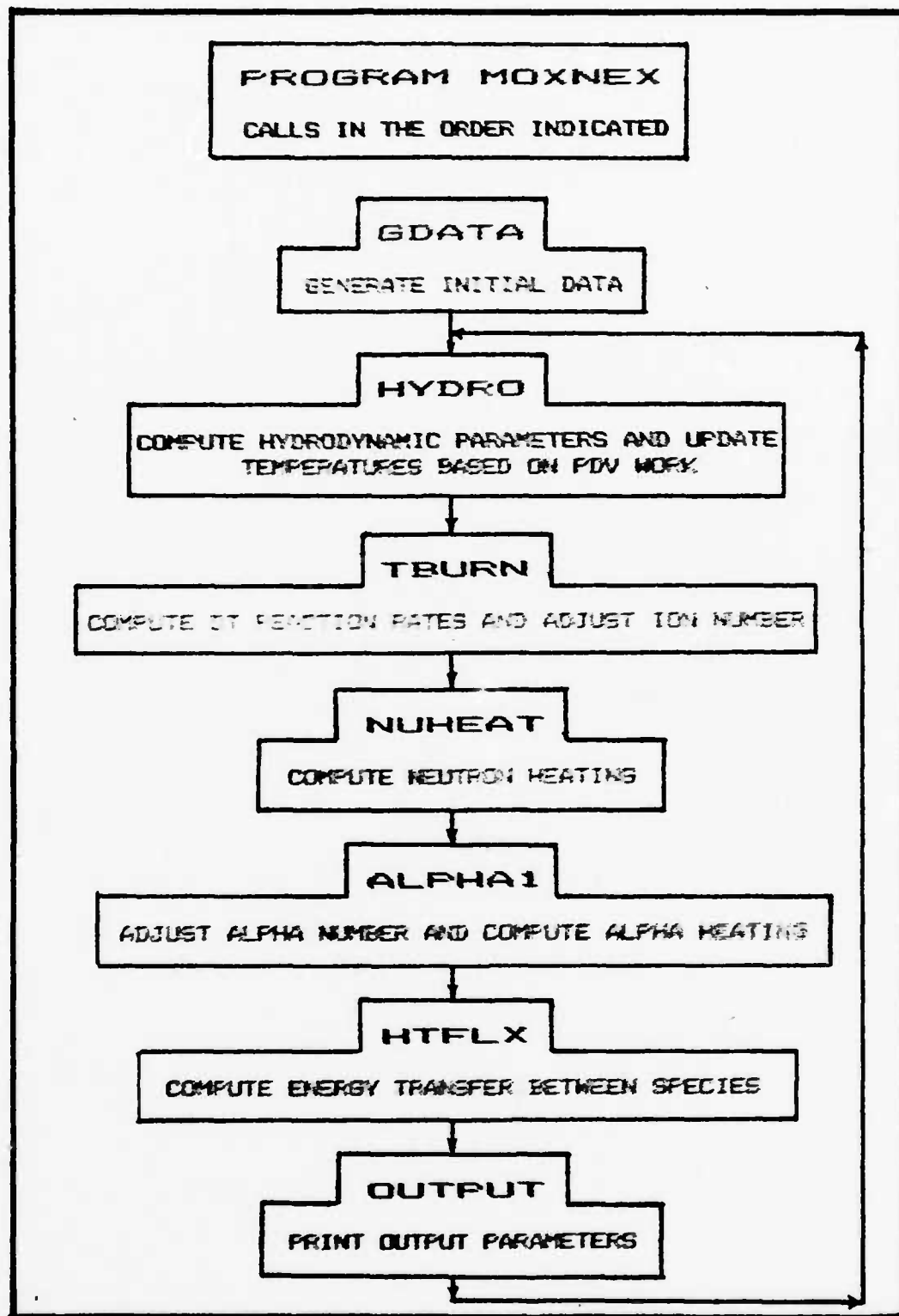
Figure 2. General flowchart for Program MOXNEX

to zero when the cell has expanded during the previous time step.

3. Subroutine TBURN. The TBURN subroutine provides reaction rates of the deuterium-tritium fusion reaction. Deuterium-deuterium reactions are not considered. Tritium created by deuterium-deuterium reactions is not included. If the ion temperature is below a specified ignition temperature of 1 kev, a figure based on bremsstrahlung power lost, no reactions are computed in any cell. The number of deuterium and tritium ions burned are subtracted from the totals in each cell.

The hydrogen fuel mix is equal amounts of deuterium and tritium at all times in TBURN. Therefore, the hydrogen number density is used in modelling the reaction rate density. The Maxwellian velocity distribution weighted average of cross section for the deuterium-tritium reaction is modelled in two ranges of ion temperature. Curve fits to data above 10 kev below 10 kev ion temperature are used for the model.

4. Subroutine NUHEAT. Subroutine NUHEAT calculates total neutron heating in each cell. Deuterium-tritium reactions are counted during one cycle and, by assuming isotropic production of one neutron per reaction, the new neutrons are placed at the center of the microsphere and attenuated during their pathlength through the plasma. Using an energy of 14.1 Mev for the neutrons and a cross section of 0.8 barns for collisions with deuterium, tritium and helium nuclei,

9

the number of interactions per cell is ascertained. An
average energy transfer per collision is used to deposit
energy into a cell based on the specific ion numbers in
the cell.

5. Subroutine ALPHA1. This subroutine is designed to
compute the energy deposited in each cell by monoenergetic
3.5 Mev alpha particles born in the deuterium-tritium
reactions. Additionally, it computes the number of alphas
produced in each zone, adjusts the helium particle mass
number in each zone, and adjusts ion and electron temperature
in each zone. Collisions with electrons are assumed to
dominate the alpha particle deceleration and are also
assumed to provide no significant scatter to the alpha parti-
cles. Upon reaching an area where ionic collisions dominate
energy loss, the motion of the alpha particle is stopped
and all residual energy is dumped in the current cell.

Subprogram ALPHA1 calls 14 other subroutines to
complete its tasks. General program organization is seen
in Figure 3.

Subroutine ALPHA1 updates the total heat added, the
number of alpha particles, total mass, electron temperature,
and ion temperature in each cell. Geometry subroutines
compute alpha particle position, direction and cell number
as the particle slows. An integration increment is computed
to integrate dE/ds along the path length in each cell using
a 4th order Runge-Kutta method. The energy deposited in
each cell is partitioned between ions and electrons.

10
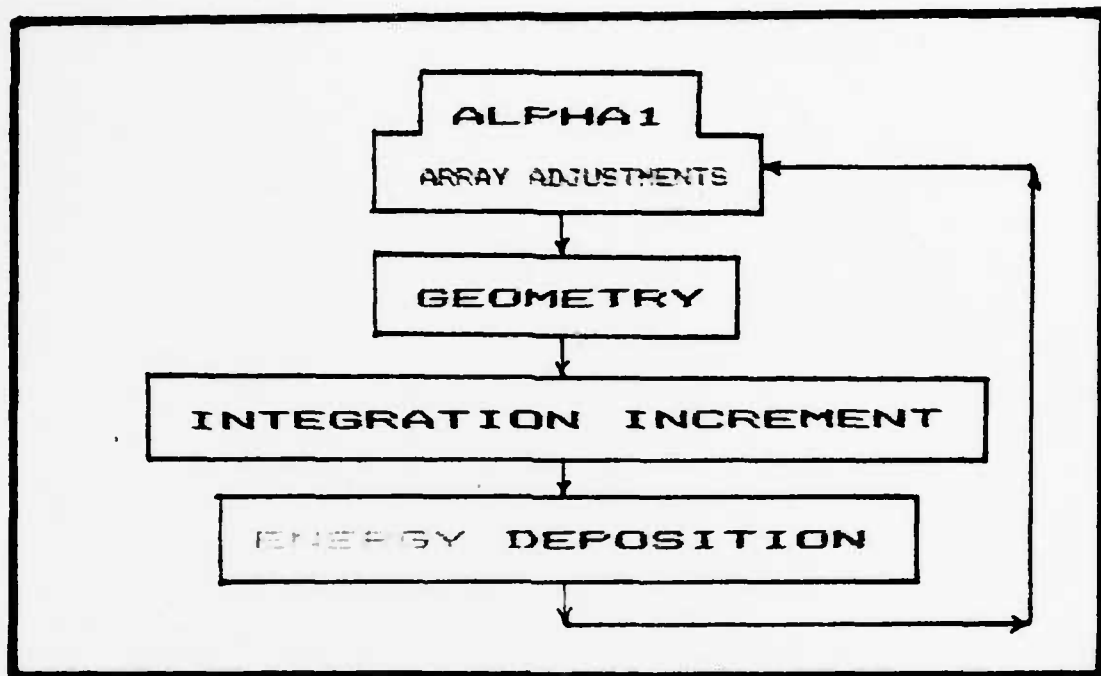
Figure 3. General Program Organization of Subroutine ALPHA1

6. Subroutine HTFLX. This subroutine computes the
energy transfer between the radiation, electron and ion
components. Drawing heavily on Appendix B of Reference 9,
HTFLX first models electron-ion energy exchange and electron
heat conduction. Ionic heat conduction is considered negligible.
Energy exchange between the photons and electrons is then
calculated. The energy exchange between photons and ions
is considered negligible.

7. Subroutine OUTPUT. This subroutine prints a variety
of information on hard copy including iteration number, time,

11

time increment used during the iteration, input energy, and output energy. Additionally, OUTPUT provides current cell radius, velocity of the cell wall, reactions during the iteration, relative density, electron, ion, and radiation temperatures, energy output, heating, and neutron fluence for each cell. Subroutine OUTPUT can be called at convenient places in the main program to provide timely output of data.

Acknowledgements

12

Approach

This report will briefly describe phenomena important to nuclear fusion for a deuterium-tritium fuel. Energy transfer processes in the plasma will then be addressed including Coulomb collisions, bremsstrahlung and Compton scatter. The equations used to code MOXNEX are then discussed as each subroutine is examined in detail.

Chapter IV discusses the validation of the hydrodynamics using a quasiequilibrium study and a point explosion. Chapter V addresses recommendations and code improvements.

Appendices include a program listing, a glossary of variables, equation derivations, and discussions of pertinent items. Each is referred to in the text where appropriate.

II. Physical Processes

Introduction

Before looking at the MOXNEX code, some basic phenomena concerning thermonuclear plasmas and fusion will be examined. The question of why fusion is attractive will be addressed, as will the nuclear reactions of interest. Knowing why the process is attractive, attention will be turned to the question of feasibility. A simple three species plasma model is then presented and energy transfer processes between these species examined. The three species plasma model is then generalized to a thermonuclear three species model that describes all MOXNEX processes.

Fusion

As mentioned previously, energy resources are a growing national concern. The following paragraphs, then, will reveal why energy can be attained from a fusion technology.

The average mass per nucleon varies slightly from 1 atomic mass unit in most nuclei. Table 1 gives values for the average mass per nucleon of selected light nuclei. If nuclear reactions can be produced such that the total mass of the reactants is greater than the total mass of the products, a net release of energy of $E = (\Delta m)c^2$ is attained. The quantity Δm is known as mass defect.

Table 1

Average Mass per Nucleon for Selected Light Nuclei
(Refs 16 and 5)

Nucleus	Ionic Mass (amu)	Mass per Nucleon (amu)
n	1.008665	1.008665
D	2.013553197	1.0067766
T	3.015501407	1.0050047
He^3	3.014932114	1.0049774
He^4	4.001506114	1.0003765

For instance, consider the reaction

$$D + T \rightarrow He^4 + n \tag{1}$$
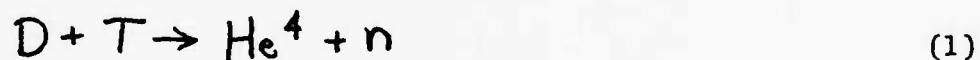
This will probably be a central reaction in a first generation
fusion reactor (Ref 6:279). The total nuclear mass of deuterium
and tritium is 5.029254604 amu and the total mass of a helium-4
nucleus and a neutron is 5.010171114 amu. The difference is
0.0188349 amu. This equates to an energy release of 17.609889
Mev. The process of exothermically combining nuclei is known
as fusion.

Although many fusion reactions are possible, the primary
reactions of interest for hydrogen fusion are listed in

15

Table 2. The excess kinetic energies of the reaction products are indicated with the reaction products.

Table 2

Reactions of Interest for Hydrogen Fusion
(Ref 19:2)

$$D + D \rightarrow {}^{3}He \ (0.82 \ MeV) + n \ (2.45 \ MeV)$$

$$D + D \rightarrow T \ (1.01 \ MeV) + H \ (3.02 \ MeV)$$

$$D + T \rightarrow {}^{4}He \ (3.5 \ MeV) + n \ (14.1 \ MeV)$$

$$D + {}^{3}He \rightarrow {}^{4}He \ (3.6 \ MeV) + H \ (14.7 \ MeV)$$
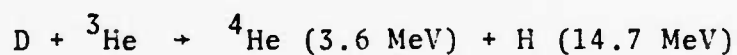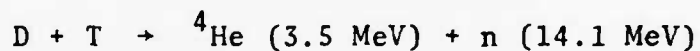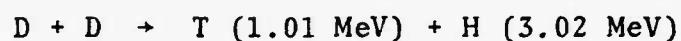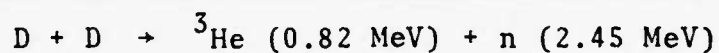
In order to bring about fusion reactions, it is necessary that the ionized nuclei collide with sufficient energy to overcome Coulombic repulsion. Classically, the relative energy required to overcome electrostatic repulsion for hydrogen is 0.28 Mev (Ref 10:7). The quantum mechanical effect of barrier penetration, however, reduces this energy threshold.

The nuclei are distributed in kinetic energy or velocity in a Maxwellian distribution. The average kinetic energy of a particle in a Maxwellian distribution is $\frac{3}{2} kT_i$. There are decreasing, but still finite, numbers of particles at many kT_i, however, and the high energy of the particles

in the "Maxwellian tail" is therefore a notable influence in overcoming Coulombic repulsion. These two factors, barrier pentration and the high energy tail on the Maxwellian distribution of the ions, make consideration of fusion reactors feasible.

Again, for a feasible system, the fusion reaction rate must be at least finite. Generally, a reaction rate may be expressed

$$RR = n_1 n_2 \sigma v \qquad (2)$$

where

    RR is the reaction rate density

    n_1 is the number density of species 1

    n_2 is the number density of species 2

    σ is the reaction cross section

    v is the relative velocity of the reactants.

The nuclear cross sections in Eq (2) are strong functions of velocity or kinetic energy. Averaging over the entire range of relative velocities, the product σv can be represented as an expectation value $\langle \sigma v \rangle$. Values of $\langle \sigma v \rangle$ which assume a Maxwellian particle distribution are shown in Figure 4. Notable from Figure 4 is the deuterium-tritium reaction is much more likely than the deuterium-deuterium reaction at any given kinetic temperature.
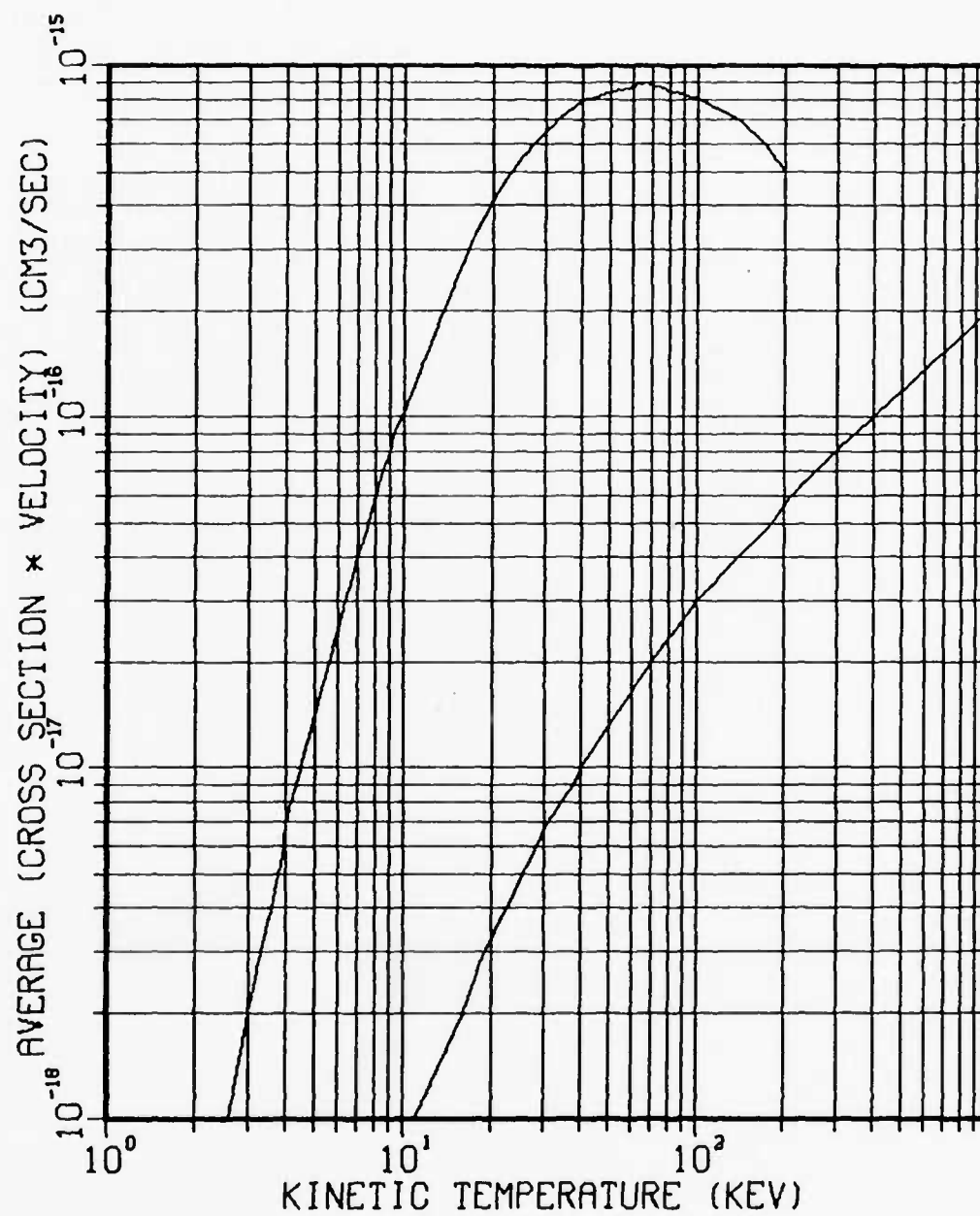
Figure 4.   Values of $\langle \sigma v \rangle$ versus Kinetic
Temperature for DT and DD (Ref 10:19)

18

The excess kinetic energy may be redeposited in the plasma or it may escape from the mixture. In order to sustain the thermonuclear burn, the redeposition of energy into the plasma is preferable. If more energy can be retained in the plasma, less energy is required from an outside input. This energy may be transferred from the reaction products by Coulomb collisions, participation in elastic collisions, or radiation-electron energy transfer. The process of redepositing the particle energy released by fusion reactions back into the plasma is known as bootstrap heating.

Singling out the deuterium-tritium reaction,

$$D + T \rightarrow He^4 \, (3.5 \; Mev) + n \, (14.1 \; Mev) \qquad (3)$$
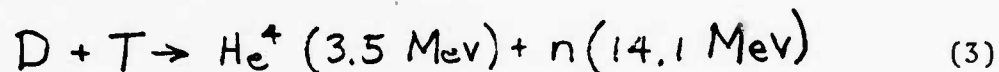
the neutrons can participate only in elastic collisions, but the alpha particles can participate in all three mechanisms named above.

The alpha particle path is dominated by Coulomb collisions with both electrons and ions. Thus, much or all of the 3.5 Mev possessed by the alpha particle is retained in the plasma promoting further fusion.

In order to retain the 14.1 Mev of the neutron within the plasma, high plasma densities are necessary (Ref 4:330). The mean free path of a 14.1 Mev neutron at typical magnetically confined thermonuclear plasma densities (10^{15} ions/cm^3) is ~10^9 cm^3 so neutrons are difficult to retain. The energy transfer from

19

radiation energy is also generally a small factor. The photon mean free path for particle number densities 10^{15} cm^3 is $\sim 10^{20}$ cm (Ref 10:29). Significant bootstrap heating comes primarily from alpha particle Coulomb collisions for the reaction given in Eq (3). A generalization can be made to other reactions that significant bootstrap heating comes primarily from the charged particle reaction products.

A primary energy loss mechanism is bremsstrahlung. As ionized particles are deflected by Coulomb interactions, they continuously radiate. The rate at which energy is radiated by an accelerating charge of $z = 1$, P_r, is expressed by the Larmor formula, namely,

$$P_r = \frac{2}{3} \frac{e^2 a^2}{c^3}$$ (4)

where

   e   is the electronic charge in statcoulombs

   a   is the acceleration in cm/sec^2

   c   is the speed of light in cm/sec.

This newly created photon energy can be redeposited through inverse bremsstrahlung or Compton collisions, but it may also escape the plasma. An optically thick plasma is desirable to recapture this radiation.

If the rate of energy loss from the plasma due to bremsstrahlung is greater than the rate of energy deposition by bootstrap heating, energy must be put into the system

from an outside source in order to sustain the thermonuclear
burn.   If the energy deposition rate is greater than brems-
strahlung loss rate, reactions may continue as long as fuel
is available.   A bremsstrahlung energy loss rate may be calcu-
lated as a function of number density and temperature.   Postu-
lating that 100% of the charged particle energy is retained
in the plasma, a bootstrap heating rate may also be calculated
as a function of number density and temperature.

Fortunately, as ion temperature increases, the bootstrap
heating rate increases faster than the bremsstrahlung loss
rate (Ref 10:33-36).   The temperature at which the bootstrap
heating rate equals the bremsstrahlung loss rate is known as
minimum ideal ignition temperature.   Below this temperature,
energy must be pumped into a system to realize sustained thermo-
nuclear burn.   Above this temperature, the reaction may be
self-sustaining and energy can be extracted from the system.

Noting the charged particle products of the reactions
from Figure 2 and the probability of reactions from Figure 3,
this "ideal ignition temperature" for deuterium-tritium is
about 4 kev and for deuterium-deuterium is about 36 kev,
almost an order of magnitude difference (Ref 10:35).

These temperatures correspond to particles with high
kinetic energies which tend to diffuse the plasma.   Coulomb
repulsion adds to dispersion effects.   Confinement of the
plasma for times long enough to achieve an economical energy
gain, therefore, becomes difficult.   Since the power density

21

depends on the reactant number density, the confinement time for energy breakeven is a function of the reactant number density. This can be stated in the Lawson criteria,

$$n\tau \geq 10^{14} \; sec/cm^3 \tag{5}$$

where τ is the confinement time (Ref 6:282).

Magnetic fusion relies on various geometries of magnetic bottles to confine the ionized particles. Typical number densities for magnetic fusion are about 10^{15} particles per cubic centimeter. This requires a confinement time of about 0.1 seconds to achieve energy breakeven.

Inertial confinement, on the other hand, realizes number densities of about 10^{26} particles per cubic centimeter and so requires a confinement time of only about 10^{-11} seconds (Ref 6:282).

Additionally, fusion reactors have some advantages over fission reactions. Deuterium for fusion fuel is readily available in seawater. Though tritium is not present in large enough quantities to be of interest in seawater and must be processed from other sources, deuterium is present in a ratio of about 1 deuterium atom to 6500 hydrogen atoms in ordinary water (Ref 10:2).

Another advantage is that radioactive reactants and by-products are minimized using fusion when compared with fission. Neutrons do activate some nuclei in the local

22

environment and some materials desirable for fusion reactions are naturally radioactive; for instance, tritium. Fusion reactions, however, create no radioactive fragments which are a necessary by-product of fission.

In summary, these paragraphs have tried to briefly develop some of the important concepts for nuclear fusion and fusion technology. Mass defect, barrier penetration, the high energy "tail" of the Maxwellian distribution, reaction rates, bootstrap heating, bremsstrahlung losses, ideal ignition temperature, and the Lawson criteria are all concepts central to nuclear fusion and fusion reactor technology. A quantitative physical model is now required that can follow some of these concepts in a time history.

Three Temperature Model

Knowing some of the central concepts of fusion, a physical model is now required that can follow macroscopic quantities through a time history of a fully ionized plasma. A simple yet physically accurate model is desired.

The motivating basis for researching nuclear fusion is that it offers the possibility of net energy gain. Energy may be calculated from power over a complete time history and power may be computed from number densities and particle velocities or particle energies. Ionic hydrogen will be the fusion reactants in the MOXNEX code so ion number densities and ion energies will be required to compute overall energy output. Ion number densities can be characterized by an

23

energy distribution. An ion species will be characterized by a Maxwellian distribution which can be denoted by a number density per unit energy at a given kinetic temperature. Ion-ion collisions partition energy throughout the species to attain a Maxwellian distribution (Ref 26:136).

But ion-ion collisions are not the only collisions occurring. Fuel pellet atoms all bind one electron prior to the driver pulse. Complete ionization, then, means as many electrons are present as are ions. Electron-electron collisions partition energy in the electron species also in a Maxwellian distribution (Ref 26:136). Electron number density can also be identified as a function of kinetic temperature. This temperature may differ, however, from the ion temperature (Ref 26:136).

If these temperatures do differ, equilibration between species will take place through electron-ion collisions. Energy exchange between these species must also be tracked.

As mentioned in the previous section, Coulombic acceleration of the electrons by the ions will result in bremsstrahlung so a photon species is present also. A third species energy distribution is required. These photons may be characterized by a Planckian distribution which requires a third species temperature. Additionally, the radiation may couple energy back into the electron species by either inverse bremsstrahlung or Compton scatter.

The minimum requirements, then, are two Maxwellian
distributions and a Planckian distribution characterized
by three species temperatures. All species can interact
with each other, although the photons will interact preferentially
with the electrons because of the mass difference between the
ions and electrons. In addition to energy flow between species,
energy flow in space, diffusion, will affect the energy distri-
butions. The more massive ions will move relatively slowly
compared to the lighter electrons, but electron diffusion must
be considered. Also, radiation diffusion will carry energy
through space.

A simple model is now apparent. A three temperature
model using separate ion, electron and radiation temperatures
accounting for electron and radiation diffusion may be used
to model a fully ionized plasma. Such a model is illustrated
in Figure 5.

The task at hand now is to develop understanding of the
pertinent energy transfer processes. This will be the topic
of the next section.

Coulombic Phenomena

Electrostatic encounters between particles of charge
Z_1 and Z_2 which are separated by a distance r are described
by the Coulomb potential, namely

$$V(r) = \frac{Z_1 Z_2 e^2}{r}$$

(6)

25
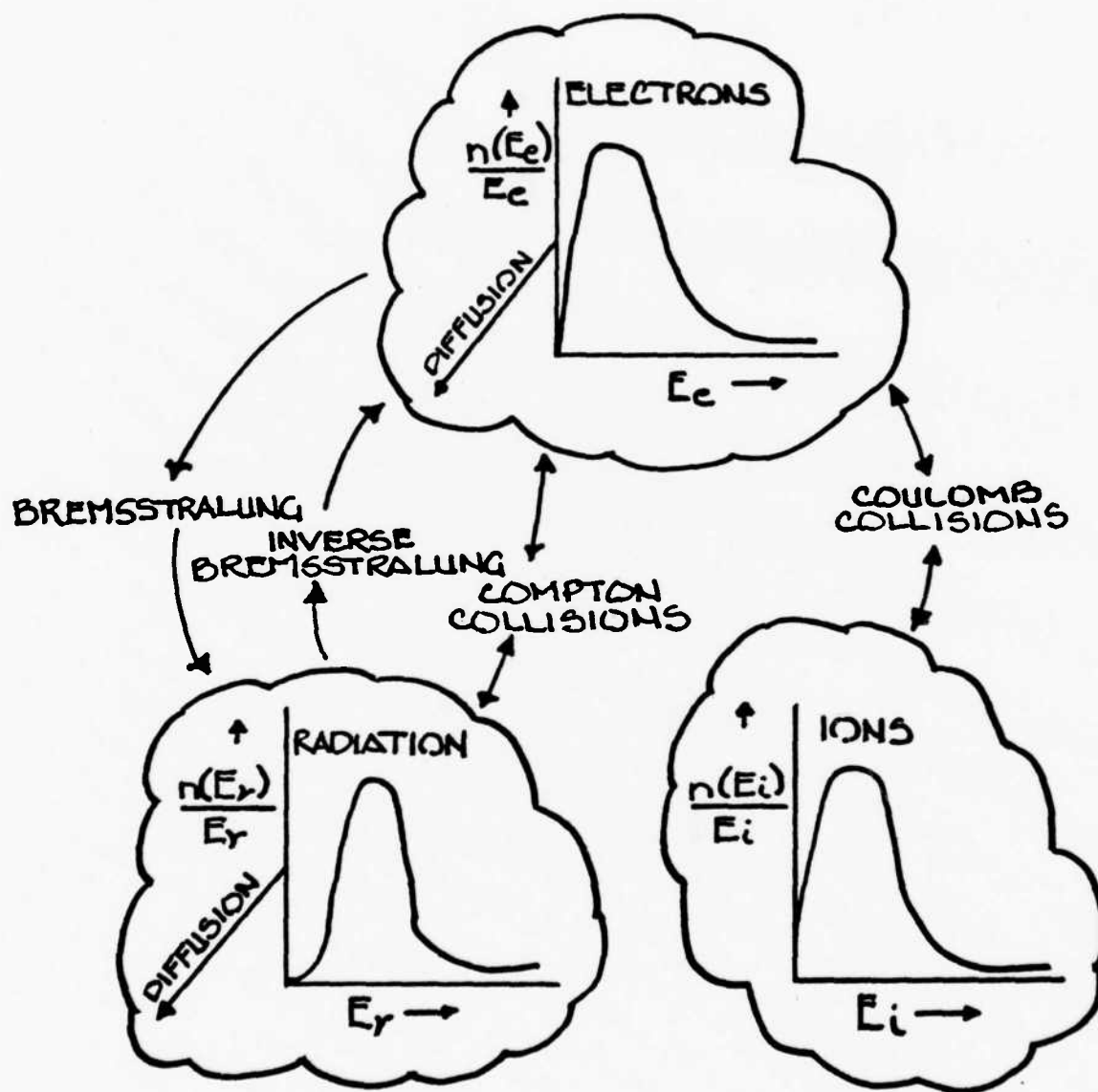
FIGURE 5: ENERGY TRANSFER BETWEEN SPECIES IN A FULLY IONIZED PLASMA

In a plasma, these electrostatic forces contribute signi-
ficantly to energy transfer between species and to species
diffusion.

The distance r is a determining factor in the magnitude
of the resulting force. In the case of charged particles
possessing kinetic energy, an impact parameter, b, is often
used to denote the distance of closest approach. Figure 6
illustrates the impact parameter of approaching particles
in the rest frame of particle 2.
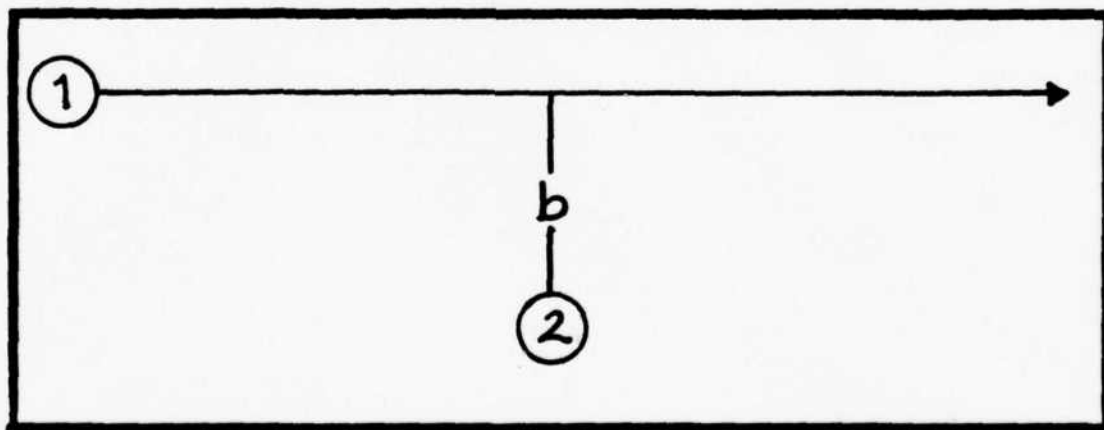
Figure 6. Illustration of Impact Parameter
Between Two Charged Particles

Figure 5 assumes a small momentum transfer so that particle 1 is basically undeflected from straight line motion. In a center of mass frame, the paths of both particles is actually hyperbolic.

In space, the range of the Coulomb force is infinite and there is no maximum interaction distance. In a plasma, however, even though the entire system is electrically neutral, random thermal motion creates small deviations from strict electrical neutrality. Electrostatic forces accentuate this and a time average will show a net negative charge density around an ion and a net positive charge density around an electron. This net opposite charge may be regarded as an "atmosphere" around each charged particle (Ref 10:84). The radius of this atmosphere based on a Maxwellian distribution and a Coulomb potential expressed in Poisson's equation is

$$\lambda_D = \left(\frac{kT_e}{4\pi n_e \Theta^2} \right)^{1/2} \tag{7}$$

(Ref 6:10). The quantity λ_D is known as the Debye length and determines the maximum shielding or screening distance at which a Coulomb force can be felt in a plasma. Notice that as electron temperature increases, the Debye length increases. It is also a function of electron number density. The Debye length is a dynamic parameter and the pseudo "atmosphere" is not static.

28

Coulomb collisions can be divided into short range encounters and long range encounters. The Debye length is the limiting distance for long range encounters. The charged particle is "screened" from charged particles farther away because of the opposite charge "atmosphere." Because of the large number of particles within a Debye radius, the number of long range encounters is large. The number of long range encounters is so great that their effect greatly outweighs the effect of short range collisions (Ref 26:123).

The cross section for a short range encounter resulting in an angle of deflection from its original path of 90° is

$$\sigma_{c_{SR}} \simeq \frac{\pi Z_1^2 Z_2^2 e^4}{4 E_1^2} \qquad (8)$$

where E_1 is the energy of the less massive particle in the rest frame of the more massive particle. In a hydrogen plasma, this can be an electron passing any positive particle.

A long range encounter may be described by a change in momentum such that

$$\left(\overline{\Delta P}\right)^2 = P_{initial}^2 \qquad (9)$$

This is equivalent to multiple scatters summing to a total 90° deflection. The cross section for this type of interaction is

$$\sigma_{C_{LR}} \simeq \frac{2\pi Z_1^2 Z_2^2 e^4}{E_1^2} \ln \Lambda \tag{10}$$

where E_1 is again the energy of the less massive particle in the rest frame of the more massive particle, and

$$\Lambda = \frac{b_{max}}{b_{min}} \tag{11}$$

or

$$\Lambda = \frac{\lambda_D}{b_{min}} \tag{12}$$

Both short range and long range Coulomb cross sections are discussed in Appendix C.

Comparing Eqs (8) and (10), note that the long range cross section is $\simeq 8 \ln \Lambda$ greater than the short range cross section. Also noting that typical values for $\ln \Lambda$ are between 10 and 25 at thermonuclear temperatures and densities (Ref 10:94), the long range interaction is much more dominant.

Relaxation times are often used to describe long range encounters and may be defined as the time required for the momentum changes to sum such that

$$\left(\overline{\Delta p_T} \right)^2 = P_{initial}^2 \tag{13}$$

The long range cross section given in Eq (10) yields for

30

electron-ion relaxation time

$$t_{ei} \simeq \frac{(2m_e)^{1/2} E_e^{3/2}}{4\pi e^4 n_i \ln \Lambda_{ei}} \tag{14}$$

Coulomb interactions between ions and electrons at different temperatures will eventually lead to equilibrium. Based on Maxwellian velocity distributions for both ions and electrons and defining t_{eq} from the relation given by Spitzer (Ref 26:135),

$$\frac{dT_1}{dt} = \frac{T_1 - T_2}{t_{eq}} \tag{15}$$

where T_j is species kinetic temperature, t_{eq} can be written

$$t_{eq} = \frac{3m_1 m_2 k^{3/2}}{8(2\pi)^{1/2} n_2 Z_1^2 Z_2^2 e^4 \ln \Lambda_{12}} \left(\frac{T_1}{m_1} + \frac{T_2}{m_2} \right)^{3/2} \tag{16}$$

Relaxation times and equilibration times are further discussed in Appendix N.

In addition to electron-ion energy exchange, Coulomb collisions add to energy transfer through heat flow. Heat conduction may be approached in the same manner as other transport phenomena using a conductivity coefficient (Ref 26:143).

In the presence of a temperature gradient (assuming no external electric field), the flow of heat, Q, can be

31

described by

$$\underline{Q} = K \underline{\nabla} T \qquad (17)$$

where T is temperature and K is the conductivity coefficient. For a Lorentz gas, a fully ionized gas in which the electrons are assumed to interact only with ions which are all at rest (Ref 26:138), this coefficient is given by Spitzer (Ref 26:144),

$$K = 20 \left(\frac{2}{\pi}\right)^{3/2} \frac{(kT)^{5/2} k}{m_e^{1/2} e^4 Z \ln \Lambda} \qquad (18)$$

Heat flow caused by a temperature gradient results in a current, however, and this current produces a secondary electric field which reduces the flow of heat by a factor of ϵ which is dependent on the net Z of the material. Additionally, for an actual gas K is further reduced by a factor of δ_T which is also dependent on the net Z . Employing these terms, the conductivity coefficient becomes

$$K_e = 20 \left(\frac{2}{\pi}\right)^{3/2} \frac{(kT_e)^{5/2} k \, e \, \delta_T}{m_e^{1/2} e^4 Z \ln \Lambda_{ei}} \qquad (19)$$

A conductivity coefficient may be derived for any charged species. Equation (19) gives this coefficient for the electron species. As the least massive charged particles in a thermonuclear plasma, the electrons should dominate heat transport if the electron temperature is not very much smaller than the ion temperature.

Bremsstrahlung Processes

Bremsstrahlung occurs when a particle having charge and
finite kinetic energy is accelerated, resulting in a photon
being radiated and decreased kinetic energy of the original
moving particle. This occurs typically in a thermonuclear
plasma as an electron is accelerated as it passes a positive
ion. The instantaneous power radiated in a non-relativistic
acceleration is given by the Larmor formula (Ref 14:469),
here for $Z = 1$,

$$P_r = \frac{2}{3} \frac{e^2 a^2}{c^3} \tag{4}$$

A bremsstrahlung emission is shown symbolically in Figure 7.
for the case of an electron passing a positive ion.
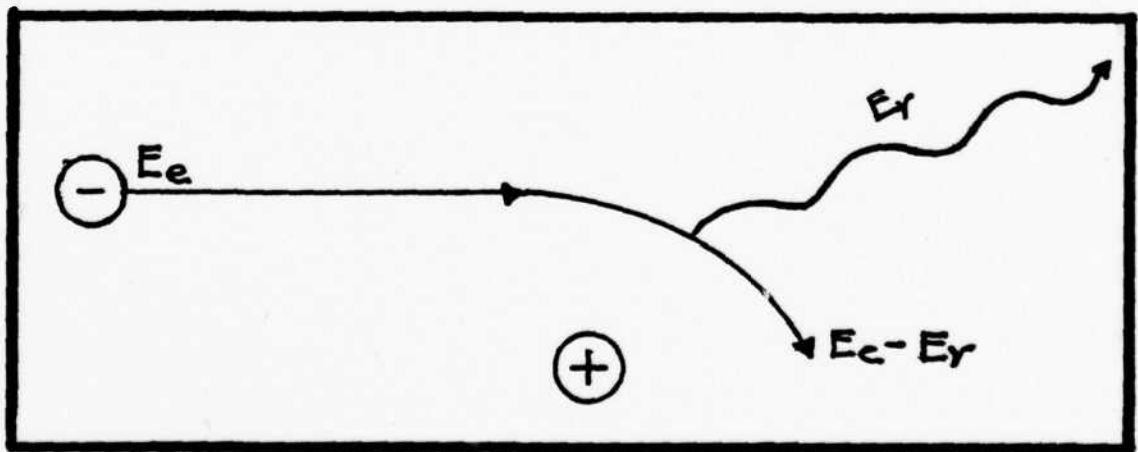
Figure 7. Symbolic Illustration of Bremsstrahlung

Inverse bremsstrahlung occurs as a photon adds energy to a particle in the presence of another particle. The second particle is necessary to conserve momentum. In the case of a photon adding energy to an electron in the presence of a positive ion, typical in a thermonuclear plasma, the kinetic energy of the electron is raised and the photon is absorbed. This is represented symbolically in Figure 8.
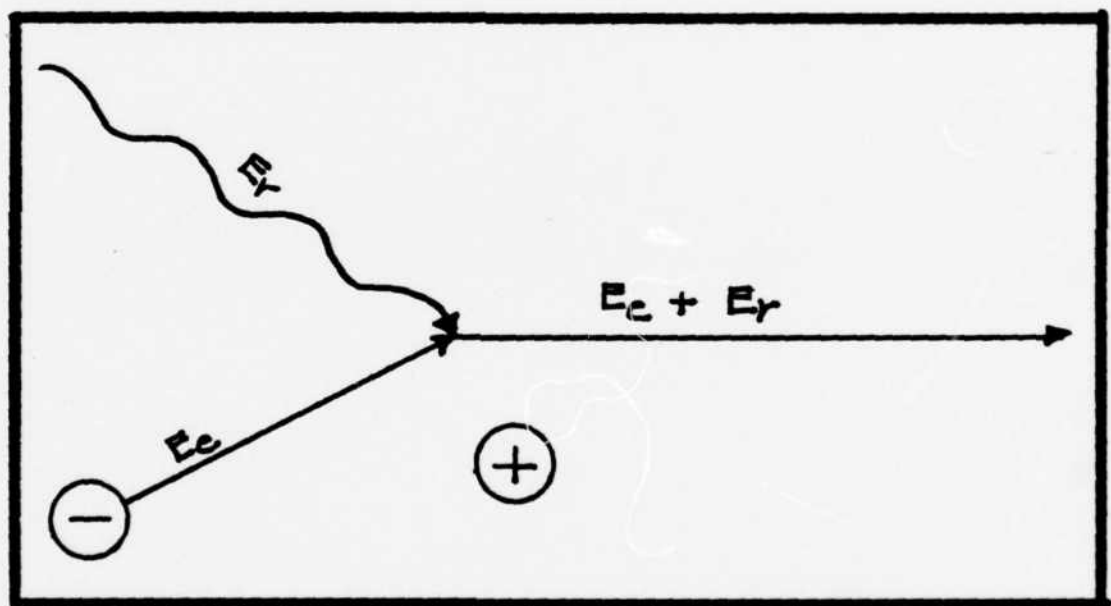
Figure 8. Symbolic Illustration of Inverse Bremsstrahlung

With these pictures in mind, some of the theory pertinent to bremsstrahlung interactions will now be developed. The equations presented in the following discussion and Appendices E through G are prompted by the unpublished notes of Dr. George H. Nickel. Significant portions of the development are contained in Reference 22.

The bremsstrahlung cross section for a non-relativistic Coulomb collision is given by Jackson (Ref 14:513) as

$$\sigma_\beta(E_1, \hbar\omega) \simeq \frac{16}{3} \frac{Z_2^2 e^2}{\hbar c} \left(\frac{Z_1^2 e^2}{M c^2}\right)^2 \left(\frac{c}{v}\right)^2 \frac{1}{\hbar\omega} \ln\left(\frac{\sqrt{E_1} + \sqrt{E_1 - \hbar\omega}}{\sqrt{\hbar\omega}}\right)^2 \quad (20)$$

where

Z_1 is the charge of the radiating particle

Z_2 is the charge of the particle providing the accelerating force

M is the mass of the radiating particle

v is the velocity of the radiating particle

or E in the rest frame of the ion.

This cross section is also supported by Bethe and Heitler (Ref 14:512). Its dimensions are area per energy.

For the case of a thermonuclear plasma, the radiating particle is usually an electron so that $Z = 1$ and $M = m_e$ and the particle providing the accelerating for ionic hydrogen or ionic helium. Referring to Appendix E and denoting the

35

ionic charge as simple Z , Eq (20) becomes

$$\sigma_{\beta}(E_e, E_\nu) = \frac{16}{3} Z^2 \alpha r_o^2 \frac{m_e c^2}{E_e E_\nu} \ln\left(\frac{\sqrt{E_e} + \sqrt{E_e - E_\nu}}{\sqrt{E_\nu}}\right) \tag{21}$$

where

$\alpha = e^2/\hbar c$ is the fine structure constant

E_e is the electron energy

E is the photon energy

The bremsstrahlung reaction rate density is then

$$RR_{\beta} = n_i n_e (E_e) \, v \, \sigma_{\beta}(E_e, E_\nu) \tag{22}$$

which has dimensions of reactions per volume per time per square energy. The inverse bremsstrahlung cross section may be derived using this reaction rate density and assuming local thermodynamic equilibrium exists. The inverse bremsstrahlung cross section, also discussed in Appendix E, is

$$\sigma_{I\beta}(E_e, E_\nu) = \frac{16}{3} Z^2 \alpha r_o^2 \left(\frac{2}{E_e m_e}\right)^{1/2} \frac{m_e c}{E_\nu n_\nu(E_\nu)} \left(\frac{e^{-E_\nu/k T_r}}{1 - e^{-E_\nu/k T_r}}\right) \ln\left(\frac{\sqrt{E_e + E_\nu} + \sqrt{E_e}}{\sqrt{E_\nu}}\right) \tag{23}$$

with dimensions area per energy.

The reaction rate densities for the respective processes can then be expressed using these cross sections. The bremsstrahlung reaction rate density can be written explicitly as

36

$$RR_\rho = n_i \int_0^\infty n_c(E_e) \left(\frac{2E_e}{m_e}\right)^{1/2} dE_e \int_0^{E_e} \sigma_\beta(E_e, E_v) \frac{dE_v}{(1 - e^{-E_v/kT_r})} \tag{24}$$

which has dimensions of reactions per volume per time. From this, the power density can be expressed as

$$P_\rho = n_i \int_0^\infty n_e(E_e) \left(\frac{2E_e}{m_e}\right)^{1/2} dE_e \int_0^{E_e} \sigma_\rho(E_e, E_v) \frac{E_v}{(1 - e^{-E_v/kT_r})} dE_v \tag{25}$$

which has dimensions of energy per unit volume per unit time. The enhancement factor

$$1 + \overline{n}(E_v) = \frac{1}{1 - e^{-E_v/kT_r}} \tag{26}$$

used for the bremsstrahlung equations is derived in Appendix D.

For inverse bremsstrahlung, the reaction rate density and the power density can be expressed as

$$RR_{I\beta} = n_i c \int_0^\infty n_e(E_e) dE_e \int_0^\infty n_v(E_v) \sigma_{I\beta}(E_e, E_v) dE_v \tag{27}$$

and

$$P_{I\rho} = n_i c \int_0^\infty n_e(E_e) dE_e \int_0^\infty n_v(E_v) \sigma_{I\beta}(E_e, E_v) E_v dE_v \tag{28}$$

Substituting explicit expressions into P_ρ , changing variables to

$$X = \frac{E_e}{E_\nu} \qquad (29)$$

$$\xi = \frac{E_\nu}{kT_e} \qquad (30)$$

and noting

$$\gamma = \frac{T_r}{T_e} \qquad (31)$$

results in

$$P_b = n_i n_e \frac{32}{3} \left(\frac{2}{\pi m_e}\right)^{1/2} z^2 \alpha r_o^2 m_e c^2 (kT_e)^{1/2} \int_0^\infty \xi \left(\frac{1}{1-e^{-\xi/\gamma}}\right) d\xi \int_1^\infty e^{-x\xi} \ln\left(\sqrt{x}+\sqrt{x-1}\right) dx \qquad (32)$$

Analogous manipulations can be performed to refine $P_{I\beta}$. This is

$$P_{I\beta} = n_i n_e \frac{32}{3} \left(\frac{2}{m_e \pi \gamma}\right)^{1/2} z^2 \alpha r_o^2 m_e c^2 (kT_e)^{1/2} \int_0^\infty \xi \left(\frac{1}{1-e^{-\xi/\gamma}}\right) d\xi \int_1^\infty e^{-\xi(x-1)} e^{-\xi/\gamma} \ln\left(\sqrt{x}+\sqrt{x-1}\right) dx \qquad (33)$$

These two power densities can be expressed using a Gaunt factor $G(\gamma)_j$, where j denotes either pure bremsstrahlung or pure inverse bremsstrahlung. Using this Gaunt factor, Eqs (32) and (33) may be written as

38

$$P_\beta = n_i n_e \frac{32}{3} \left(\frac{2}{m_e \pi} \right)^{1/2} Z^2 \alpha r_0^2 m_e c^2 \left(\frac{1}{kT_e} \right)^{1/2} G(\gamma)_\beta \left(kT_e - kT_r \right) \tag{34}$$

where

$$G(\gamma)_\beta = \frac{1}{1-\gamma} \int_0^\infty \xi \left(\frac{1}{1-e^{-\xi/\gamma}} \right) d\xi \int_1^\infty e^{-x\xi} \ln\left(\sqrt{x} + \sqrt{x-1} \right) dx \tag{35}$$

and

$$P_{I\beta} = n_i n_e \frac{32}{3} \left(\frac{2}{m_e \pi} \right)^{1/2} Z^2 \alpha r_0^2 m_e c^2 \left(\frac{1}{kT_e} \right)^{1/2} G(\gamma)_{I\beta} \left(kT_e - kT_r \right) \tag{36}$$

where

$$G(\gamma)_{I\beta} = \frac{1}{1-\gamma} \int_0^\infty \xi \left(\frac{1}{1-e^{-\xi/\gamma}} \right) d\xi \int_1^\infty e^{-\xi(x-1)} e^{-\xi/\gamma} \ln\left(\sqrt{x} + \sqrt{x-1} \right) dx \tag{37}$$

Recognize that these power densities are limiting cases.
Equation (34) models a case of pure bremsstrahlung and
Eq (36) models the case of pure inverse bremsstrahlung. For
practical applications, the power density equations must be
extended from the limiting cases of either pure bremsstrahlung
or pure inverse bremsstrahlung to a situation of competing
processes. This is done by simple subtraction.

Note that the power density equations have a common
coefficient, which may be denoted by A_{er}^Δ , and is

$$A_{er}^{\beta} = \frac{32}{3} \left(\frac{2}{\pi m_e} \right)^{1/2} Z^2 \alpha \, r_o^2 \, m_e \, c^2 \, \frac{n_i \, n_e}{(kT_e)^{1/2}} \, G(\gamma) \tag{38}$$

Substituting explicit expressions for α , r_o , n_e , and n_i , this becomes

$$A_{er}^{\beta} = \frac{32}{3} \left(\frac{2}{\pi m_e} \right)^{1/2} \frac{e^4 \, N_a}{\hbar \, c} \, k \left(\frac{Z^2}{A^2} \right) \frac{e^2}{m_e \, c^2} \, \frac{\rho^2 \, Z}{(kT_e)^{1/2}} \, G(\gamma) \tag{39}$$

Thus the net rate of energy flow into the radiation field from bremsstrahlung processes is

$$P_{\beta}^{NET} = P_{\beta} - P_{I\beta} \tag{40}$$

which is

$$P_{\beta}^{NET} = A_{er}^{\beta} \left(kT_e - kT_r \right) \left(G(\gamma)_{\beta} - G(\gamma)_{I\beta} \right) \tag{41}$$

Denoting

$$G(\gamma) = G(\gamma)_{\beta} - G(\gamma)_{I\beta} \tag{42}$$

this can be written

$$P_{\beta}^{NET} = A_{er}^{\beta} \left(kT_e - kT_r \right) G(\gamma) \tag{43}$$

where

$$G(\gamma) = \frac{1}{1-\gamma} \int_0^\infty \xi \left(\frac{1 - e^{-\xi(\frac{1}{\gamma}-1)}}{1 - e^{-\xi/\gamma}} \right) d\xi \int_1^\infty e^{-x\xi} \ln\left(\sqrt{x} + \sqrt{x-1}\right) dx \tag{44}$$

or

$$G(\gamma) = \int_0^\infty \frac{\xi \, d\xi \, f(\xi)\left(1 - e^{-\xi(1/\gamma - 1)}\right)}{(1-\gamma)\left(1 - e^{-\xi/\gamma}\right)} \tag{45}$$

where

$$f(\xi) = \int_1^\infty \ln\left(\sqrt{x} + \sqrt{x-1}\right) e^{-\xi x} dx \tag{46}$$

Note that $G(\gamma)$ is dimensionless.

The values of $G(\gamma)$ as $\gamma \to 0$ and as $\gamma \to \infty$ may be found analytically. These are

$$G(0) = 1 \tag{47}$$

and

$$G(\infty) = \frac{\pi^2}{4} \tag{48}$$

Appendix F discusses the reaction rate densities, power densities, Gaunt factors, and the bremsstrahlung coupling coefficient in more depth. Appendix G discusses the Gaunt factor and its limiting values.

Compton Processes

The quantum theory of light postulates that photons behave like particles except for the absence of rest mass. This concept provides a foundation for radiation-material energy interaction to be treated as an elementary mechanical collision. Figure 9 symbolically illustrates such a collision known as a Compton collision.
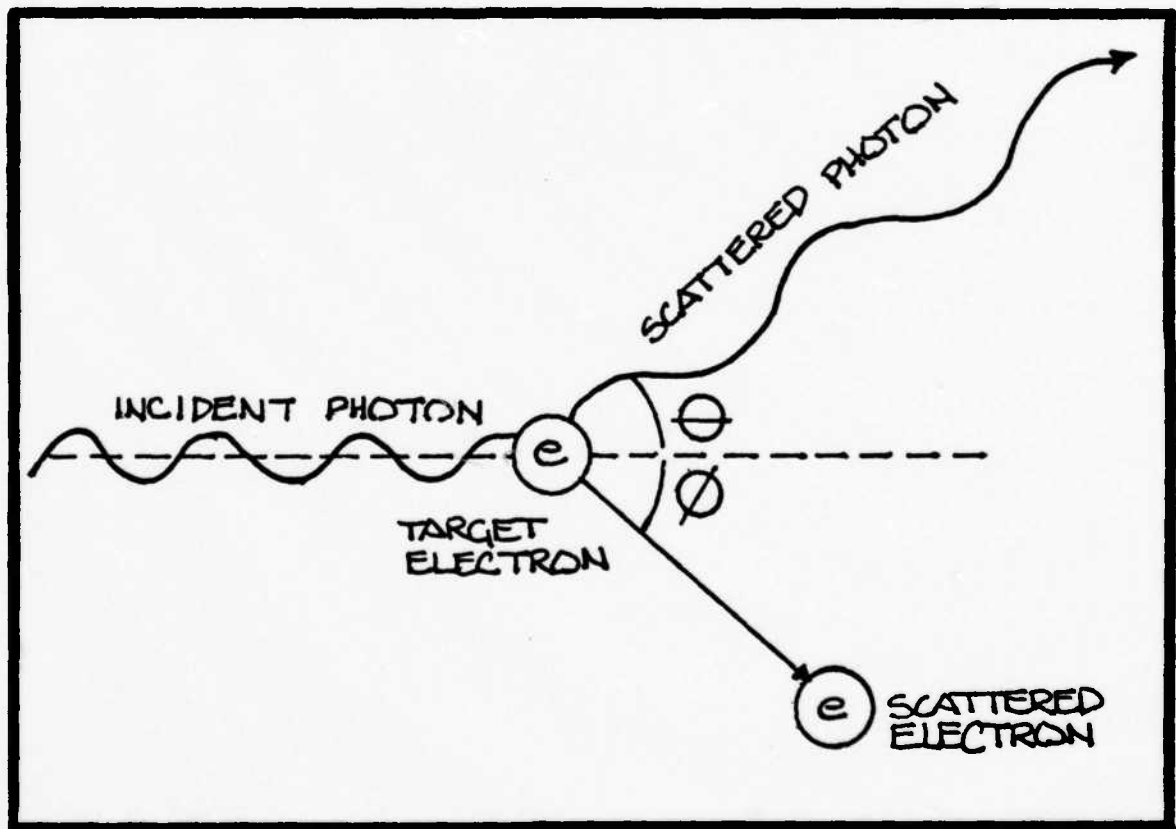
Figure 9 . Symbolic Illustration of a Compton Collision

The energy transfer can be described by the wavelength change of the photon which is (Ref 2:71)

$$\lambda' - \lambda = \frac{h}{m_e c}(1 - \cos\Theta)$$

(49)

Since the photon is not absorbed and a photon exits from the interaction, Compton collisions are a scattering process as opposed to absorption processes such as pair production or photoelectric effect.

The classical cross section for Compton scatter is

$$\sigma_T = \frac{8\pi r_0^2}{3}$$

(50)

where

$$r_0 = \frac{e^2}{m_e c^2}$$

(51)

is the classical electron radius. This cross section, known as the Thomson cross section, becomes suspect at higher photon energies.

At higher photon energies, Compton scatter can be described by

$$\sigma_{KN} = \sigma_T \left[1 - 2\left(\frac{E_\nu}{m_e c^2}\right) + \frac{26}{5}\left(\frac{E_\nu}{m_e c^2}\right)^2 + \cdots \right]$$

(52)

(Ref 3:124), where E_ν is the energy of the incident photon.

43

This is known as the Klein-Nishina cross section and applies only for photon energies such that $E_\nu \ll m_e c^2$.

Inverse Compton collisions are also possible and such an interaction is symbolically represented in Figure 10.
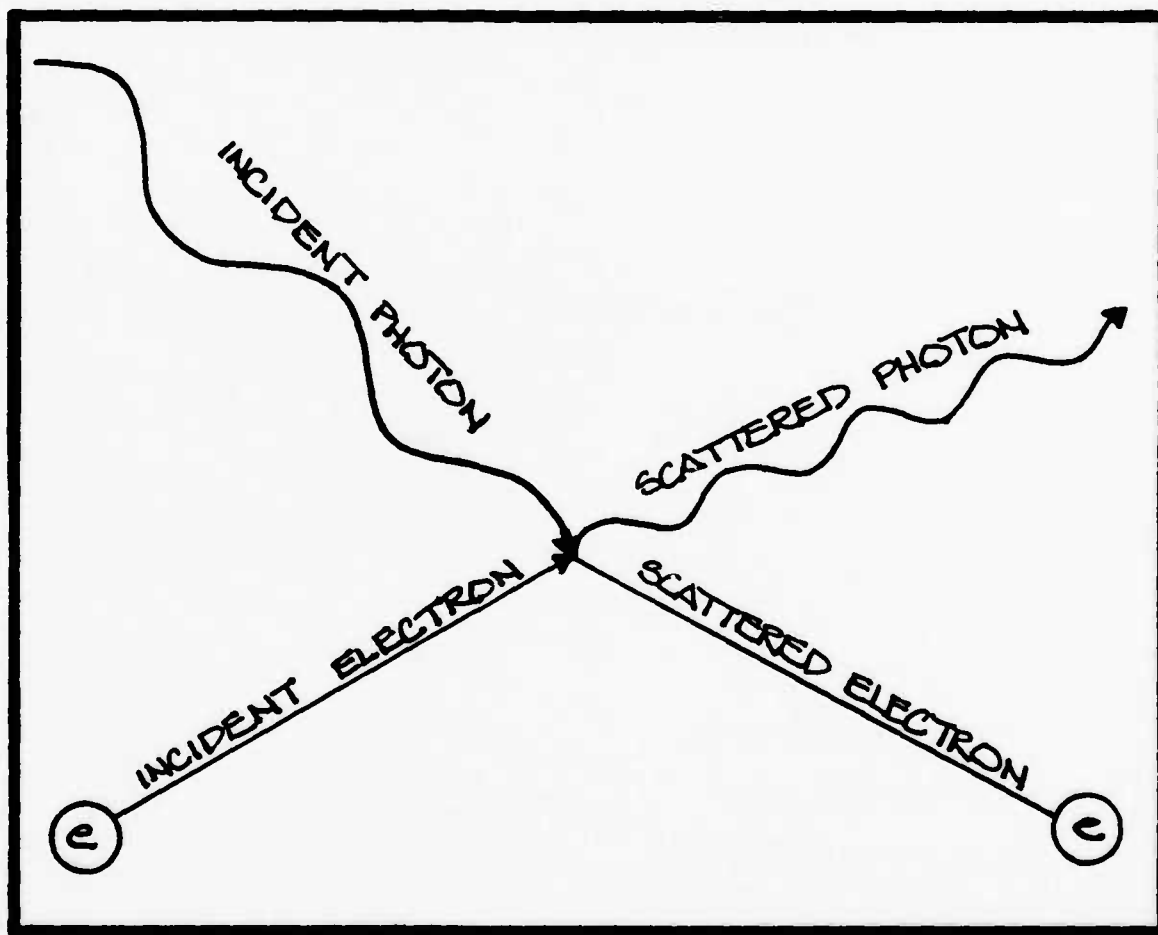
Figure 10. Symbolic Illustration of an Inverse Compton Collision

Note that in both processes a photon is emitted. Again, since photons are Bose particles, the photon population will be enhanced by photons already existing in the plasma and this enhancement factor can be expressed as

$$1 + \overline{n}_\nu(E_\nu) = \frac{1}{1 - e^{-E_\nu/k T_r}}$$

(26)

Again, much of the following development is due to George H. Nickel (Ref 22).

The reaction rate density for Compton scatter now can be written as

$$RR_c = n_e \, n_\nu(E_\nu) \, \sigma_T \, c \, \frac{1}{1 - e^{-E_\nu/k T_r}}$$

(53)

which has dimensions of reactions per volume per time per energy. This formula assumes the electrons are at rest. The cross section, however, is dependent on electron energy. Note from Eq (52) that if $E_\nu \lll m_e c^2$ that the Klein-Nishina cross section reduces to the Thomson cross section. This is well approximated in a thermonuclear plasma as typical photon temperatures can be expected to be on the order of 1 kev (Ref 9:475). As the electron rest mass is $m_e c^2 = 511$ kev , an approximation might be made assuming $\sigma_{KN} \rightarrow \sigma_T$ for a thermonuclear plasma and using σ_T for the reaction rate density.

45

A power density may be written from the reaction rate
by including the energy exchange per collision and integrating
over the entire range of photon energies. This average
energy exchange per collision can be approximated by

$$\langle \Gamma E \rangle = \frac{E_\nu^2}{m_e c^2} \tag{54}$$

This quantity is discussed in Appendix H.

The power going from radiation to electrons per unit
volume is

$$P_c = n_e \int_0^\infty n_\nu (E_\nu) \sigma_T \, c \left(\frac{E_\nu^2}{m_e c^2} \right) \frac{1}{1 - e^{-E_\nu / h T_r}} \, dE_\nu \tag{55}$$

No integration is done over electron energy as the electrons
are again assumed to be at rest. Using explicit expressions,
this becomes

$$P_c = \frac{8}{3} \frac{1}{\pi} \left(\frac{1}{\hbar c} \right)^3 \frac{c \, n_e}{m_e c^2} \, r_0^2 \int_0^\infty \frac{E_\nu^4 \, e^{E_\nu / k T_r}}{\left(e^{E_\nu / k T_r} - 1 \right)^2} \, dE_\nu \tag{56}$$

By multiplying and dividing by $(kT_r)^5$, and substituting
$y = E / k \, Tr$,

$$P_c = \frac{8}{3} \frac{1}{\pi} \left(\frac{1}{\hbar c} \right)^3 \frac{c \, n_e}{m_e c^2} \, r_0^2 \left(h T_r \right)^5 \int_0^\infty \frac{y^4 e^{-y}}{\left(1 - e^{-y} \right)^2} \, dy \tag{57}$$

The value of the integral is $4\pi^4/15$, therefore

$$P_c = \frac{32}{45} \pi^3 \left(\frac{1}{\hbar c}\right)^3 \frac{c\, n_e}{m_e\, c^2}\, r_o^2 \left(k T_r\right)^5 \tag{58}$$

This is the rate of energy flow from radiation to electrons for pure Compton scatter.

The calculation for inverse Compton scatter is fairly complicated and will not be included in this report. Inverse Compton requires that the electron have non-zero kinetic energy prior to incidence with the photon. The calculation first requires a transformation to the rest frame of the electron. The energies of the incident and emerging photons are also transformed in the electron rest frame. Rates are calculated in this reference frame and transformation back to the original frame is required. The result is (Ref 20)

$$P_{xc} = \frac{32}{45} \pi^3 \left(\frac{1}{\hbar c}\right)^3 \frac{c\, n_e}{m_e\, c^2}\, r_o^2 \left(k T_r\right)^4 \left(k T_e\right) \tag{59}$$

This equation represents pure inverse Compton scatter.

The net flow of energy from electrons to radiation can be found by subtracting the power from radiation to electrons due to Compton scatter from the power from electrons to radiation due to inverse Compton scatter, or

47

$$P_C^{NET} = P_{IC} - P_C \tag{60}$$

Inserting Eqs (58) and (59) for P_{IC} and P_C

$$P_c^{NET} = \frac{32}{45} \pi^3 \left(\frac{1}{\hbar c}\right)^3 \frac{c n_e}{m_e c^2} r_0^2 \left(kT_r\right)^4 \left(kT_e - kT_r\right) \tag{61}$$

The coupling coefficient for Compton scatter may then be written

$$A_{er}^c = \frac{32}{45} \pi^3 \left(\frac{1}{\hbar c}\right)^3 \frac{c n_e}{m_e c^2} r_0^2 \left(kT_r\right)^4 \tag{62}$$

This can be expressed in terms of the Stephan-Boltzmann constant and explicit expressions as

$$A_{er}^c = \frac{128}{3} \pi \sigma \frac{e^2}{(m_e c^2)^2} N_a \left(\frac{Z}{A}\right) r_0 \rho \, T_r^4 \tag{63}$$

Pertinent information on the Compton power density and Compton coupling coefficient may be found in Appendix I.

Thermonuclear Three Temperature Model

Complete ionization does occur in a thermonuclear plasma. Nuclear interactions, however, are not modelled in Figure 4. Neutral particles in the form of neutrons exist

in a thermonuclear state and are also not modelled in
Figure 5. Figure 11 includes these items.

The neutrals are a result of the nuclear reaction

$$D + T \rightarrow He^4 (3.5 \, Mev) + n \, (14.1 \, Mev) \tag{3}$$
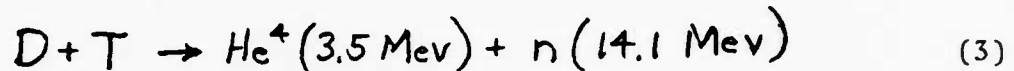
Note that one particle is returned to the ion distribution with
an additional 3.5 Mev of energy. One neutron at 14.1 Mev is
added to the neutral distribution for each nuclear reaction,
also. The nuclear reactions, then, affect both the ion and
neutral particle distributions, and are shown affecting both
in Figure 11.

Once born, however, the 14.1 Mev neutron may undergo
elastic collisions with the ions, adding energy to the ion
distribution. This interaction is illustrated in Figure 11
also. The neutrons have no mechanism with which to interact
with the photons and, though the neutrons can collide elast-
ically with the electrons, the collision cross section is
negligible when compared to the ion collision cross section.

The energy distributions of the ions, electrons and photons
remain the same as do the interactions between these species.
The energy distribution of the neutrons is represented as a
Maxwellian distribution in Figure 11. At extremely high
densities, this should be the case as neutrons, being particles,
will tend toward a Maxwellian distribution. But at lesser
densities, many 14.1 Mev neutrons will escape the plasma after
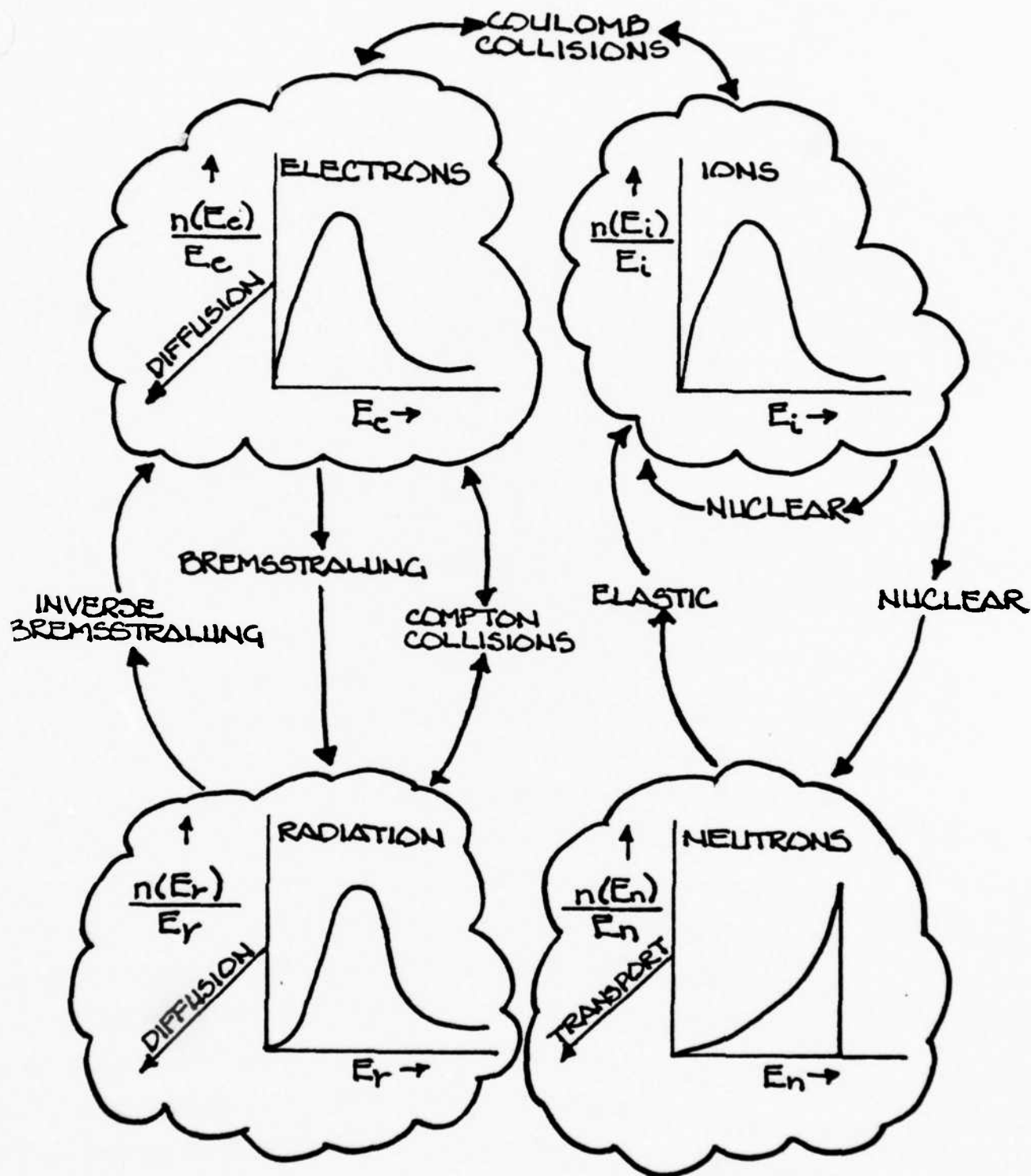
FIGURE 11: ENERGY TRANSFER BETWEEN SPECIES IN A THERMONUCLEAR PLASMA

only few, if any, collisions. Few will thermalize. The escaping particles will not be in the distribution long, however, so the actual distribution may be a Maxwellian distribution with a peak at high temperatures.

The nuclear interaction will dramatically add to the energy of the total system and is indeed the motivating process for this study. Chapter II, then, addresses the system illustrated in Figure 11 and how these processes are modelled in the MOXNEX code.

III. Theory and Coding

Introduction

This chapter discusses specific theory and how it is
coded into program MOXNEX. Remembering energy transfer
theory developed in Chapter II, the specific equations of
MOXNEX will first be presented. A comparison of this set
of equations with another formalism will then be given.
Finally, the coding of the formalism into the specific
equations of MOXNEX will be discussed.

MOXNEX Formalism

The MOXNEX one-dimensional, three temperature, spherical,
Lagrangian code uses the momentum equation

$$\frac{\partial v}{\partial t} = - \frac{1}{\rho} \frac{\partial}{\partial r} \left(P_T + q \right) \tag{64}$$

where P_T is the sum of the three species pressures or

$$P_T = P_e + P_i + P_r \tag{65}$$

and q is the artificial viscosity. The coupled energy
equations are

$$\frac{\partial(kT_i)}{\partial t} = \frac{1}{c_{vi}} \left\{ -\left(P_i + q\right)\frac{\partial V}{\partial t} - A_{ie}^\rho \left(kT_i - hT_e\right) + \frac{V}{r^2}\frac{\partial}{\partial r}\left(r^2 K_i \frac{\partial T_i}{\partial r}\right) \right\} \quad (66)$$

$$\frac{\partial(kT_e)}{\partial t} = \frac{1}{c_{ve}} \left\{ -P_e \frac{\partial V}{\partial t} + A_{ie}^\rho \left(kT_i - hT_e\right) - A_{er}^\rho \left(kT_e - hT_r\right) \right. $$
$$\left. + \frac{V}{r^2}\frac{\partial}{\partial r}\left(r^2 K_e \frac{\partial T_e}{\partial r}\right) \right\} \quad (67)$$

$$\frac{\partial(kT_r)}{\partial t} = \frac{1}{c_{vr}} \left\{ -\left(P_r + \frac{I_r}{\partial V}\right)\frac{\partial V}{\partial t} + A_{er}^\rho \left(kT_e - kT_r\right) + \frac{V}{r^2}\frac{\partial}{\partial r}\left(r^2 K_r \frac{\partial T_r}{\partial r}\right) \right\} \quad (68)$$

The coupling coefficients in the equations are

$$A_{jk}^\rho = \frac{A_{jk}}{\rho} \quad (69)$$

where j and k denote specific species. Each energy
equation is derived using the chain rule

$$\frac{\partial I_j}{\partial t} = c_{vj}\frac{\partial T_j}{\partial t} + \frac{\partial I_j}{\partial V}\frac{\partial V}{\partial t} \quad (70)$$

j denoting species, where

53

$$C_{v_{\perp}} = \frac{\partial I_{\perp}}{\partial T_{\perp}}$$

(71)

and for an ideal gas

$$\frac{\partial I_{\perp}}{\partial V} = 0$$

(72)

The energy densities and specific heats for the three species are

$$E_{DENSITY\ e} = \rho_m I_e$$

(73)

and

$$C_{ve} = \frac{3}{2} \frac{Z}{m_i}$$

(74)

for electrons,

$$E_{DENSITY\ i} = \rho_m I_i$$

(75)

and

$$C_{vi} = \frac{3}{2m_i}$$

(76)

for ions,

$$E_{DENSITY \ r} = \frac{4\pi \sigma}{c}(T_r)^4 \tag{77}$$

and

$$C_{yr} = \frac{4 I_r}{T_r} \tag{78}$$

where

$$I_r = \frac{4\pi \sigma}{c \rho_m}(T_r)^4 \tag{79}$$

Ion and electron species pressures are computed using an
ideal gas equation of state. Radiation pressure is

$$P_r = \left(\frac{4\sigma}{c}\right)\frac{T_r^4}{3} \tag{80}$$

The ion electron fields are coupled by

$$A_{ie}^\rho = C_{ye} \, \nu_{eq} \tag{81}$$

where

$$\nu_{eq} \quad \frac{8(2\pi)^{1/2} e^4 N_a^2 Z^2 \rho \ln \Lambda_{ei}}{3 A^2 (k T_e)^{3/2}} \tag{82}$$

The electron diffusion coefficient is

$$K_e = 20\left(\frac{2}{\pi}\right)^{3/2}\frac{(kT_c)^{5/2}k\,\epsilon\,\delta_T}{m_e^{1/2}e^4\,Z\,\ln\Lambda_{ei}}\tag{19}$$

where

$$\epsilon\,\delta_T = \frac{0.43\,Z}{(3.44 + Z + 0.26\ln[Z])}\tag{83}$$

and

$$\ln\Lambda_{ei} = \ln\left\{\frac{3}{2e^3}\left(\frac{A}{Z}\frac{(kT_e)^3}{\pi\,N_a\rho}\right)^{1/2}\frac{1}{\left[Z + \left(\frac{1}{2\alpha c}\right)\left(\frac{3kT_e}{m_e}\right)^{1/2}\right]}\right\}\tag{84}$$

and is defined to have a minimum value of 1. The electron radiation coupling coefficient, A_{er} , is

$$A_{er} = A_{er}^{\beta} + A_{er}^{c}\tag{85}$$

where

$$A_{er}^{\beta} = \frac{32}{3}\left(\frac{Z}{\pi m_e}\right)^{1/2}\frac{e^4 N_a^2}{\hbar c}k\left(\frac{Z^2}{A^2}\right)\frac{\rho^2 Z}{(kT_c)^{1/2}}r_o\,G(\gamma)\tag{86}$$

and

56

$$A_{er}^c = \frac{128}{3} \pi \sigma \frac{e^2}{(m_e C^2)^2} N_a \left(\frac{Z}{A}\right) r_o \rho \left(T_r\right)^4 \qquad (87)$$

with

$$G(\gamma) = \int_0^\infty \frac{\xi \, d\xi \, f(\xi) \left[1 - e^{-\xi(1/\gamma - 1)}\right]}{(1 - \gamma)(1 - e^{-1/\gamma})} \qquad (88)$$

where

$$f(\xi) = \int_1^\infty \ln\left(\sqrt{x} + \sqrt{x-1}\right) e^{-\xi x} dx \qquad (89)$$

The Rosseland mean free path is

$$\lambda_r = \frac{1.3 \, T_e^{7/2}}{\rho^2} \qquad (90)$$

from which the radiation diffusion coefficient is attained, namely

$$K_r = \frac{16 \sigma}{3} \lambda_r T_r^3 \qquad (91)$$

Only the deuterium-tritium nuclear reaction is modelled assuming a fuel that is 50% deuterium and 50% tritium so the nuclear reaction rate density is modelled as

$$RR_{DT} = \frac{n_H^2}{4} \langle \sigma v \rangle_{DT} \qquad (92)$$

57

Two hydrogens are subtracted from the hydrogen number array for each reaction.

Radiation-Electron Energy Transfer Formalism Comparison

Reference 9 presents the bremsstrahlung Gaunt factor as

$$G(\gamma) = \int_0^\infty \frac{d\xi \, f(\xi) \left[1 - e^{-\xi(1/\gamma - 1)} \right]}{(\gamma - 1)(1 - e^{-\xi/\gamma})} \tag{93}$$

where

$$f(\xi) = \int_1^\infty \ln\left(\sqrt{x} + \sqrt{x+1}\right) e^{-\xi x} dx \tag{94}$$

Appendix F derives these quantities as

$$G(\gamma) = \int_0^\infty \frac{\xi \, d\xi \, f(\xi) \left[1 - e^{-\xi(1/\gamma - 1)} \right]}{(1 - \gamma)(1 - e^{-\xi/\gamma})} \tag{88}$$

where

$$f(\xi) = \int_1^\infty \ln\left(\sqrt{x} + \sqrt{x-1}\right) e^{-\xi x} dx \tag{89}$$

All quantities are dimensionless. The bremsstrahlung Gaunt factor is used in the project as derived.

Reference 9 gives the bremsstrahlung coupling coefficient as

$$A_{er}^{\beta} = \frac{32}{3} \left(\frac{2}{\pi m_e}\right)^{1/2} \frac{e^4 N_a^2}{\hbar c} k \left(\frac{Z^2}{A^2}\right) \frac{\rho Z}{(kT_e)^{1/2}} G(\gamma) \qquad (95)$$

and the Compton coupling coefficient as

$$A_{er}^{c} = \frac{128}{3} \frac{\pi e^2 \sigma}{(m_e c^2)^2} N_a \left(\frac{Z}{A}\right) T_r^4 k \qquad (96)$$

These are used according to the relation

$$\frac{\partial T_j}{\partial t} = \pm \frac{A_{er}}{C_{y_j}} (T_e - T_r) \qquad (97)$$

where

$$A_{er} = C_{y_j} \left(A_{er}^{\beta} + A_{er}^{c}\right) \qquad (98)$$

and j denotes either electron or radiation. The quantity A_{er} , then, should have dimensions of 1/mt . The dimensions of A_{er} in Eq (98), however, are 1/(t-m-ℓ).

The coupling coefficients used in this study may be expressed

59

$$A_{er}^{\beta} = \frac{32}{3} \left(\frac{2}{\pi m_e} \right)^{1/2} \frac{e^4 N_a^2}{\hbar c} h \left(\frac{Z^2}{A^2} \right) \frac{\rho^2 Z}{(kT_e)^{1/2}} r_0 G(\gamma) \qquad (86)$$

and

$$A_{er}^{c} = \frac{128}{3} \pi \sigma \frac{e^2}{(m_e c^2)^2} N_a \left(\frac{Z}{A} \right) r_0 \rho (T_r)^4 \qquad (87)$$

where

$$A_{er} = A_{er}^{\beta} + A_{er}^{c} \qquad (85)$$

For computations in MOXNEX

$$\frac{\partial T_J}{\partial t} = \pm \frac{A_{er}^{\rho}}{C_{yJ}} (T_e - T_r) \qquad (99)$$

where

$$A_{er}^{\rho} = \frac{A_{er}}{\rho} \qquad (100)$$

Comparing Eqs (86) and (95), it is seen that they differ by a factor of ρr_0. Equations (87) and (96) differ by the same factor. The dimensions of A_{er}^{ρ} from Eq (100) should be $1/mt$ also. The dimensions of A_{er} in Eq (85) are $1/(t-\ell^3)$. The quantity A_{er}^{ρ}, then, is

1/mt , consistent with Eq (99). Derivations of these coupling coefficients are included in Appendices F and I.

Subroutine GDATA

This subroutine sets initial conditions by initializing variables and is called one time prior to the execution of physical processes. Constants are gathered at the front of the subroutine, then specific zone values are computed. The radii of the zones are the inside radius, that is $r_1 = 0$. This requires one more radius element than the number of zones. Thus, two loops are necessary; one having an upper limit of the number of zones and another to the number of zones + 1.

Hydrogen density and pusher mass are constants of interest for parameter study. Additionally, zone thickness and number of zones may be changed.

Energy is introduced in the microsphere by initializing the ion, electron, and radiation temperatures as desired. If a cell has no other initial energy specified, it is set at a value of 1.16 °K or 1×10^{-7} kev. Typically, the radiation temperature is set at 1 kev and the electron and ion temperatures are set between 1.8 and 100 kev following procedures outlined in Reference 9.

Subroutine HYDRO

Subroutine HYDRO is a one dimensional spherical Lagrangian hydrodynamics code. It is based on the Lagrangian energy equation

$$\frac{\partial T}{\partial t} = \frac{1}{C_\nu}\left[-\left(P+q\right)\frac{\partial V}{\partial t}\right] \qquad (101)$$

where

T is species temperature

C_ν is the specific heat

P is species pressure

q is artificial viscosity

I is species internal energy

V is volume

t is time.

Appendix J discusses this equation. Viscosity is assumed to be due only to the ions, and is modelled by artificial viscosity. Thus, q is seen only in the ion species equation.

The first lines of the subroutine initializes constants and steps the cycle counter. Initial densities are then calculated and viscosities are set to zero for the first cycle. Ion and electron pressures are computed using a perfect gas law and species populations computed in other subroutines. Radiation pressure is calculated from

62

$$P_r = \left(\frac{4\sigma}{c}\right) \frac{T_r^4}{3} \tag{80}$$

An effective temperature is calculated for the case of electron degeneracy and is used as a minimum electron temperature according to the relation

$$T_{e(effective)} = 0.00565\rho^{2/3} \tag{102}$$

This is discussed in Appendix K. At low values of T_e, this effective minimum provides electron pressures which create a disassembly rate higher than classically anticipated (Ref 9:477). Total pressure is the sum of the species pressures, or

$$P_T = P_i + P_e + P_r \tag{65}$$

The time step is computed using a fractional value of the time required for a shock wave to travel across the thinnest cell or

$$\Delta t_{iteration} = F \frac{\Delta r_{min}}{c} \tag{103}$$

where

F   is the fractional value specified

c   is the speed of sound in the medium.

63

The speed of sound is computed using

$$C = \left(\frac{\gamma P_i}{\rho}\right)^{1/2}$$

(104)

This assumes a perfect gas so that $\gamma = 5/3$ and also that viscous pressure is due only to the ions. A minimum time step is specified in subroutine GDATA and a maximum time step is specified early in the HYDRO subprogram. The fractional value used may be varied between 1/10 and 1/2.

Cell wall accelerations and velocities are computed using total pressure and artificial viscosities. New cell wall positions are then determined.

With these new positions, densities are updated. Artificial viscosities are now updated according to the relation

$$q = \rho(\Delta r)^2 (\nabla \cdot v)^2$$

(105)

where

q is the artificial viscosity

$\nabla \cdot v$ is the divergence of velocity (Ref 27:136).

In the instance of cell expansion, artificial viscosity is set to zero.

Species temperatures are then updated accounting for compression or expansion. Computations assume the total

64

Pdv work can be divided between the ion, electron
and radiation energies based on the species pressures.
Ion and electron calculations are done using the ideal gas
law. Viscosity is not used in the electron temperature
update equation, again reflecting the assumption that
viscous pressure is due only to ions. Radiation tempera-
ture is updated using

$$T_r^{(n+1)} = T_r^{(n)} \left[\frac{\left(V^{(n)} - \Delta V/3 \right)}{V^{(n+1)}} \right]^{1/4}$$

(106)

where

$V^{(n+1)}$ is the updated volume

ΔV is the change in volume

n is the iteration.

This assumes adiabatic compression and is discussed in
Appendix M. Minimum species energies are specified.
Finally, the total time is re-calculated.

Subroutine TBURN

Subroutine TBURN provides the reaction rates of the
deuterium-tritium fusion reaction. Deuterium-deuterium
reactions are not computed. Tritium created by deuterium-
deuterium reactions is not considered. Constant tempera-
tures and number densities of deuterium and tritium are
assumed at the time of the subroutine call.

A minimum ignition temperature flag, TSTART, is set at 1 kev, a figure based on bremsstrahlung power lost. If the ion temperature is below the TSTART temperature, no reactions are computed in any cell. The flag TBURN is used to carry this information to other subroutines; TBURN = 1 signals ignition and TBURN = 0 denotes no thermonuclear burn. The number of deuterium and tritium ions burned are subtracted from the totals in each cell.

The reaction of interest in TBURN is

$$D + T \rightarrow He^4 + n \tag{1}$$
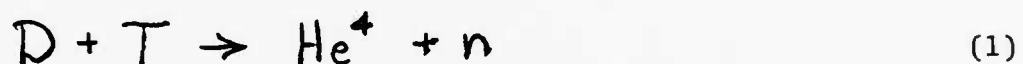
The reaction rate density for this reaction is

$$RR_{DT} = n_D n_T \langle \sigma v \rangle_{DT} \tag{107}$$

where $\langle \sigma v \rangle_{DT}$ is the Maxwell Boltzmann velocity distribution weighted average of cross section for the deuterium-tritium reaction times the velocity of approach of the reactants (Ref 4:358). The weighted average of the product $\langle \sigma v \rangle_{DT}$ is modelled in two ranges, one for ion temperatures less than or equal to 10 kev, namely

$$\langle \sigma v \rangle_{DT}\Big|_{T_i \leq 10 \, kev} = (3.8 \times 10^{-12}) T_i^{-2/3} e^{(-19.02 T_i^{-1/3})} \tag{108}$$

66

and for ion temperatures greater than 10 kev

$$\langle \sigma v \rangle_{DT} \Big|_{T_i > 10 \, kev} = (3.41 \times 10^{-14}) T_i^{-2/3} e^{\left[(3.638 T_i^{-1/3}) - (22.217 T_i^{-2/3}) \right]}$$ (109)

Values of $\langle \sigma v \rangle_{DT}$ from these functions are seen in Figure 11.

Since the original hydrogen mix is specified as 50% deuterium and 50% tritium, only the hydrogen number density is used modelling the reaction rate density as

$$RR_{DT} = \frac{n_H^2}{4} \langle \sigma v \rangle_{DT}$$ (92)

Subroutine NUHEAT

Subroutine NUHEAT calculates total neutron heating in each cell. The uncharged neutrons do not participate in Coulomb collisions as do alpha particles though neutrons can add significantly to plasma heating at high fuel densities (Ref 4:330). Most neutrons born at 14.1 Mev, however, escape unscattered for conditions of interest (Ref 4:359). Expense is minimized by using a beam attenuation model. This simplification is an economical consideration balanced by the relative importance of neutron heating.

67
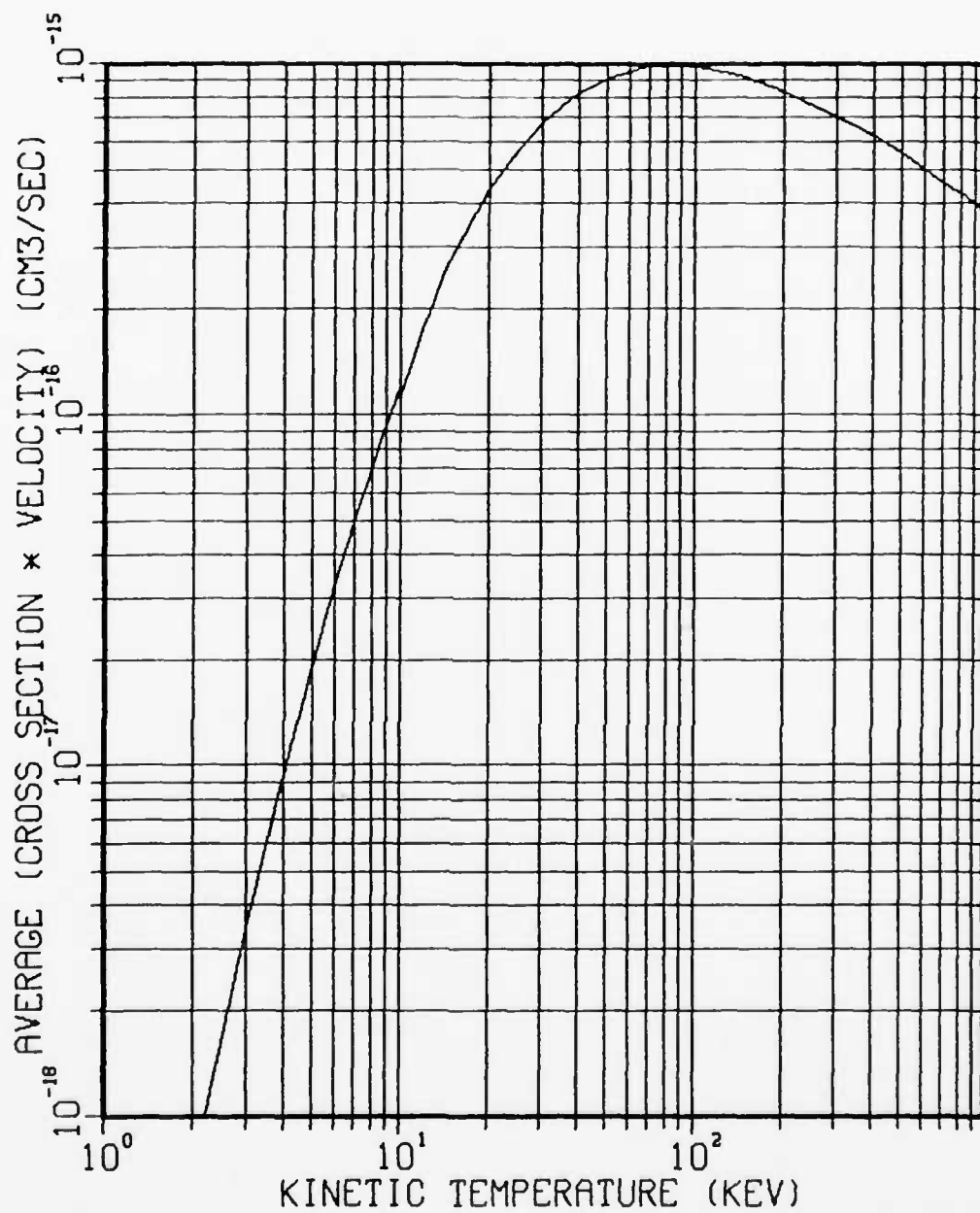
Figure 12.   Graphical Values of $\langle \sigma v \rangle_{DT}$ Used in Subroutine TBURN.

Deuterium-tritium reactions are counted during one cycle and, by assuming isotropic production of one neutron per reaction, the new neutrons are placed at the center of the microsphere and attenuated during their path length through the plasma. Using an energy of 14.1 Mev for the neutrons and a cross section of 0.8 barns for collisions with deuterium, tritium and helium nuclei, the number of interactions per cell is ascertained according to

$$\text{NUMBER OF INTERACTIONS} = (\text{TOTAL NEUTRON NUMBER}) *$$
$$(1 - \text{PROBABILITY A NEUTRON PENETRATES THE CELL}) \tag{110}$$

The probability the neutron penetrates the cell is

$$P_{PENETRATE} = e^{-(\text{NUMBER OF IONS} * \sigma_n * \text{RADIAL DISTANCE THROUGH CELL})} \tag{111}$$

and the ion number denisty is

$$n_{ION} = (n_H + n_{He})/V_J \tag{112}$$

The cross sections from BNL 325 for deuterium, tritium and helium at 14.1 Mev are shown in Table 3. Noting the values in Table 3, 0.8 barns seems low for this treatment.

The average energy per collision is multiplied by the number of interactions to attain total heating. The average energy per collision is given by

Table 3

Cross Sections for 14.1 Mev
Neutron Interactions with Selected Nuclei

Nucleus	Cross Section (barns)
Deuterium	0.93
Tritium	1.15
Helium-4	1.21

$$\text{Average Energy} = \frac{\frac{1}{2} n_H (2.35) + \frac{1}{2} n_H (1.7625) + n_{He}(1.4)}{n_H + n_{He}} \tag{113}$$

The factors of $\frac{1}{2}$ in front of the hydrogen number densities signify a 50% mix of deuterium with a 50% mix of tritium.

Finally, subprogram NUHEAT calculates the number of 3.5 Mev alpha particles that will give an equivalent amount of heating if all 3.5 Mev is deposited in the plasma. This number density of alpha particles is passed in the NUHEAT argument list to other subroutines.

Subroutine ALPHA1

The subroutine is designed to compute the energy deposited in each cell by monoenergetic 3.5 Mev alpha particles born in deuterium-tritium reactions. Also, it

70

computes the number of alpha particles produced in each zone, recomputes helium particle number density, recalculates total zone mass and adjusts ion and electron temperatures.

Subprogram ALPHA1 calls 14 other subroutines to accomplish tasks. Subprogram organization is illustrated in Figure 13.
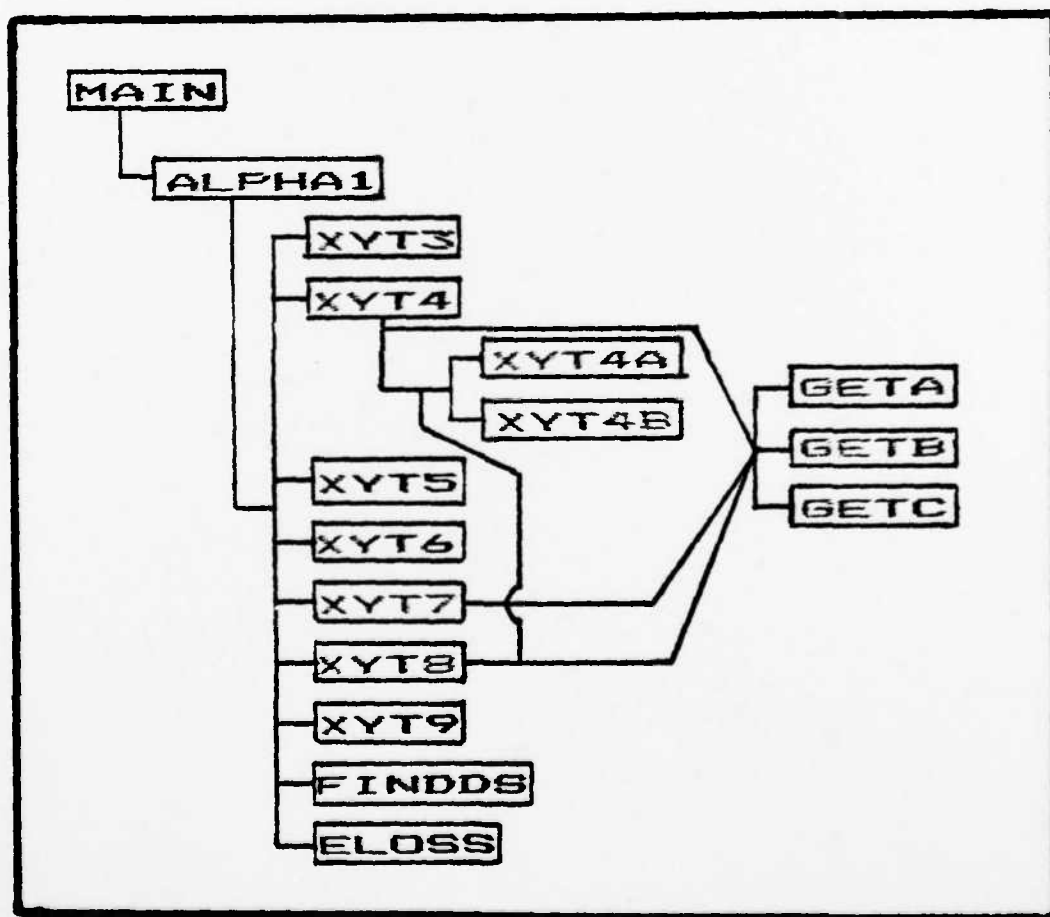
Figure 13. Subprogram ALPHA1 Substructure

The main subroutine, ALPHA1, is the location where temperatures, zone mass, alpha number densities, and heating are computed. Subroutines XYT3 through XYT9 and GETA through GETB are geometry subroutines. Subroutine FINDDS calculates an integration increment and ELOSS computes energy deposition and energy partition. A logical flag, IALPH, is set according to remaining alpha particle energy and signals particle behavior. Table 4 defines parameter IALPH. Before each call IALPH is set to 0. This value is changed by the geometry subroutines. The logical flag value ISTOP = 0 signals thermalization.

Table 4

Logical Flag IALPH Definitions

IALPH Value	Behavioral Treatment of Alpha Particle
2	Particle travels line of sight until thermalization; electron collisions dominate
1	Particle travels line of sight until ion collisions dominate; scatter becomes significant and particle stops
0	Particle stops in birth zone
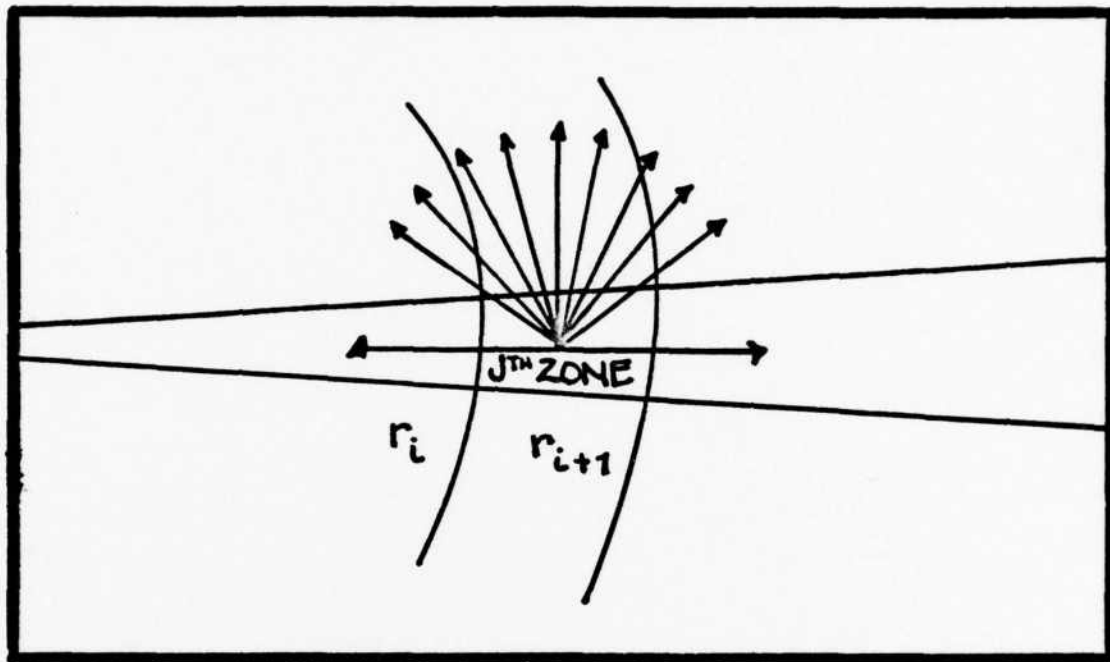
Figure 14. Angular Directions for Alpha Particle
Leaving the jth Zone

The geometry used by the coding is summarized in
Figure 14. Alpha particles are assumed to be at zone
center at birth. Angles are most finely divided at $\pi/2$.
The paths are weighted by the amount of angle considered
assuming isotropic propagation from particle birth location.
The purpose of the geometry subroutines is to find the
distance traveled within a zone, thus enabling energy
deposition modelling. The particle direction is assumed to
be unchanged by collisions with electrons. Appendix M
describes the geometry models.

The energy is deposited by subroutine ELOSS. It used
the range energy described by Fraley et al. (Ref 9:475),
namely

$$\frac{du}{ds} = -23.2\left(\frac{\rho}{\rho_o}\right)\frac{U^{\frac{1}{2}}}{T_e^{\frac{3}{2}}}\left\{1+0.17\ln\left[T_e\left(\frac{\rho_o}{\rho}\right)^{\frac{1}{2}}\right]\right\} - 0.047\left(\frac{\rho}{\rho_o}\right)\frac{1}{U}\left\{1+0.075\ln\left[T_e^{\frac{1}{2}}\left(\frac{\rho_o}{\rho}\right)^{\frac{1}{2}}U^{\frac{1}{2}}\right]\right\}$$

(114)

where

s   is distance in centimeters

ρ_0 =   0.213 grams per cubic centimeter for solid DT

and

$$U = \frac{E_\alpha}{3.5\,MeV}$$

(115)

E_α being the residual energy of the alpha particle in Mev.
The first term represents energy deposited in electrons and
the second term represents energy deposited by ions. The
fraction of energy partitioned to the ions, F_i, during alpha
particle transit is described by

$$F_i = \left[1 - \frac{(32 - 0.868\ln\rho)}{T_e}\right]^{-1}$$

(116)

74

The energy deposition rate is much higher near the end of the alpha particle path due to ionic collisions (Ref 9:475). Subroutine ELOSS models this by comparing the electron and ion terms and stopping the particle in the current zone when the ion term dominates.

The range of the alpha particle when only the electron term of Eq (114) is considered is

$$\lambda_{\alpha e} = T_e^{3/2}\left(\frac{\rho_o}{\rho}\right)0.086\left\{1+0.17\ln\left[T_e\left(\frac{\rho_o}{\rho}\right)^{1/2}\right]\right\}^{-1} \tag{117}$$

The range when only the ion term is considered is

$$\lambda_{\alpha i} = \left(\frac{\rho_o}{\rho}\right)10.65\left\{1+0.075\ln\left[T_e^{1/2}\left(\frac{\rho_o}{\rho}\right)^{1/2}\right]\right\}^{-1} \tag{118}$$

These relationships are used in subroutine FINDDS dividing λ_α by 50 to attain an integration increment. When the electron temperature is below 20 kev, $\lambda_{\alpha e}$ is used denoting electron collision domination. Above 20 kev, $\lambda_{\alpha\ i}$ is used to model ion collision domination.

This integration increment is always computed prior to energy deposition. The actual integration is accomplished in ELOSS using a 4th order Runge-Kutta method.

Subroutine HTFLX

Subroutine HTFLX calculates the energy transfer between radiation, electron and ion components. Flux continuity at cell boundaries is used in electron and radiation diffusion calculations.

Constants used include pi, electron mass and charge, the speed of light, Boltzmann's constant, the fine structure constant, and the Stephan-Boltzmann constant. Constants for coefficients of thermal conductivity, equilibration frequency, Compton coupling and bremsstrahlung coupling coefficients are grouped in front. Constant terms from the Coulomb logarithm are found in initial subroutine stages. Heat and radiation fluxes are initialized to zero.

Electron-ion energy exchange is the first process addressed. The Coulomb logarithm for electron-ion energy exchange is

$$\ln \Lambda_{ei} = \ln \left\{ \frac{3}{2e^3} \left(\frac{A}{Z} \frac{(kT_e)^3}{\pi N_a \rho} \right)^{1/2} \frac{1}{\left[Z + \left(\frac{1}{2\alpha c} \right) \left(\frac{3kT_e}{m_e} \right)^{1/2} \right]} \right\} \tag{84}$$

The minimum value of the Coulomb logarithm is set at 1. The term $A/(ZN_a\rho)$ is coded as volume per number of electrons.

Using this, the thermal conductivity is given by (Ref 26:144)

$$K_e = 20 \left(\frac{2}{\pi}\right)^{3/2} \frac{(kT_e)^{5/2}}{e^4 m_e^{1/2}} \frac{k}{Z} \frac{\epsilon \delta_T}{\ln \Lambda_{ei}} \qquad (19)$$

The factor ϵ is due to the secondary electric fields origin-
ated by the flow of charged particles. The factor δ_T is
dependent on the Z of the material and is included to model
a real gas vice the Lorentz gas on which the derivation of
Eq (19) is based (Ref 26:144). The product $\epsilon\delta_T$ is modelled

$$\epsilon \delta_T = \frac{0.43 Z}{(3.44 + Z + 0.26 \ln[Z])} \qquad (83)$$

The equilibration frequency, $1/t_{eq}$, is

$$\nu_{eq} = \frac{8(2\pi m_e)^{1/2} e^4 N_a^2}{3} \left(\frac{Z}{A}\right)^2 \ln \Lambda_{ei} \frac{\rho}{(kT_e)^{3/2}} \qquad (82)$$

The quantity

$$\left(\frac{Z}{A}\right)^2 N_a^2 \rho = \frac{N_{ej}^2}{A V_j} \qquad (119)$$

where N_{ej} is the number of electrons in zone j.

77

It is so coded. The Z's used are net charge N_e/N_i . Array values for all but the last zone are averaged over two zones. Array values for the last zone are used without average.

A term of $(1 - \frac{3}{2} \frac{T_i}{T_e} \frac{m_e}{m_i})$ is included in Reference 9 for ν_{eq} . It is not used in this study, as it will be insignificant if T_i and T_e are within an order of magnitude. These terms are discussed in Chapter II and Appendix N.

The derivative for flux calculations is

$$\frac{dT_e}{dr} = \frac{T_e^{J+2} - T_e^{J}}{r_{J+2} - r_{J}} \tag{120}$$

except for the final two zones where

$$\frac{dT_e}{dr} = \frac{T_e^{J+1} - T_e^{J}}{r_{J+1} - r_{J}} \tag{121}$$

The heat flux is then

$$F_{LUX} = r^2 K_e \frac{dT_e}{dr} \tag{122}$$

The updated electron temperature comes from a combination of ion electron energy transfer and electron heat conduction. This is

$$\frac{dT_e}{dt} = \frac{8\pi}{3kN_e}\left(r^2 K_e \frac{dT_e}{dr}\right) + \nu_{eq}\left(T_i - T_e\right) \tag{123}$$

This equation is discussed in Appendix N. The ion temperature is then

$$\frac{dT_i}{dt} = -Z \nu_{eq}\left(T_i - T_e\right) \tag{124}$$

where again Z is net charge.

The electrons are much lighter than the ions and so conduct much more energy through diffusion than do ions. Consequently, ion heat conduction is not considered.

Radiation-electron energy transfer is treated using a Rosseland mean free path

$$\lambda_r = \frac{1.3\, T_e^{7/2}}{\rho^2} \tag{90}$$

from Fraley et al. (Ref 9:476). A radiation diffusion coefficient

$$K_r = \frac{16\sigma}{3} \lambda_r T_r^3 \tag{91}$$

is then evaluated. Radiation flux is then calculated by

$$RFLUX = r^2 K_r \frac{dT_r}{dr} \tag{125}$$

79

where the spatial derivative of the radiation temperature
is treated similarly to the spatial derivative of the
electron temperature.

A bremsstrahlung Gaunt factor is computed using

$$G(\gamma) = \frac{\pi^2}{4} - \left(\frac{\pi^2}{4} - 1\right) e^{-(0.2\gamma)} \tag{126}$$

where $\gamma = T_r/T_e$. The Gaunt factor for bremsstrahlung
processes is discussed in Appendix G. This Gaunt factor
is used in computing the bremsstrahlung coupling coefficient
which is

$$A_{er}^{\beta} = \frac{32}{3} \left(\frac{2}{\pi m_e}\right)^{1/2} \frac{e^4 N_a^2}{\hbar c} k \left(\frac{Z^2}{A^2}\right) \frac{\rho^2 Z}{(kT_e)^{1/2}} r_o \, G(\gamma) \tag{86}$$

The Compton coupling coefficient is denoted

$$A_{er}^{c} = \frac{128}{3} \pi \sigma \frac{e^2}{(m_e c^2)^2} N_a \left(\frac{Z}{A}\right) r_o \rho \, T_r^4 \tag{87}$$

These are added to arrive at the complete coupling coeffi-
cient or

$$A_{er} = A_{er}^{\beta} + A_{er}^{c} \tag{85}$$

These coupling coefficients are discussed in Chapter II
and also in Appendices F and I.

A
806

‖ 1.0   ▪ 2.8   ▪ 2.5
         ▪ 3.2   ▪ 2.2
         ▪ 3.6

‖ 1.1   ▪ 4.0   ‖ 2.0

                  ‖ 1.8

‖ 1.25   ‖ 1.4   ‖ 1.6
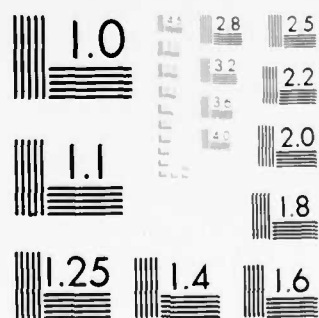
MICROCOPY RESOLUTION TEST CHART
NATIONAL BUREAU OF STANDARDS 1963-A

Specific heats are required and are

$$C_{\nu e} = \frac{3}{2} \frac{k Z}{m_i}$$ (127)

and

$$C_{\nu r} = \frac{16 \sigma T_r^3}{c \rho}$$ (128)

The radiation temperature can then be updated using

$$\frac{dT_r}{dt} = \frac{A_{er}}{C_{\nu r}} (T_e - T_i) + \frac{4\pi}{\rho C_{\nu r} V_J} \left(r^2 K_r \frac{dT_r}{dt} \right)$$ (129)

This equation is discussed in Appendix O. The electron temperature is updated using

$$\frac{dT_e}{dt} = - \frac{A_{er}^{\rho}}{C_{\nu e}} (T_e - T_i)$$ (130)

Because of the mass difference between ions and electrons, radiation interaction with electrons is highly preferential. Radiation-ion energy exchange is, therefore, not considered.

Subroutine OUTPUT

This subroutine can be called at timely locations to provide a variety of information. A summary of the data printed on hard copy is given in Tables 5 and 6.

Table 5

Cyclic Data Printed by Subroutine OUTPUT

Parameter	Dimension
Cycle Number	Pure Integer Number
Total Time	Nanoseconds
Time Step	Picoseconds
Input Energy	Kilojoules
Output Energy	Kilojoules

Table 6

Zone Data for the Given Cycle Number
Printed by Subroutine OUTPUT

Parameter	Dimension
Zone Number	Pure Integer Number
Radius	Millimeters
Cell Wall Velocity	Millimeters per nanosecond
Reactions	Reactions per time step
Density	Density times normal
Electron Temperature	kev
Ion Temperature	kev
Radiation Temperature	kev
Output	Joules
Heating	Joules
Neutron Fluence	-----

The cyclic information is printed at the top of the page followed by zone information in columns. Neutron fluence is a parameter of interest currently not computed in program MOXNEX. Conversions are made in subroutine OUTPUT to attain the desired parameter dimensions.

IV. Validation Arguments

Introduction

Code validation for the MOXNEX program is a goal that must be satisfied to enable its use as a vehicle for further study. Because the code is not yet running, comparison with published data is not possible. Steps were taken, however, to analyze specific analytic cases and to validate program modules. The efforts to verify the MOXNEX coding and, in particular, the HYDRO and HTFLX subroutines are discussed in the following paragraphs.

Analytic Cases

The radiation-electron energy transfer coefficient $A_{er}^{\prime}$ used in subroutine HTFLX is discussed in Chapter III. Chapter III also includes a comparison between the radiation-electron energy transfer coefficients used for this study and those coefficients used in Reference 9. Chapter III further points out that the coefficient used by Reference 9 is dimensionally incorrect. It also notes the MOXNEX bremsstrahlung and Compton coupling coefficients differ from those used in Reference 9 by a factor of ρr_0 . This means the radiation-electron energy transfer coefficients used in the two studies differ by a factor of $r_0 = 2.8178 \times 10^{-13}$ centimeters (Ref 3:501), or a difference of

almost 13 orders of magnitude. A difference of this size
in the radiation-electron energy transfer coefficient should
make a substantial difference in the results attained from
the two codes and is further discussed in Chapter V.
Critical examination of the processes that are included in
the radiation-electron energy transfer coefficient, then,
is central to this study in order to confirm the value of
this coefficient. Appendices include derivations of the
radiation-electron energy transfer coefficient components,
the bremsstrahlung coupling coefficient and the Compton
coupling coefficient. The locations in appendices of
derivations of the bremsstrahlung and Compton coupling
coefficients, along with other derivations and analytic
verifications used directly in MOXNEX coding, are summarized
in Table 7.

In many cases supporting calculations for derivations
are presented in prior appendices. Cross section derivations
for short and long range Coulomb collisions are derived in
Appendix C. Appendix E discusses cross sections for
bremsstrahlung and inverse bremsstrahlung collisions which
support bremsstrahlung coupling coefficient calculations.
Bremsstrahlung Gaunt factor modelling is addressed in
Appendix G. The enhancement factor for bosons used in both
bremsstrahlung and Compton calculations is derived in
Appendix L. The average energy exchange during a Compton
collision is discussed in Appendix H. The geometrical models

85

Table 7

Analytic Verifications of Specific Terms and Equations

Used for MOXNFX Coding

Appendix	Derivation	Subroutine Where Used	Page
F	Bremsstrahlung Process Coupling Coefficient	HTFLX	
F	Bremsstrahlung Gaunt Factor	HTFLX	
I	Compton Process Coupling Coefficient	HTFLX	
J	Lagrangian Energy Equation	HYDRO	
K	Equivalent Fermi Electron Temperature	HYDRO	
L	Radiation Temperature Adiabatic Update Equation	HYDRO	
N	HTFLX Electron Temperature Update Equation	HTFLX	
O	HTFLX Radiation Temperature Update Equation	HTFLX	

used for subroutine ALPHA1 are presented in Appendix M.
These derivations and mathematical discussions are presented
to support presentations in Chapters II and III, but also
to provide an analytical check on the self consistency of
the coupled rate equations.

An error was discovered in the original HTFLX differencing
scheme for temperature update equations that required cor-
rection. Temperature update equations in subroutine HTFLX

86

use the first derivative, dT/dr, where dT denotes
either the electron or radiation species temperature. This
temperature gradient is approximated by the quotient of
finite differences between cells. The temperatures used
for this finite difference must be the temperatures at
the time of the subroutine call. The temperature differ-
ences in the original equations used already updated temper-
atures in the outer 3 cells yielding an erroneous gradient.
A new differencing scheme is now employed to ensure that
the gradient is computed in all cells using the temperature
values at the time of the subroutine call.

Other discrepancies were found in the signs of the
temperature update equations in subroutine HTFLX. These
sign errors were changed ensuring that energy flows in
the correct direction.

Quasistatic Equilibrium Study for Subroutine HYDRO

Subroutine HYDRO updates species temperatures based
only on adiabatic changes. No energy transfer mechanisms
are modelled in the subroutine. Consequently, species
temperatures should be updated only by cell expansion or
contraction independent of differences in temperatures
between species. If the species temperatures are nonzero
and approximately the same between cells within the species
inside the microsphere, cell expansion should be most
rapid in the outer cells since the species pressures outside

87

of the last cell are very close to zero (all species temperatures outside of the last cell are initialized to $1. \times 10^{-7}$ kev). After a time period short compared to the time required for microsphere kinetic disassembly and in the absence of other processes, the inner cells should demonstrate no temperature changes or energy exchanges and the outer shells should have decreased temperatures due to expansion.

These phenomena were tested and observed by calling subroutine HYDRO consecutively 100 times after initializing species temperatures at equilibrium conditions and then at various non-equilibrium conditions. Using 40 cells, no temperature changes were observed in the inner 34 cells in any calculation and temperatures lower than initial temperatures were seen in at least the outer 3 cells in all species in all calculations. Table 8 lists the initial temperatures and final temperatures in cell 40 and the total time for the run for the 4 runs completed. The reason that total time on the second run is different from the other three is that a different time step was used.

Table 8

Quasiequilibrium Studies for Subroutine HYDRO

(100 Iterations, All Temperatures in kev)

Run No.	Electron Temp		Ion Temp		Radiation Temp		
	Initial (All Cells)	Final (Cell 40)	Initial (All Cells)	Final (Cell 40)	Initial (All Cells)	Final (Cell 40)	TOTAL TIME
1	6	2.770	6	2.770	6	4.954	0.0808 nsec
2	6	2.647	3	1.323	6	4.898	0.1 nsec
3	6	2.796	6	2.796	3	2.483	0.0808 nsec
4	3	1.505	6	3.010	6	5.056	0.0808 nsec

Point Explosion Calculation for Subroutine HYDRO

An analytic solution, due to Sedov (Ref 25) is available for pressure at a shock wave front resulting from an explosion at a dimensionless point (Ref 25:238-240). This solution for spherical geometry is

$$P_s = \frac{P_o}{\gamma+1} \frac{2\gamma - (\gamma-1)g}{g} \tag{131}$$

where

$$g = \gamma \left(\frac{5}{2}\right)^2 \alpha \ell^3 \tag{132}$$

where

$$\lambda = \frac{r_s}{\left(E_0/P_0\right)^{1/3}} \tag{133}$$

and

$$\alpha = E_0/E_c \tag{134}$$

In these equations

P_0 is ambient pressure

P_s is pressure at the shock front

γ is the ratio of specific heats

r_s is the distance of the shock front from the
sphere center

E_c is the energy of the explosion charge

E_0 = E_c

The constant α is a function of γ and is approximately
0.84 for γ = 1.4 and 0.48 for γ = 1.67 (Ref 25:231-240).

A hydrodynamics scheme may be validated by initiating
an explosion obtaining values for pressure at the shock
front and shock front distance from the sphere center, and
comparing these values with values obtained from the analytic
solution. A dimensionless point can only be approximated
in a hydrodynamics scheme by placing the charge energy in

the smallest possible volume. This should lead to error
in the form of small random deviations from the analytic
solution.

The calculations were done using $\gamma = 1.67$ and compared
to the Sedov solution curve (Ref 27:142) for $\gamma = 1.4$. The
slope and shpae of this curve was duplicated in each calcu-
lation. The differences in the ratios of specific heats,
γ, and the scaling of E_0 with γ is felt to be the
reason that actual coincidence was not attained. A solution
for $\gamma = 1.67$ can be constructed using Eqs (131) through
(134). It is felt that coincidence with such a solution
would be attained with a point explosion calculation in
subroutine HYDRO. These calculations were not pursued,
however, in view of limited time and resources.

V.   Recommendations

Code Completion

Without code completion, the work presented is largely inconclusive. Code completion and subsequent comparison with published data is central to any further code development or modification.

Time Step Selection

Currently, the time step used for the entire MOXNEX program is determined in subroutine HYDRO. As noted in Chapter III, this time step is defined by a fraction (less than or equal to 1/2) of the time required for a shock wave to travel across the thinnest microsphere zone. Using this time step, erratic values of the temperature gradient are observed in subroutine HTFLX resulting in temperature changes of as much as three orders of magnitude in electron temperature during one iteration. These dramatic variations in the temperature gradient, as well as the resulting electron temperatures, are uncharacteristic of inertially confined fusion microspheres (Refs 4, 6).

Consideration may be given to redefining the time step selection method to obtain time step values yielding gradient values compatible with HTFLX equations. One method that could be employed would be modifying the program to allow the electron temperature and/or the radiation temperature

update modules to define the time step for the entire program. The first derivative, dT/dr , could be iterated until a favorable value of dt is attained. A favorable value of dt would be the largest value of dt that yielded well behaved temperature changes between cells. This value of dt could then be used as the time step for the entire program. This process, however, may yield a very small time step. This time step may result in stable difference equations in sub-routine HTFLX, but also insignificant changes in other sub-routines. For instance, cell walls in subroutine HYDRO may move so little that their movement is barely consequential so that an increased number of iterations is required for the overall run. A very small time step, then, may greatly increase the total number of computer operations required per run and inefficiently treat the overall problem.

Efficiency might be regained by letting the HTFLX and HYDRO subroutines proceed at separate time steps character-istic of the processes modelled. If the characteristic time step for the HTFLX subroutine is significantly smaller than the time step computed in the HYDRO subroutine, HTFLX could be sub-cycled independently from the rest of the program. When total time over many HTFLX iterations is equal to the HYDRO time step, the HTFLX subroutine can be interfaced into the rest of the program. This approach may provide stable equations throughout the MOXNEX code and still achieve a minimum of computer operations.

93

Literature Comparison

Once the code is completed, validation by comparison
with published literature should follow. Brueckner and
Jorna give graphical data of ion temperature versus micro-
sphere radius at different times for 40 micrometer deuterium-
tritium microsphere with a uniform initial density of 600
grams per cubic centimeter and initial uniform electron and
ion temperatures of 5 kev in the center six micrometers
(Ref 4:361) to which MOXNEX results may be compared. This
data is seen in Figure 15.   The MOXNEX model incorporates
many features of the Brueckner-Jorna code. The thermo-
nuclear reaction rate modelling for MOXNEX is taken directly
from the Brueckner-Jorna coding description (Ref 4:358).
Some differences, however, exist in the equations used
for charged particle and neutron heating, radiative transfer
and the equation of state. A tabular Fermi-Thomas equation
of state is used for the electron species (Ref 4:357) which
should model electron energy much more closely than does the
MOXNEX coding which accounts for electron degeneracy only at
low temperatures and uses a perfect gas law as the equation
of state. Still, similarities in the processes modelled
lead to anticipation the MOXNEX code will duplicate the
curves seen on page 361 of Reference 4 by much less than an
order of magnitude for the same input parameters.
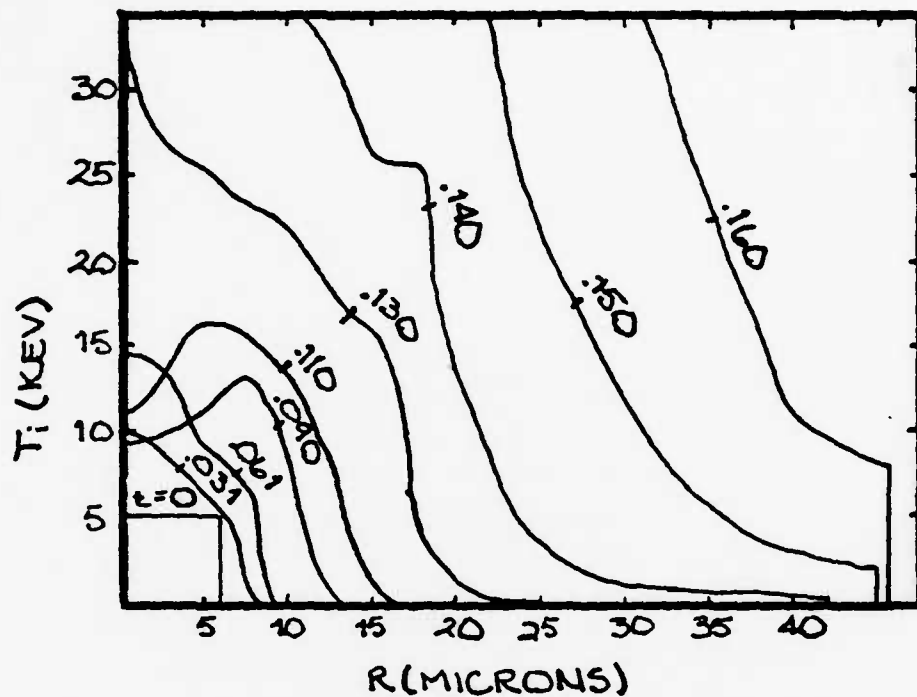
Figure 15. The propagation of the burning front in
initially uniformly compressed DT. The initial
density is 600 gm/cm³ and the initial radius
40 μm. The central region initially heated to
5 kev has a 6 μm radius. The curves are labeled
by the time in units of 10^{-10} sec (Ref 4:361).

The radiation temperature used by Brueckner and Jorna are not given for the above example. The radiation temperature in the MOXNEX program might be initialized at 1 kev following the lead of Reference 9, with the hope of duplicating the Brueckner-Jorna data.

A second basis paper, written by Gary S. Fraley and others, gives extensive data for numerous microsphere sizes, densities, and temperatures on pages 479 through 483 of Reference 9. The MOXNEX coding of alpha particle heating is patterned after equations appearing in this paper. The coding of the energy transfer processes in MOXNEX for species temperature update in the three temperature model closely parallel the equations of Appendix B of Reference 9. A tabular Fermi-Thomas-Dirac equation of state is used in the Fraley code (Ref 9:474), so once again differences may be anticipated when MOXNEX results are compared with Fraley code results due to differences in the equation of state.

A large difference exists, however, between the MOXNEX code and the Fraley code in the values of the radiation-electron energy transfer coefficient. This difference, discussed in Chapters III and IV, may result in a much different energy partitioning among species between the two codes. This energy partitioning difference will affect many other areas which are temperature dependent such as thermonuclear reaction rates and species pressures. The disagreement should propagate and magnify as the codes

progress in time. The degree of similarity between the MOXNEX
code and the Fraley code hinges on the relative importance
of the radiation-electron energy transfer process. This
process may be dominated numerically by thermonuclear, Cou-
lombic, or other processes in both codes in which case the
MOXNEX results should closely approximate the Fraley results
because of the similarities in the processes modelled and
similarities in the equations. Much better than order of
magnitude agreement may be seen.

If, on the other hand, other processes do not numerically
dominate the radiation-electron energy transfer process,
correlation between the MOXNEX code and the Fraley code
should be hard to recognize. Radiation-electron energy
transfer should be a significant process (Refs 4, 10, 18, 26).
Doubt exists whether this process is so totally dominated that
a coefficient difference of almost 13 orders of magnitude
will be inconsequential.

Nevertheless, Reference 9 reports agreement with other
published literature (Clarke, J.S., H.N. Fisher, and R.J.
Mason. "Laser-Driven Implosion of Spherical DT Targets to
Thermonuclear Burn Conditions," Physical Review Letters, 30
(2): 89-92, (January 1973).) in total microsphere energy
yield. The three temperature code used in this paper is the
basis for the three temperature model used for the Fraley
code (Ref 9:474). Both Reference 9 and the paper by Clarke
and others were written at the Los Alamos Scientific Laboratory

between 1972 and mid-1973. In fact, one author, R.J. Mason, is a common author for both papers. The possibility exists that the agreement in results is at least in part a consequence of the similarity in their coding. Further, the possibility exists that the radiation-electron energy transfer coefficient used in both codes is the same.

With this background in mind, the Brueckner-Jorna code results should be considered as the primary comparison standard. Differences in results between the MOXNEX code and the Fraley code might be explained by the difference in the radiation-electron energy transfer coefficient. Results from both codes are computed using one dimensional, spherical Lagrangian coding.

Another inertial confinement fusion code to which MOXNEX results could be compared are the LASNEX code results from the Lawrence Livermore National Laboratory. LASNEX models sophisticated physics in a large and expensive computer simulation to support experimental laser fusion studies at Lawrence Livermore National Laboratory. Some LASNEX code results might be attained from recent volumes of the Lawrence Livermore National Laboratory laser program annual reports. Additionally, these annual reports contain information concerning experimental laser fusion. A strong validation argument is made if MOXNEX results agree with LASNEX results or experimental results for total yield, disassembly times,

neutron fluence, and species temperature profiles in time
within an order of magnitude.

Driver Incorporation

A final recommendation is to incorporate an energy
delivery mechanism or driver into the MOXNEX code. Driver
incorporation will add completeness to the MOXNEX code and
make it more comparable to other studies of its type, for
instance, the Brueckner-Jorna code. Study may be augmented
in many additional areas such as laser-plasma coupling,
particle beam-plasma coupling, and microsphere design by
using and/or further developing the MOXNEX code. Procedures
outlining driver incorporation to a fusion microsphere are
included in the paper by Brueckner and Jorna (Ref 4).
Additional modelling information can be found in recent
laser program annual reports by the Lawrence Livermore
National Laboratory.

Bibliography

1. Abramowitz, Milton and Irene A. Stegun. Handbook of Mathematical Functions. New York: Dover Publications, Inc., 1965.

2. Beiser, Arthur. Perspectives on Modern Physics. New York: McGraw-Hill, 1969.

3. Bond, John W. Jr., Kenneth M. Watson and Jasper A. Welch, Jr. Atomic Theory of Gas Dynamics. Reading MA: Addison-Wesley, 1965.

4. Brueckner, Keith A. and Siebe Jorna. "Laser-Driven Fusion," Reviews of Modern Physics, 46 (2): 325-367 (April 1974).

5. Chemical Rubber Company. CRC Handbook of Chemistry and Physics, 60th Edition. Boca Raton FL: CRC Press, 1980.

6. Chen, Francis F. Introduction to Plasma Physics. New York: Plenum Press, 1974.

7. Eisberg, Robert and Robert Resnick. Quantum Physics. New York: John Wiley & Sons, Inc., 1974.

8. Evans, Robley D. The Atomic Nucleus. New York: McGraw-Hill, 1955.

9. Fraley, G.S., E.J. Linnebur, R.J. Mason, and R.L. Morse. "Thermonuclear Burn Characteristics of Compressed Deuterium-Tritium Microspheres," The Physics of Fluids, 17 (2): 474-489 (February 1974).

10. Glasstone, Samuel and Ralph H. Lovberg. Controlled Thermonuclear Reactions. Huntington NY: Robert E. Krieger Publishing Company, 1975.

11. Gradshteyn, I.S. and I.M. Ryzhik. Table of Integrals, Series, and Products. New York: Academic Press, 1965.

12. Harlow, Francis H. and Anthony A. Amsden. Fluid Dynamics. LA 4700. Los Alamos NM: Los Alamos Scientific Laboratory of the University of California, June 1971.

13. Hornbeck, Robert W. Numerical Methods. New York: Quantum Publishers, 1975.

14. Jackson, John David. Classical Electrodynamics.
     New York: John Wiley & Sons, Inc., 1962.

15. Knolls Atomic Power Laboratory. Chart of the Nuclides.
     San Jose CA: General Electric, 1977.

16. Martin, Charles R. Private Communication. Wright-
     Patterson AFB OH: School of Engineering, Department
     of Physics, Air Force Institute of Technology,
     December 1981.

17. Mitchner, M. and Charles H. Kruger, Jr. Partially
     Ionized Gases. New York: John Wiley & Sons, Inc.,
     1973.

18. Motz, H. The Physics of Laser Fusion. New York:
     Academic Press, 1979.

19. National Energy Plan II. Washington DC: U.S. Depart-
     ment of Energy, May 1979.

20. "News: State and Society; Budgets for 1981 and 1982,"
     Physics Today. New York: American Institute of Physics,
     April 1981.

21. Nickel, George H. Private Communication. Wright-
     Patterson AFB OH: School of Engineering, Department
     of Physics, Air Force Institute of Technology.

22. Nickel, George H. Unpublished Notes. Wright-Patterson
     AFB OH: School of Engineering, Department of Physics,
     Air Force Institute of Technology, 1981.

23. O'Shea, Donald C., W. Russel Callen and William T. Rhodes.
     Introduction to Lasers and Their Applications. Reading
     MA: Addison-Wesley, 1978.

24. Reif, F. Fundamentals of Statistical and Thermal Physics.
     New York: McGraw-Hill, 1965.

25. Sedov, L.I. Similarity and Dimensional Methods in
     Mechanics. New York: Academic Press, 1959.

26. Spitzer, Lyman, Jr. Physics of Fully Ionized Gases.
     New York: Interscience, 1962.

27. Stamm, Michael Richard. The Formulation, Propagation
     and Structure of Laser Supported Detonation Waves and
     Their Effect on Laser-Target Interactions. PhD Disser-
     tation, Lincoln NE: University of Nebraska, December
     1976.

28. Zel'Dovich Ya. B. and Yu. P. Raizer. Physics of
     Shock Waves and High-Temperature Hydrodynamic Phenomena.
     New York: Academic Press, Inc., 1966.

APPENDIX A

Program Listing

```
100=        PROGRAM MOYNEX
110=        DIMENSION R(101),AMASS(101),VEL(101),V(101),
120=        DIMENSION H(101),HE(101),PUSH(101),ELEC(101),TE(101),
130=      * TI(101),TR(101),REAC(101),THEAC(101),FR(101),FLU(101)
140=        DIMENSION RELRHO(101),THEAT(101),DELV(101),                ,ALPH
A(101)
150=C******************************************
160=C     HYDRODYNAMICS VARIABLES---------
170=C       R(I) IS RADIUS OF ITH ZONE IN CM
180=C       AMASS(I) IS TOTAL MASS OF ITH ZONE IN GRAMS
190=C       P(I) IS TOTAL PRESSURE IN ITH ZONE IN ERG/CM3
200=C       Q(I) IS ARTIFICIAL VISCOSITY IN ITH ZONE IN ERG/CM3
210=C       VEL(I) IS VELOCITY OF ITH ZONE IN CM/SEC
220=C       V(I) IS VOLUME OF ITH ZONE IN CM3
230=C******************************************
240=C     INDIVIDUAL PARTICLE VARIABLES----------
250=C       H(I) IS TOTAL NUMBER OF D+T ATOMS IS ITH ZONE (50-50 MIX)
260=C       HE(I) IS TOTAL NUMBER OF ALPHAS IN ITH ZONE
270=C       PUSH(I) IS TOTAL NUMBER OF PUSHER "ATOMS" IN ITH ZONE
280=C       ELEC(I) IS TOTAL NUMBER OF ELECTRONS IN ITH ZONE (NEUTRAL)
290=C       TE(I) IS ELECTRON TEMP IN ITH ZONE IN KEV
300=C       TI(I) IS ION TEMP IN ITH ZONE IN KEV
310=C       TR(I) IS RADIATION TEMP IN ITH ZONE IN KEV
320=C       REAC(I) IS TOTAL NUMBER OF REACTIONS IN ITH ZONE THIS DT
330=C******************************************
340=C     SINGLE VARIABLES------------
350=C       DT IS TIME STEP IN SECONDS
360=C       NSPACE IS NUMBER OF ZONES IN ENTIRE PROBLEM
370=C       NFUEL IS NUMBER OF LAST FUEL ZONE
380=C       ZPUSH IS AVERAGE ATOMIC NUMBER OF PUSHER "ATOMS"
390=C******************************************
400=C     TASKS--------------
410=C       SET INITIAL CONDITIONS
420=        CALL GDATA          (R,DT,TE,TI,TR,NSPACE,NFUEL,TIME,H,HE,PUSH
,CYCLE,
430=      1   ZPUSH,FMASS,DMASS,TMASS,AMASS,ELEC,V,HEMASS,DELV,FR,HD,P
USHD,
440=      *   HMASS,DRVENG,TREAC,THEAT,VEL,ALPHA)
450=        DRENG = 0.0
460=        DO 10 I=1,NSPACE
470=        REAC(I) = 0.0
480=        RELRHO(I) = 1.
490=     10 FLU(I) = 0.0
500=        CALL        OUTPUT(R,CYCLE,TIME,DT,DRENG,NFUEL,NSPACE,VEL,RHO
Z,FMASS
510=      %,ZPUSH,ELEC,TE,TI,TR,REAC,TREAC,THEAT,FLU,RELRHO,H,HE,PUSH,
DRVENG)
520=C     UPDATE HYDRO VARIABLES, PARTICLE VARIABLES BY HYDRO (WADE/W
EBER)
530=        CALL HYDRO          (R,VEL,DT,TR,TI,TE,NSPACE,TIME,CYCLE,IBURN,
RELRHO,
540=      1 H,HE,ELEC,PUSH,AMASS,FMASS,DMASS,TMASS,HEMASS,FR,DELV,HD,P
USHD,
550=      2  NFUEL,V)
```

104

```
    560=       CALL        OUTPUT(R.CYCLE.TIME.DT.DRENG.NFUEL.NSPACE.VEL.RHO
Z.PMASS
    570=       %.ZPUSH.ELEC.TE.TI.TR.REAC.TREAC.THEAT.FLU.RELRHO.H.HE.PUSH.
DRVENG)
    580=C       COMPUTE THERMONUCLEAR REACTION RATES. REMOVE DT MASS
    590=       CALL        TNBURN(NSPACE.NFUEL.DT.V.H.TI.REAC.TREAC.IBURN)
    600=       CALL        OUTPUT(R.CYCLE.TIME.DT.DRENG.NFUEL.NSPACE.VEL.RHO
Z.PMASS
    610=       %.ZPUSH.ELEC.TE.TI.TR.REAC.TREAC.THEAT.FLU.RELRHO.H.HE.PUSH.
DRVENG)
    620=C       DEPOSIT NEUTRON ENERGY. COMPUTE NEUTRON OUTPUT
    630=       CALL        NEUHEAT(NSPACE.  R.REAC.ALPHA.THEAT.V.H.HE)
    640=       CALL        OUTPUT(R.CYCLE.TIME.DT.DRENG.NFUEL.NSPACE.VEL.RHO
Z.PMASS
    650=       %.ZPUSH.ELEC.TE.TI.TR.REAC.TREAC.THEAT.FLU.RELRHO.H.HE.PUSH.
DRVENG)
    660=C       DEPOSIT ALPHA ENERGY. ADD ALPHA MASS
    670=       IALPH = 0
    680=       CALL ALPHA1(R.AMASS.V.H.HE.PUSH.ELEC.TE.TI.REAC.DT.NSPACE.
    690=       +            NFUEL.ZPUSH.PMASS.IALPH.THEAT.ALPHA)
    700=       CALL        OUTPUT(R.CYCLE.TIME.DT.DRENG.NFUEL.NSPACE.VEL.RHO
Z.PMASS
    710=       %.ZPUSH.ELEC.TE.TI.TR.REAC.TREAC.THEAT.FLU.RELRHO.H.HE.PUSH.
DRVENG)
    720=C       CALCULATE RADIATION ENERGY. HEAT CONDUCTION
    730=       CALL        HTFLX(R.TE.TI.TR.ELEC.V.H.HE.PUSH.AMASS.NSPACE.H
MASS.
    740=       *   HEMASS.PMASS.DT.FR)
    750=       CALL        OUTPUT(R.CYCLE.TIME.DT.DRENG.NFUEL.NSPACE.VEL.RHO
Z.PMASS
    760=       %.ZPUSH.ELEC.TE.TI.TR.REAC.TREAC.THEAT.FLU.RELRHO.H.HE.PUSH.
DRVENG)
    770=C*********************************************************
    780=       END
    790=C*********************************************************
    800=       SUBROUTINE GDATA (R.DT.TE.TI.TR.NSPACE.NFUEL.TIME.H.HE.PUSH
.CYCLE.
..LIST 800.2500

    800=       SUBROUTINE GDATA (R.DT.TE.TI.TR.NSPACE.NFUEL.TIME.H.HE.PUSH
.CYCLE.
    810=       1    ZPUSH.PMASS.DMASS.TMASS.AMASS.ELEC.V.HEMASE.DELV.FR.HD.P
USHD.
    820=       *    HMASS.DRVENG.TREAC.THEAT.VEL.ALPHA)
    830=       DIMENSION R(101).TE(101).TI(101).TR(101).H(101).HE(101).PUS
H(101).
    840=       1    ELEC(101).AMASS(101).DELV(101).FR(101).V(101).VEL(101)
    850=       DIMENSION DRVENG(101).TREAC(101).THEAT(101).ALPHA(101)
    860=       INTEGER CYCLE
    870=       PIE = 4.*ATAN(1.)
    880=C   SET MASSES OF COMPONENTS (GMS)
    890=       DMASS = 3.34E-24
    900=       TMASS = 5.02E-24
    910=       HMASS = (DMASS + TMASS) / 2.
    920=       HEMASS=6.64E-24
```

105

```
930=       AMASS=10.6E-24
940=C   INITIALIZE TIME AND CYCLE # TO ZERO
950=       TIME = 0.0
960=       CYCLE = 0
970=C   SET NUMBER OF CELLS
980=       NSPACE=40
990=       NSPP1=NSPACE+1
1000=C   SET HYDROGEN DENSITY (GM/CM3)
1010=       HD=600.
1020=C   SET ZONE WIDTH (CM) AND 1ST RM3=0.
1030=       DR=.0001
1040=       RM3=0.
1050=C   MINIMUM TIME STEP
1060=       DT=1.E-12
1070=C   FIND AVERAGE Z OF PUSHER ATOMS
1080=       ZPUSH=SQRT(37.)
1090=       DO 1 N=1,NSPP1
1100=C   COMPUTE WALL POSITIONS (CM) AND VOLUMES (CM3)
1110=       R(N) = DR*(N-1)
1120=       RP3 = (R(N)+DR)**3
1130=       V(N) = 4.*PIE*(RP3-RM3)/3.
1140=       RM3 = RP3
1150=C   COMPUTE MASS IN CELL (GM)
1160=       AMASS(N) = HD*V(N)
1170=C   COMPUTE NUMBER OF PARTICLES
1180=       H(N) = AMASS(N)/HMASS
1190=       HE(N) = 0.0
1200=       PUSH(N) = 0.0
1210=       ELEC(N) = H(N)
1220=       ALPHA(N) = 0.0
1230=C   SET VELOCITIES (CM/SEC) AND VOLUME CHANGES (CM3)
1240=       VEL(N) = 0.0
1250=       DELV(N)=0
1260=C   INITIALIZE RADIATION PRESSURE
1270=       PR(N)=0.
1280=C   SET CELL OUTPUT (ERGS), REACTIONS, AND CELL HEATING (ERGS)
1290=       DRVENG(N)=0.
1300=       TREAC(N)=0.
1310=       THEAT(N)=0.
1320=C   AMBIENT TEMPERATURE FOR CELLS WITH NO ENERGY INPUT (KEV)
1330=       TE(N) = 1.E-7
1340=       TI(N) = 1.E-7
1350=       TR(N) = 1.E-7
1360=     1 THEAT(N) = 0.0
1370=C   YOU HAVE TO HAVE MORE R-VALUES THAN OTHER VARIABLES,
1380=C    SO THAT THERE IS A VALUE OF R(N+1) FOR THE LAST ZONE
1390=C
1400=C   SET NUMBER OF FUEL CELLS
1410=       NFUEL = NSPACE
1420=C   INPUT ENERGY (KEV)
1430=       DO 2 N=1,NSPACE
1440=       TR(N)=1.
1450=       TI(N)=5.
1460=     2 TE(N)=5.
1470=       RETURN
```

```
1480=      END
1490=      SUBROUTINE BURN(NSPACE,NFUEL,DT,V,H,TI,REAC,TREAC,IBURN)
1500=      DIMENSION V(101),TREAC(101),H(101),TI(101),REAC(101)
          C  SUBROUTINE BY FOR N. EGELI
          C  STEP 1 OF BURN AT ISTART TEMPERATURE IN KEV SET BELOW
1520=      TSTART= 1.0
1530=      IBURN= 0
1550=C  SET NUMBER OF REACTIONS TO ZERO FOR ALL CELLS IN THIS DT INIT
TALLY
1560=      DO 1 I=1,NSPACE
1570=    1 REAC(I)= 0.0
1580=C  TEST FUEL TO SEE IF THERMONUCLEAR BURN IGNITION TEMPERATURE H
AS BEEN
1590=C    REACHED AT ANY CELL IN THE FUEL.   RETURN WITH IBURN=0 IF BU
RN NOT
1600=C     INITIATED
1610=      DO 2 I=1,NFUEL
1620=    2 IF(TI(I).GE.TSTART) IBURN=1
1630=      IF(IBURN.EQ.0) RETURN
1640=C  COMPUTE NUMBER OF REACTIONS (D+T ONLY) IN EACH CELL OF FUEL.
1650=      DO 3 I=1,NFUEL
1660=      IF (TI(I).LT.0.01) THEN
1670=         REAC(I) = 0.0
1680=         GO TO 3
1690=         ENDIF
1700=      TM13= (TI(I))**(-0.333333)
1710=      TM23= (TI(I))**(-0.666667)
1720=      IF (TI(I).LE.10.0) GO TO 4
1730=      SIGVDT= (3.41E-14)*TM23*EXP((3.638*TM13)-(27.217*TM23))
1740=      GO TO 5
1750=    4 SIGVDT= (3.8E-12)*TM23*EXP(-19.02*TM13)
1760=    5 REAC(I)= DT*(H(I)**2)*SIGVDT/(4.0*V(I))
1770=C  REMOVE BURNED FUEL NUCLEI FROM CELL
1780=      H(I)= H(I) - (2.0*REAC(I))
1790=C  ADD NUMBER OF REACTIONS IN THIS DT TO TOTAL FOR EACH CELL
1800=      TREAC(I)= TREAC(I) + REAC(I)
1810=    3 CONTINUE
1820=C  ADJUSTMENT OF ELECTRON NUMBER IN EACH CELL WILL BE PERFORMED
BY
1830=C    ANOTHER SUBROUTINE WHEN THE CHARGED PARTICLES PRODUCED IN T
HE
1840=C    REACTION HAVE BEEN TRANSPORTED TO OTHER CELLS.
1850=C  UNITS IN THIS SUBROUTINE ARE: TEMP IN KEV, VOLUME IN CM CUBED
1860=C                    REACTIONS IN NUMBER OF REACTIONS IN EACH CEL
L.
1870=C    AND SIGVDT IN PER CM CUBED PER SECOND.
1880=      RETURN
1890=      END
1900=      SUBROUTINE HYDRO(R,VEL,DT,TR,TI,TE,NSPACE,TIME,CYCLE,IBURN,
RELRHO,
1910=     1 H,HE,ELEC,PUSH,AMASS,PMASS,DMASS,TMASS,HEMASS,PR,DELV,HD,P
USHD,
1920=     2  NFUEL,V)
1930=      DIMENSION R(101),PT(101),PI(101),PE(101),PR(101),
```

```
1540=      1  Q(101),VEL(101),TR(101),TE(101),AMASS(101),TI(101),
1550=      2  H(101),HE(101),PUSH(101),ELEC(101),V(101),
1560=      3  DELV(101),RELRHO(101),RHO(101),ACC(101)
1570=         INTEGER CYCLE
1580=         SIGMA = 5.67E-5 * (1.161E7)**4
1990=         A = 4. * SIGMA / 2.997E10
2000=         HMASS = (DMASS + TMASS)/2.
2010=         DTMAX = 1.E-10
2020=         CYCLE = CYCLE + 1
2030=         PIE = 4.*ATAN(1.)
2040=         DO 10 I=1,NSPACE+1
2050=         IF(IBURN.NE.0) AMASS(I)=H(I)*HMASS+HE(I)*HEMASS+PUSH(I)*PMA
==S
2060=         PI(I) = (H(I)+HE(I)+PUSH(I))*TI(I)*1.6E-9   /V(I)
2070=         PR(I) = A * TR(I)**4 / 3.
2080=C    NOW OBTAIN EFFECTIVE ELECTRON TEMP TO ACCOUNT FOR DEGENERACY
2090=         EFFTE = 0.00565*(AMASS(I)/V(I))**(2./3.)
2100=         IF((I.GT.NFUEL).OR.(EFFTE.LT. TE(I))) EFFTE=TE(I)
2110=         PE(I) = ELEC(I) * EFFTE * 1.6E-9 /V(I)
2120=         PT(I) = PE(I) + PI(I) + PR(I)
2130=C    INITIALIZE DENSITIES AND SET Q=0 FOR FIRST CYCLE
2140=         IF (CYCLE.EQ.1) RHO(I)=AMASS(I)/V(I)
2150=         IF (CYCLE.EQ.1) Q(I)=0.
2160=      10 CONTINUE
2170=         NOW FIND TIME STEP
2180=         DO 15 I=1,NSPACE
2190=         C = SQRT(5./3.*PI(I)*V(I)/AMASS(I))
2200=         FRACT=.5
2210=         DTI=FRACT*(R(I+1)-R(I))/C
2220=         IF (DTI.LT.DTMAX) DTMAX=DTI
2230=         IF (DTMAX.LT.DT) DT=DTMAX
2240=      15 CONTINUE
2250=C    NEXT FIND ACCELERATIONS OF CELL WALL
2260=         DO 17 I=1,NSPACE
2270=         AN=-(PT(I+1)+Q(I+1)-PT(I)-Q(I))
2280=         IF (I.NE.NSPACE) AD=(R(I+2)-R(I))/2.*(RHO(I+1)+RHO(I))/2.
2290=         IF (I.EQ.NSPACE) AD=(R(I+1)-R(I))*(RHO(I+1)+RHO(I))/2.
2300=         ACC(I)=AN/AD
2310=C    NOW FIND VELOCITIES OF CELL WALL
2320=         VEL(I)=VEL(I)+ACC(I)*DT
2330=      17 CONTINUE
2340=C    FIND NEW POSITIONS OF CELL WALL
2350=         DO 19 I=1,NSPACE
2360=         R(I+1)=R(I+1)+VEL(I)*DT
2370=      19 CONTINUE
2380=C    COMPUTE NEW DENSITIES AND VISCOSITIES
2390=         DO 20 I=1,NSPACE
2400=         RHOOLD=RHO(I)
2410=         VOLD = V(I)
2420=         V(I) = 4./3.*PIE*(R(I+1)**3-R(I)**3)
2430=         DELV(I) = V(I) - VOLD
2440=         RHO(I)=AMASS(I)/V(I)
2450=         RELRHO(I)=RHO(I)/.213
2460=         DIV=(1.-RELRHO(I))/DT
2470=         Q(I)=RHO(I)*(R(I+1)-R(I))*(R(I+1)-R(I))*DIV*DIV
```

108

```
  2480=        IF (DIV.GE.0) Q(I)=0.
  2490=   30   CONTINUE
  2500=        TI(I)=TI(I)-(2./3.)*(PI(I)+Q(I))*DELV(I)/(1.6E-9*(H(I)+HE(I
)))
```

```
  2500=        TI(I)=TI(I)-(2./3.)*(PI(I)+Q(I))*DELV(I)/(1.6E-9*(H(I)+HE(I
)))
  2510=        TE(I)=TE(I)-(2./3.)*PE(I)*DELV(I)/(1.6E-9*ELEC(I))
  2520=        TR(I) = TR(I)*((VOLD-DELV(I)/3.)/V(I))**.25
  2530=        IF(TI(I).LT.1.E-7)   TI(I)=1.E-7
  2540=        IF(TE(I).LT.1.E-7)   TE(I)=1.E-7
  2550=        IF(TR(I).LT.1.E-7)   TR(I)=1.E-7
  2560= 30   CONTINUE
  2570=        TIME=TIME+DT
  2580=        RETURN
  2590=        END
  2420=        SUBROUTINE NEUHEAT(NSPACE,   R,REAC,ALPHA,THEAT,V,H,HE)
  2430=        DIMENSION ALPHA(101),REAC(101),EX(0:101),D(101),R(101)
  2440=        DIMENSION THEAT(101),V(101),H(101),HE(101),ANO(101),AVGEN(1
01)
  2450=C
  2460=C        D, T. AND HE CROSS-SECTIONS ARE APPROXIMATELY
  2470=C        .8 BARNS FOR 14.1 MEV NEUTRONS.   AN AVERAGE
  2480=C        ENERGY PER COLLISION IS FOUND BY AVERAGING EACH
  2490=C        REACTION'S ENERGY DEPOSITION AND THEN SUMMING
  2500=C        BASED ON NUMBER FRACTIONS.   THEAT RECEIVES THE
  2510=C        NEUTRON ENERGY DEPOSITED IN EACH CELL.   ALPHA
  2520=C        IS THE EQUIVALENT NUMBER OF 3.5 MEV ALPHA
  2530=C        PARTICLES FOR THE NEUTRON ENERGY DEPOSITED.
  2540=C
  2550=        SIGMA = .8E-24
  2560=        TOTINT = 0.
  2570=        DO 1 I=1,NSPACE
  2580=           BNO = H(I) + HE(I)
  2590=           AVGEN(I) = ((.5*H(I)*2.35)/BNO) + ((.5*H(I)*1.7625)/BNO)
+
  2600=        *              ((HE(I)*1.4)/BNO)
  2610=           ANO(I) =(H(I) + HE(I)) / V(I)
  2620=           TOTINT = TOTINT + REAC(I)
  2630= 1    CONTINUE
  2640=        S = TOTINT
  2650=        EX(0) = 1.
  2660=        DO 2 I=1,NSPACE
  2670=           RI = R(I+1) - R(I)
  2680=           EE = EXP(-ANO(I)*SIGMA*RI)
  2690=           EX(I)=EE * EX(I-1)
  2700=           ACTIONS = S * (1. - EE) * EX(I-1)
  2710=           THEAT(I) = ACTIONS*AVGEN(I)*(1.6E-6)
  2720=           ALPHA(I) = THEAT(I) / (3.5*(1.6E-6))
  2730= 2    CONTINUE
  2740=        RETURN
  2750=        END
  2760=        SUBROUTINE ALPHA1(R,AMASS,V,H,HE,PUSH,ELEC,TE,TI,REAC,DT,NS
PACE,
```

109

```
2770=            +                          NFUEL,IPUSH,PMASS,IALPH,THEAT,ALPHA)
2780=          DIMENSION ALPHA(101)
2790=          DIMENSION THETA(11),EELEC(101),EION(101)
2800=          DIMENSION R(101),AMASS(101),V(101),HE(101),PUSH(101),ELEC(1
01),
2810=          +                TE(101),TI(101),REAC(101),H(101),THEAT(101)
2820=         DATA THETA/0.,.7467880321,.9899779077,1.196752093,1.3871656
22,
2830=          +                1.570796327,1.754427031,1.944840561,2.151614746,
2840=          +                2.394604621,3.141592654/
2850=         DATA PI/3.141592654/
2860=         DO 10 I=1,101
2870=         EELEC(I)=0.
2880=      10 EION(I)=0.
2890=         DO 2000 IZONE=1,NFUEL
2900=         IF(IALPH.EQ.0) GO TO 250
2910=         DO 1000 ITHET=1,11
2920=         ISTOP=0
2930=         THET=THETA(ITHET)
2940=         U=1.
2950=         XO=(R(IZONE)+R(IZONE+1))/2.
2960=         THETO=THET
2970=         INOW=IZONE
2980=C
2990=C******* STAGE FOR BIRTH SHELL
3000=C
3010=         IF(ITHET.EQ.1) CALL XYT6(INOW,R,XN,THETN,DIST,IDUM,XO)
3020=         IF(ITHET.NE.1.AND.THET.LT.PI/2.) CALL XYT7(XO,INOW,THETO,R,
DIST,
3030=          +                                ICELL,XN,THETN)
3040=         IF(ITHET.EQ.6) CALL XYT3(XO,XN,DIST,THETO,THETN,INOW,R)
3050=         IF(ITHET.NE.11.AND.THET.GT.PI/2.) CALL XYT4(XO,XN,DIST,THET
O,
3060=          +                                THETN,INOW,R)
3070=         IF(ITHET.EQ.11) CALL XYT5(XO,XN,DIST,THETN,INOW,R)
3080=         XO=XN
3090=         THETO=THETN
3100=C
3110=C****** COMPUTE THE INTEGRATION INCREMENT
3120=C
3130=         ALPHS=REAC(IZONE)/11.
3140=         IF(ITHET.EQ.1) ALPHS=REAC(IZONE)/11.+ALPHA(IZONE)
3150=         TEMPE=TE(IZONE)
3160=         DENSE=AMASS(IZONE)/V(IZONE)
3170=         CALL FINDDS(TEMPE,DENSE,DS,DIST,IDS)
3180=         ICELL=IZONE
3190=         CALL ELOSS(DENSE,TEMPE,U,DS,DIST,EELEC,EION,ICELL,ISTOP,IAL
PH,
3200=          +                IDS,THEAT,ALPHS)
3210=         IF(ISTOP.EQ.1) ICELS=ICELL
3220=         IF(ISTOP.EQ.1) GO TO 600
3230=C
3240=C****** STAGE FOR SUBSEQUENT MOTION OUT OF BIRTH SHELL
3250=C
3260=         DO 500 ILOOP=1,1000
```

110

```
3270=         IF(XO.GE.R(NSPACE+1)) GO TO 600
3280=         IF(THETO.EQ.O.) CALL XYT6(INOW,R,XN,THETN,DIST,ICELL,XO)
3290=         IF(THETO.GT.O.O.AND.THETO.LE.PI/2.) CALL XYT7(XO,INOW,THETO
3300=        +                              R,DIST,ICELL,XN,THETN)
3310=         IF(THETO.GT.PI/2.O.AND.THETO.LT.PI) CALL XYT8(INOW,THETO,XO
3320=        +                              THETN,XN,DIST,R)
3330=         IF(THETO.EQ.PI) CALL XYT9(INOW,XO,THETO,R,ICELL,DIST,XN,THE
TN)
3340=         IF(ICELL.GT.NSPACE) GO TO 1000
3350=         TEMPE=TE(ICELL)
3360=         DENSE=AMASS(ICELL)/V(ICELL)
3370=         CALL FINDDS(TEMPE,DENSE,DS,DIST,IDS)
3380=         CALL ELOSS(DENSE,TEMPE,U,DS,DIST,EELEC,EION,ICELL,ISTOP,IAL
PH,
3390=        +              IDS,THEAT,ALPHS)
3400=         IF(ISTOP.EQ.1) ICELS=ICELL
3410=         IF(ISTOP.EQ.1) GO TO 600
3420=         XO=XN
3430=         THETO=THETN
3440=   500 CONTINUE
3450=   600 CONTINUE
3460=         HE(ICELL)=HE(ICELL)+ALPHS
3470=         AMASS(ICELL)=AMASS(ICELL)+ALPHS*6.635E-24
3480=  1000 CONTINUE
3490=         GO TO 2000
3500=   250 CONTINUE
3510=         ALPHS=REAC(IZONE)+ALPHA(IZONE)
3520=         HE(IZONE)=HE(IZONE)+ALPHS
3530=         AMASS(IZONE)=AMASS(IZONE)+ALPHS*6.635E-24
3540=         DENSE = AMASS(IZONE)/V(IZONE)
3550=         FI = 1./(1.+(32.-.868*ALOG(DENSE))/TE(IZONE))
3560=         EION(IZONE)=3500.*ALPHS*FI
3570=         EELEC(IZONE)=3500.*ALPHS*(1.-FI)
3580=         THEAT(IZONE)=3.5*1.602E-6*ALPHS
3590=  2000 CONTINUE
3600=C
3610=C****** COMPUTE NEW TE, TI
3620=C
3630=         DO 700 IZONE=1,NSPACE
3640=         ETOTE=3./2.*TE(IZONE)*ELEC(IZONE)
3650=         ETOTE=ETOTE+EELEC(IZONE)
3660=         TE(IZONE)=ETOTE*2./3./ELEC(IZONE)
3670=         ETOTI=3./2.*TI(IZONE)*H(IZONE)
3680=         ETOTI=ETOTI+EION(IZONE)
3690=         TI(IZONE)=ETOTI*2./3./H(IZONE)
3700=   700 CONTINUE
3710=         RETURN
3720=         END
3730=         SUBROUTINE XYT3(XO,XN,DIST,THETO,THETN,INOW,R)
3740=         DIMENSION R(101)
3750=         RR=R(INOW+1)
3760=         XN=RR
3770=         ANG=ACOS(XO/RR)
```

```
3780=          YTEMP=RR*SIN(ANG)
3790=          THETN=THETO-ANG
3800=          DIST=YTEMP
3810=          INOW=INOW+1
3820=          RETURN
3830=          END
3840=          SUBROUTINE XYT4(XO,XN,DIST,THETO,THETN,INOW,R)
3850=          DIMENSION R(101)
3860=          CALL GETA(THETO,A)
3870=          CALL GETB(XO,THETO,B)
3880=          RR=R(INOW)
3890=          RR1=R(INOW+1)
3900=          CALL GETC(RR,XO,THETO,C)
3910=          CALL GETC(RR1,XO,THETO,C1)
3920=          DISC=B**2-4.*A*C
3930=          DISC1=B**2-4.*A*C1
3940=          IF(DISC.GE.O.) CALL XYT4A(THETO,RR,XO,B,DISC,A,XN,THETN,DIS
T,
3950=         +                    O,IDUM)
3960=          IF(DISC.LT.O.) CALL XYT4B(INOW,RR1,THETO,XO,A,DISC1,B,THETN
,XN,
3970=         +                    DIST,O,IDUM)
3980=          RETURN
3990=          END
4000=          SUBROUTINE XYT4A(THETO,RR,XO,B,DISC,A,XN,THETN,DIST,IFLAG,I
CELL)
4010=          PI=3.141592654
4020=          YTEMP=(-B-SQRT(DISC))/2./A
4030=          XTEMP=(YTEMP-XO*TAN(PI-THETO))/TAN(THETO)
4040=          DIST=SQRT((XO-XTEMP)**2+YTEMP**2)
4050=          XN=RR
4060=          THETN=THETO-ASIN(YTEMP/RR)
4070=          ICELL=INOW-1
4080=C         INOW=INOW
4090=          IF(IFLAG.EQ.1) INOW=INOW-1
4100=          RETURN
4110=          END
4120=          SUBROUTINE XYT4B(INOW,RR1,THETO,XO,A,DISC1,B,THETN,XN,DIST,
IFLAG,
4130=         +                    ICELL)
4140=          PI=3.141592654
4150=          YTEMP=(-B+SQRT(DISC1))/2./A
4160=          XTEMP=(YTEMP-XO*TAN(PI-THETO))/TAN(THETO)
4170=          DIST=SQRT((XO-XTEMP)**2+YTEMP**2)
4180=          XN=RR1
4190=          THETN=THETO-ASIN(YTEMP/RR1)
4200=          ICELL=INOW
4210=          INOW=INOW+1
4220=          IF(IFLAG.EQ.1) INOW=INOW-1
4230=          RETURN
4240=          END
4250=          SUBROUTINE XYT5(XO,XN,DIST,THETN,INOW,R)
4260=          DIMENSION R(101)
4270=          PI=3.141592654
4280=          XN=R(INOW)
```

```
4290=        THETN=PI
4300=        INOW=INOW
4310=        DIST=ABS(XN-XO)
4320=        IF(R(INOW).LE.0.) THETN=0.
4330=        RETURN
4340=        END
4350=        SUBROUTINE GETA(THETO,A)
4360=        A=1.+1./(TAN(THETO))**2
4370=        RETURN
4380=        END
4390=        SUBROUTINE GETB(XO,THETO,B)
4400=        PI=3.141592654
4410=        ANUM=-2.*XO*TAN(PI-THETO)
4420=        DEN=(TAN(THETO))**2
4430=        B=ANUM/DEN
4440=        RETURN
4450=        END
4460=        SUBROUTINE GETC(R,XO,THETO,C)
4470=        PI=3.141592654
4480=        ANUM=(XO*TAN(PI-THETO))**2
4490=        DEN=(TAN(THETO))**2
4500=        C=-1.*R**2+ANUM/DEN
4510=        RETURN
4520=        END
4530=        SUBROUTINE XYT6(INOW,R,XN,THETN,DIST,ICELL,XO)
4540=        DIMENSION R(101)
4550=        XN=R(INOW+1)
4560=        THETN=0.
4570=        ICELL=INOW
4580=        INOW=INOW+1
4590=        DIST=XN-XO
4600=        RETURN
4610=        END
4620=        SUBROUTINE XYT7(XO,INOW,THETO,R,DIST,ICELL,XN,THETN)
4630=        DIMENSION R(101)
4640=        PI=3.141592654
4650=        CALL GETA(THETO,A)
4660=        CALL GETB(XO,THETO,B)
4670=        RR=R(INOW+1)
4680=        CALL GETC(RR,XO,THETO,C)
4690=        YTEMP=(-B+SQRT(B**2-4.*A*C))/2./A
4700=        XTEMP=(YTEMP-XO*TAN(PI-THETO))/TAN(THETO)
4710=        THETN=THETO-ASIN(YTEMP/RR)
4720=        XN=RR
4730=        ICELL=INOW
4740=        INOW=INOW+1
4750=        DIST=SQRT((XO-XTEMP)**2+YTEMP**2)
4760=        RETURN
4770=        END
4780=        SUBROUTINE XYT8(INOW,THETO,XO,THETN,XN,DIST,R)
4790=        DIMENSION R(101)
4800=        CALL GETA(THETO,A)
4810=        CALL GETB(XO,THETO,B)
4820=        RR=R(INOW-1)
4830=        RR1=R(INOW)
```

113

```
4840=        CALL GETC(RR,XO,THETO,C)
4850=        CALL GETC(RR1,XO,THETO,C1)
4860=        DISC=B**2-4.*A*C
4870=        DISC1=B**2-4.*A*C1
4880=        IF(DISC.GE.O.) CALL XYT4A(THETO,RR,XO,B,DISC,A,YN,THETN,DIS
T,1,
4890=     +              ICELL)
4900=        IF(DISC.LT.O.) CALL XYT4B(INOW,RR1,THETO,XO,A,DISC1,B,THETN
,XN,
4910=     +              DIST,1,ICELL)
4920=        RETURN
4930=        END
4940=        SUBROUTINE XYT9(INOW,XO,THETO,R,ICELL,DIST,XN,THETN)
4950=        DIMENSION R(101)
4960=        THETN=THETO
4970=        XN=R(INOW-1)
4980=        DIST=ABS(XN-XO)
4990=        ICELL=INOW-1
5000=        INOW=INOW-1
5010=        IF(XN.EQ.0.)THETN=0.
5020=        RETURN
5030=        END
5040=        SUBROUTINE FINDDS(TEMPE,DENSE,DS,DIST,IDS)
5050=        RATIO=.213/DENSE
5060=        ANUME=TEMPE**1.5*0.086*RATIO
5070=        DENE=1.+0.17*ALOG(TEMPE*SQRT(RATIO))
5080=        DE=ANUME/DENE
5090=        ANUMI=10.65*RATIO
5100=        DENI=1.+0.75*ALOG(SQRT(TEMPE*RATIO))
5110=        DI=ANUMI/DENI
5120=        IF(TEMPE.LE.20.) D=DE
5130=        IF(TEMPE.GT.20.) D=DI
5140=        D=D/50.
5150=        IDS=INT(DIST/D)
5160=        IF(IDS.LE.1) IDS=1
5170=        DS=DIST/IDS
5180=        RETURN
5190=        END
5200=        SUBROUTINE ELOSS(DENSE,TEMPE,U,DS,DIST,EELEC,EION,ICELL,IST
OP,
5210=     +              IALPH,IDS,THEAT,ALPHS)
5220=        DIMENSION THEAT(101)
5230=        DIMENSION EELEC(101),EION(101)
5240=        SPE(D,U,T)=-23.2/D*SQRT(U)/T**1.5*(1.+.17*ALOG(T*SQRT(D)))
5250=        SPI(D,U,T)=-.047/D/U*(1.+0.075*ALOG(SQRT(T*D*U)))
5260=        RATIO=.213/DENSE
5270=        IF(RATIO.EQ.0..OR.TEMPE.EQ.0.) STOP
5280=        DO 100 I=1,IDS
5290=        FRACE=SPE(RATIO,U,TEMPE)
5300=        FRACI=SPI(RATIO,U,TEMPE)
5310=        U=U+DS*(FRACE+FRACI)
5320=        UTHERM=3./2./3500.*TEMPE
5330=        IF(U.LE.UTHERM) ISTOP=1
5340=        IF(U.LE.UTHERM) GO TO 200
5350=        EE=3500.*DS*ABS(FRACE)*ALPHS
```

114

```
5360=          EI=3500.*DS*ABS(FRACI)*ALPHS
5370=          EELEC(ICELL)=EELEC(ICELL)+EE
5380=          EION(ICELL)=EION(ICELL)+EI
5390=          THEAT(ICELL)=THEAT(ICELL)+0.5*DS*ABS(FRACE+FRACI)*1.602E-6*
ALPHS
5400=          IF(IALPH.EQ.1.AND.EI.GE.EE) GO TO 300
5410=  100 CONTINUE
5420=  200 CONTINUE
5430=          RETURN
5440=  300 ISTOP=1
5450=          EION(ICELL)=EION(ICELL)+U*3500.*ALPHS
5460=          THEAT(ICELL)=THEAT(ICELL)+3.5*1.602E-6*U*ALPHS
5470=          RETURN
5480=          END
5490=          SUBROUTINE HTFLX(R,TE,TI,TR,ELEC,V,H,HE,PUSH,AMASS,NSPACE,H
MASS,
5650=     *  HEMASS,PMASS,DT,PR)
5690=          DIMENSION R(101),TE(101),TR(101),TI(101),ELEC(101),
5700=     %  V(101),PR(101),AMASS(101),H(101),HE(101),PUSH(101)
5710=          REAL LOGLAM,ME,MI,K,KP,NU,NUB,NUC,KROS,LAMROS,NAZOVA,NEP,MC
2
5720=C   HEAT CONDUCTION IS CONSIDERED USING COEFFICIENTS TAKEN FROM
5730=C   FRALEY, ET AL. PHYS FL. VOL 17. NO 2, FEB 74. USING FLUX-CONSE
RVATIVE
5740=C   DIFFERENCING AT ZONE BOUNDRIES IN CGS UNITS
5750=C
5760=C   ELECTRON MASS
5770=          ME=.911E-27
5780=C   BOLTZMANNS CONSTANT IN ERGS/KEV
5790=          K=1.38E-16*1.161E+7
5800=C   ELECTRON CHARGE
5810=          E=4.8E-10
5820=C   FINE STRUCTURE CONSTANT
5830=          ALF=1/137.04
5840=          PI=3.14159
5850=C   SPEED OF LIGHT
5860=          C=2.9979E10
5870=C   STEPHAN-BOLTZMANN SIGMA IN ERGS/CM2/SEC/KEV4
5880=          SIGMA = 5.67E-5*(1.161E+7)**4
5890=          FLUXM=0.0
5900=          RFLUXM = 0.0
5910=C   COLLECT ALL OF THE CONSTANTS IN FRONT OF THE DO-LOOP
5920=C   A AND B ARE USED IN LOG LAMBDA = LOGLAM (EQN B4C)
5930=C   D IS USED IN ELECTRONIC HEAT DIFFUSION COEFFICIENT = KP (EQN
B4C)
5940=C   F IS USED IN ELECTRON-ION RELAXATION RATE = NU (EQN B4A)
5950=C   H1 AND H2 ARE USED IN ELECTRON-RADIATION RELAXATION RATE
5960=C        =AERB + AERC
5970=C   FLUXP AND FLUXM ARE EACH AN ELECTRON HEAT CONDUCTION FLUX TIM
ES AREA
5980=C   RFLUXP AND RFLUXM ARE SIMILAR FLUXES TIMES AREA FOR RADIATION
5990=          A=(1.5/E**2)**1.5/SQRT(PI)
6000=          B=.5/ALF/C*SQRT(3./ME)
6010=          D=20.*((2./PI)**1.5)*K/(SQRT(ME)*(E**4))
```

115

```
6020=        F = 8.0*SQRT(2.*PI*ME)*E**4/3.
6030=        HBARC=6.63E-27/2./PI*C
6040=        MC2=ME*C*C
6050=        RO=E*E/MC2
6060=        H1=32./3.*SQRT((2./PI/ME))*(E*E*E*E)*K*RO/HBARC
6070=        H2=(128./3.)*PI*(E/MC2)*(E/MC2)*SIGMA*RO
6080=        DO 100 N=1,NSPACE
6090=C    ELECTRON-ION EXCHANGE AND ELECTRON HEAT CONDUCTION
6100=        RP=R(N)
6110=        Z2=ELEC(N)/(H(N)+HE(N)+PUSH(N))
6120=        IF (N.LT.NSPACE) GO TO 10
6130=        TP=TE(N)
6140=        NEP=ELEC(N)/V(N)
6150=        ZP=Z2
6160=        GO TO 20
6170=   10   TP=.5*(TE(N+1)+TE(N))
6180=        NEP=.5*(ELEC(N+1)/V(N+1)+ELEC(N)/V(N))
6190=        Z1=ELEC(N+1)/(H(N+1)+HE(N+1)+PUSH(N+1))
6200=        ZP=.5*(Z1+Z2)
6210=   20 EDT = .43*ZP/(3.44+ZP+.26*ALOG(ZP))
6220=        SQTE=SQRT(TP)
6230=        LOGLAM=ALOG(SQTE**3/NEP/(ZP+B*SQTE))
6240=        IF (LOGLAM.LT.1.)  LOGLAM=1.
6250=        KP=D*(TP**2.5)*EDT/(ZP*LOGLAM)
6300=        MI = (HMASS*H(N)+HEMASS*HE(N)+PMASS*PUSH(N))/
6310=      %    (H(N)+HE(N)+PUSH(N))
6320=        NU=F*ELEC(N)*ELEC(N)*LOGLAM/(AMASS(N)*V(N)*TE(N)**1.5
6330=        IF(N.GE.NSPACE-2) GO TO 22
6340=        DTDRP = (TE(N+2)-TE(N))/(R(N+2)-R(N))
6350=        GO TO 23
6360=   22 DTDRP=(TE(N+1)-TE(N))/(R(N+1)-R(N))
6370=   23 FLUXP=-R(N+1)*R(N+1)*KP*DTDRP
6380=        TE(N) = TE(N) + 8.*PI/(3.*K*ELEC(N))*(FLUXP-FLUXM)*DT
6390=      1    +NU*(TI(N)-TE(N))*DT
6400=        TI(N)=TI(N)-Z2*NU*(TI(N)-TE(N))*DT
6410=        FLUXM = FLUXP
6420=C    RADIATION DIFFUSION CALCULATION
6430=        IF (N.LT.NSPACE-2)GO TO 32
6440=        TRP = TR(N)
6450=        TRP3 = TRP*TRP*TRP
6460=        DTDRP = (TR(N)-TR(N-1))/(R(N)-R(N-1))
6470=        TEP = TE(N)
6480=        TEP72 = TEP**3.5
6490=        RHOP2 =  (AMASS(N)/V(N))**2
6500=        RP=R(N)*R(N)
6510=        GO TO 33
6520=   32 TRP = (TR(N+1)+TR(N))/2.
6530=        TRP3 = TRP*TRP*TRP
6540=        DTDRP = (TR(N+2)-TR(N))/(R(N+2)-R(N))
6550=        TEP = (TE(N+1)+TE(N))/2.
6560=        PRINT*,TEP
6570=        TEP72 = TEP**3.5
6580=        RHOP2 = (AMASS(N+1)/V(N+1)+AMASS(N)/V(N))**2/4.
6590=        RP2 = R(N+1)**2
```

116

116

```
6600=      13 LAMRDS = FLOATER?3/RHOL?
6610=         AEC=16./3.+-3GMA*LAMRDS*TR*3
6620=         RFLUXP = RF2*RHOS*DTDRP
6630=C     RADIATION-ELECTRON ENERGY TRANSFER
6640=         A1=.2*TR(N)/TE(N)
6650=         G=PI*PI/4.-(PI*PI/4.-1)*EXP(-A1)
6670=         TR4 = (TR(N)**2)**2
6680=         TR3 = TR4/TR(N)
6700=         AERR=H1/SQRT(TE(N))*(ELEC(N)*ELEC(N)/V(N)/V(N))*ZZ*G
6710=         AERC=H2*NEF*TR4
6720=         CNUI = 1.5*R/MI
6730=         CNUE = CNUI*ZZ
6740=         AER=AERR+AERC
6750=         CNUR=16*SIGMA/C*V(N)/AMASS(N)*TR3
6760=         TE(N) = TE(N) - AER*(TE(N)-TR(N))*DT/CNUE
6770=         TR(N) = TR(N) + AER*(TE(N)-TR(N))*DT/CNUR
6780=      %     +(RFLUXP-RFLUXM)*4.*PI*DT/(A(N)*CNUR)
6790=         RFLUXM = RFLUXP
6810=     100 CONTINUE
6820=         RETURN
6830=         END
6680=         SUBROUTINEOUTPUT(R,CYCLE,TIME,DT,DRENG,NFUEL,NSPACE,VEL,RHO
Z,PMASS
6690=      %,ZPUSH,ELEC,TE,TI,TR,REAC,TREAC,THEAT,FLU,RELRHO,H,HE,PUSH,
DRVENG)
6700=         DIMENSION VEL(101),RELRHO(101),H(101),HE(101),PUSH(101),ELE
C(101),
6710=      % TE(101),TI(101),TR(101),REAC(101),TREAC(101),THEAT(101),FL
U(101),
6720=      %  DRVENG(101),R(101)
6730=         INTEGER CYCLE
6740=         TPLOT=TIME*1.E9
6750=         DTPLOT=DT*1.E12
6760=         EIPLOT=DRENG*1.E-10
6770=         EOPLOT=0.
6780=         DO 2 N=1,NFUEL
6790=       2 EOPLOT=EOPLOT+REAC(N)*2.816E-15
6800=C    EOPLOT IS KJ RELEASED BY DT BURN
6810=         PRINT 101, CYCLE,TPLOT,DTPLOT,EIPLOT,EOPLOT
6820=         PRINT 102
6830=         PRINT 104
6840=         DO 10 N=1,NFUEL
6850=         RPLOT=R(N)*10.
6860=         VPLOT=VEL(N)*1.E-8
6870=         OUTFL=TREAC(N)*2.816E-12
6880=         HTPLT=THEAT(N)*1.E-7
6890=      10 PRINT 103,N,RPLOT,VPLOT,REAC(N),RELRHO(N),TE(N),TI(N),TR(N)
6900=      %OUTFL ,HTPLT,FLU(N)
6910=         IF(NFUEL.LE.NSPACE) GO TO 200
6920=         PRINT 105
6930=         NFP=NFUEL+1
6940=         DO 20 N=NFP,NSPACE
6950=         RPLOT=R(N)*10.
6960=         VPLOT=VEL(N)*1.E-8
```

117

```
6970=          OUTPLOT=DRVENG(N)*1.E-7
6980=          HTPLT=THEAT(N)*1.E-7
6990=       20 PRINT 103,N,RPLOT,VPLOT,REAC(N),RELRHO(N),TE(N),TI(N),TR(N)
7000=          %OUTPLOT,HTPLT,FLU(N)
7010=      101 FORMAT ('1CYCLE =',I4,3X,'TIME =',F8.4,'NS    DT =',
7020=          %F8.4,'FS    INPUT =',F8.4,'KJ    OUTPUT =',F8.3,'KJ',///)
7030=      102 FORMAT (12X,'RADIUS',4X,'VELOCITY',3X,'REACTIONS',
7040=          1 4X,'DENSITY',5X,'EL. TEMP',4X,'ION TEMP',4X,'RAD TEMP',
7050=          2 5X,'OUTPUT',4X,'HEATING',5X,'NEUTRON',/,3X,'I',5X,'(MM)',
7060=          3 6X,'(MM/NS)',4X,'THIS DT',3X,'(X NORMAL)',4X,'(KEV)',
7070=          47X,'(KEV)',7X,'(KEV)',5X,'(JOULES)',2X,'(JOULES)',5X,'FLUEN
CE',//
7080=          5)
7090= 103    FORMAT(1X,I5,2F12.6,1PE12.4,0P,6F12.3,1PE12.4)
7100=  104 FORMAT (' FUEL',//)
7110=  105 FORMAT (//,' PUSHER',90X,'INPUT',//)
7120= 200 CONTINUE
7130=      RETURN
7140=      END
```

118

APPENDIX B

Glossary of Variables

Variables used in program MOXNEX are defined or
described below. Global variables are discussed, followed
by the non-global variables used in each subroutine.

Table 9

Global Variables

Variable	Definition or Description
ALPHA(I)	Equivalent number of 3.5 Mev alpha particles computed from energy transfer from neutron-ion collisions.
AMASS(I)	Total mass in grams in zone i
CYCLE	Total program iteration counter
DMASS	Deuterium mass in grams
DRVENG(I)	Output in ergs of zone i
DT	Time step in seconds
ELEC(I)	Total number of electrons in zone i
H(I)	Total hydrogen nuclei in zone i
HD	Hydrogen density in grams per cubic centimeter
HE(I)	Total number of helium-4 nuclei in zone i
HMASS	Average hydrogen mass in grams
HEMASS	Helium mass in grams

NFUEL	total number of fuel zones
NSPACE	Total number of zones
PMASS	Pusher mass in grams
PUSH(I)	Total number of pusher atoms in zone i
PUSHD	Pusher material density in grams per cubic centimeter
R(I)	Radial distance of zone i in centimeters
TE(I)	Electron species temperature in kev in zone i
THEAT(I)	Total heating in ergs of zone i
TI(I)	Ion species temperature in kev in zone i
TIME	Time in seconds
TMASS	Tritium mass in grams
TR(I)	Radiation temperature in zone i
TREAC(I)	Total number of reactions in zone i
V(I)	Volume in cubic centimeters of zone i
VEL(I)	Velocity of cell wall i in centimeters per second
ZPUSH	Average atomic number of pusher material

Table 10

Subroutine GDATA Variables

Variable	Definition or Description
DELV(I)	Change in volume in cubic centimeters
DR	Zone width in centimeters
NSSP1	NSPACE + 1

120

PIE	π
PR(I)	Radiation pressure in ergs per cubic centimeter
RM3	Inside zone radius in centimeters cubed
RP3	Outside zone radius in centimeters cubed

Table 11

Subroutine HYDRO Variables

Variable	Definition or Description
A	Constant = $4\sigma/c$ for radiation pressure calculation
ACC(I)	Acceleration of zone wall i in centimeters per second
AD	Denominator for acceleration computation
AN	Numerator for acceleration computation
C	Speed of sound
DIV	Divergence of velocity
DTI	Interval time step
DTMAX	Maximum time step
EFFTE	Effective electron temperature
FRACT	Fractional value for time step calculation
PE(I)	Pressure in ergs per cubic centimeter due to electron species
PI(I)	Pressure in ergs per cubic centimeter due to ion species

121

PIE	π
PR(I)	Pressure in ergs per cubic centimeter due to radiation
PT(I)	Total pressure in ergs per cubic centimeter
Q(I)	Artificial viscosity in ergs per cubic centimeter
RELRHO(I)	Relative density, current density over ambient density
RHO(I)	Density in grams per cubic centimeter
RHOOLD	Density during previous iteration
SIGMA	Stephan-Boltzmann constant in ergs per square centimeter per second per kev^4
VEL(I)	Cell wall velocity in centimeters per second
VOLD	Volume during previous iteration

Table 12

Subroutine TBURN Variables

Variable	Definition or Description
IBURN	Logical flag used to carry burn status to other subroutines
SIGVDT	$\langle\sigma v\rangle_{DT}$
TM13	Cubic root of ion temperature
TM23	Ion temperature to the 2/3 power
TSTART	GO/NO GO temperature for thermonuclear burn

122

Table 13

Subroutine NUHEAT Variables

Variable	Definition or Description
ACTION	Total number of interactions
ALPHA(I)	Equivalent number of 3.5 Mev alpha particles computed from energy transfer from neutron-ion collisions
ANO(I)	Ion number density in zone i
AVGEN(I)	Average energy lost by a neutron during collision with an ion
BNO(I)	Total ion number in zone i
EE	Probability neutron penetrates zone i
EX(I)	Probability neutron penetrates zone i+1
S	Total number of neutrons
SIGMA	Neutron-ion cross section
TOTINT	Total number of neutrons

Subprogram ALPHA1 is discussed by subroutines.

Table 14

Subroutine ALPHA1 Variables

1. Subprogram ALPHA1

Variable	Definition or Description
ALPHS	Number of new alpha particles
DENSE	Zone density in grams per cubic centimeter
EELEC(I)	Energy transferred to electrons in zone i

EION(I)	Energy transferred to ions in zone i
ETOTI	Total energy of ions
ETOTE	Total energy of electrons
FI	Fraction of energy deposited in ions
IALPH	Logical flag for energy deposition position
ICELL	Zone number into which alpha particle is about to decelerate
ICELS	Vestigial statement
ILOOP	Simple loop parameter
INOW	Current alpha particle position on radial mesh
ITHET	Index for angular mesh
ISTOP	Logical flag to signal alpha particle thermalized
IZONE	Radial zone number
TEMPE	Electron temperature
THET	Particular angle of angular grid
THETA(I)	Angles of angular grid
THETN	New theta angle
THETO	Old theta angle
U	Remaining fraction of alpha energy
XN	New x coordinate
XO	Old x coordinate

2. Subroutine XTY3

Variable	Definition or Description
ANG	Angle measured from microsphere center from birth point to exit position
DIST	Distance traveled within the zone
RR	Radius of zone being entered
YTEMP	Distance traveled within the zone in the y direction

3. Subroutine XYT4

Variable	Definition or Description
DISC	Discriminant of the solution of the equation of the line of travel with the circle representing the next inner zone
DISC1	Discriminant of the solution of the equation of the line of travel with the circle representing the next outer zone
RR1	Radius to the outside of the zone being entered

4. Subroutine XYT4A

Variable	Definition or Description
XTEMP	Distance traveled within the zone in the x direction

125

5. Subroutine XYT4B

No New Variables

6. Subroutine XYT5

New New Variables

7. Subroutine GETA

Variable	Definition or Description
A	Coefficient of the solution of the intersection of a line with a circle

8. Subroutine GETB

Variable	Definition or Description
ANUM	Numerator for coefficient calculation
B	Coefficient of the solution of the intersection of a line with a circle
DEN	Denominator for coefficient calculation

9. Subroutine GETC

Variable	Definition or Description
C	Coefficients of the solution of the intersection of a line with a circle

10. Subroutine XYT6

No New Variables

11. Subroutine XYT7

No New Variables

12. Subroutine XYT8

No New Variables

13. Subroutine XYT9

No New Variables

14. Subroutine FINDDS

Variable	Definition or Description
ANUME	Numerator for range calculation if electrons only decelerate alpha particle
ANUMI	Numerator for range calculation if ions only decelerate alpha particle
D	Intermediate variable supporting integration increment calculation
DE	Range of alpha particle in zone if zone goes to infinity and only electrons decelerate it
DENE	Denominator of range calculation if electrons only decelerate alpha particle

127

DENI	Denominator of range calculation if ions only decelerate alpha particle
DI	Range of alpha particle in zone if zone goes to infinity and only ions decelerate it
DS	Integration increment
IDS	Number of integration increments within current zone
RATIO	Relative ratio of deuterium-tritium compared to ambient

15. Subroutine ELOSS

Variable	Definition or Description
EE	Energy to electrons in kev
EI	Energy to ions in kev
FRACE	Electron term for energy deposition
FRACI	Ion term for energy deposition
SPE	Electron term for energy deposition
SPI	Ion term for energy deposition
UTHERM	Energy of thermal ions

Table 15

Subroutine HTFLX Variables

Variable	Definition or Description
A	Constant for Coulomb logarithm computation
AER	Radiation-electron energy transfer coupling coefficient
AERB	Bremsstrahlung coupling coefficient
AERC	Compton scatter coupling coefficient
ALP	Fine structure constant
A1	Constant for bremsstrahlung Gaunt factor calculation
B	Constant for Coulomb logarithm computation
CNUE	Specific heat for electron species
CNUI	Specific heat for ion species
CNUR	Radiation specific heat
D	Constant for coefficient of thermal conductivity calculation
DTDRP	Spatial derivative of temperature
E	Electronic charge in esu
EDT	Term $\varepsilon\delta_T$ for coefficient of thermal conductivity calculation
F	Constant for equilibration coefficient computation
FLUXM	Heat flux at zone inner radius

129

FLUXP	Heat flux at zone outer radius
G	Bremsstrahlung Gaunt factor
H1	Constant for bremsstrahlung coupling coefficient calculation
H2	Constant for Compton scatter coupling coefficient calculation
KP	Coefficient of thermal conductivity
KROS	Diffusion coefficient for radiation
LAMPOS	Mean free path of photons
LOGLAM	Coulomb logarithm
MI	Average ion mass
NEP	Electron density
NU	Equilibration frequency for electron-ion energy transfer
RFLUXM	Radiation energy flux at inner zone radius
RFLUXP	Radiation energy flux at outer zone radius
RHOP2	Square of zone density
RP	Cell wall radius from center in centimeters of zone in loop
SQTE	Square root of electron temperature
TEP	Electron temperature in kev of zone in loop
TEP72	Electron temperature to 7/2 power
TP	Average electron temperature over two zones
TRP	Radiation temperature in kev of zone in loop
TRP3	Cube of radiation temperature
TR3	Cube of radiation temperature

TR4	Radiation temperature to the fourth power
ZP	Net electronic charge averaged over zones i and $i+1$
Z1	Net electronic charge in zone $i+1$
Z2	Net electronic charge in zone i

Table 16

Subroutine OUTPUT Variables

Variable	Definition or Description
DTPLOT	Time step in picoseconds
E1PLOT	Energy in kilojoules input by driver
E0PLOT	Energy in kilojoules released by thermo-nuclear burn
HTPLT	Bootstrap heating in kilojoules
NFP	Loop Index = NFUEL + 1
OUTPL	Cell output in joules in fuel zones
OUTPLOT	Cell output in joules in pusher zones
RPLOT	Zone radii in millimeters
TPLOT	Total time in nanoseconds
VPLOT	Cell wall velocity in millimeters per nanosecond

APPENDIX C

Derivation of the Coulomb Cross Sections

for Short and Long Range Collisions

Figure 16 illustrates the hyperbolic paths of two passing particles of equal charge and mass. It also defines the geometry and parameters necessary to this discussion.
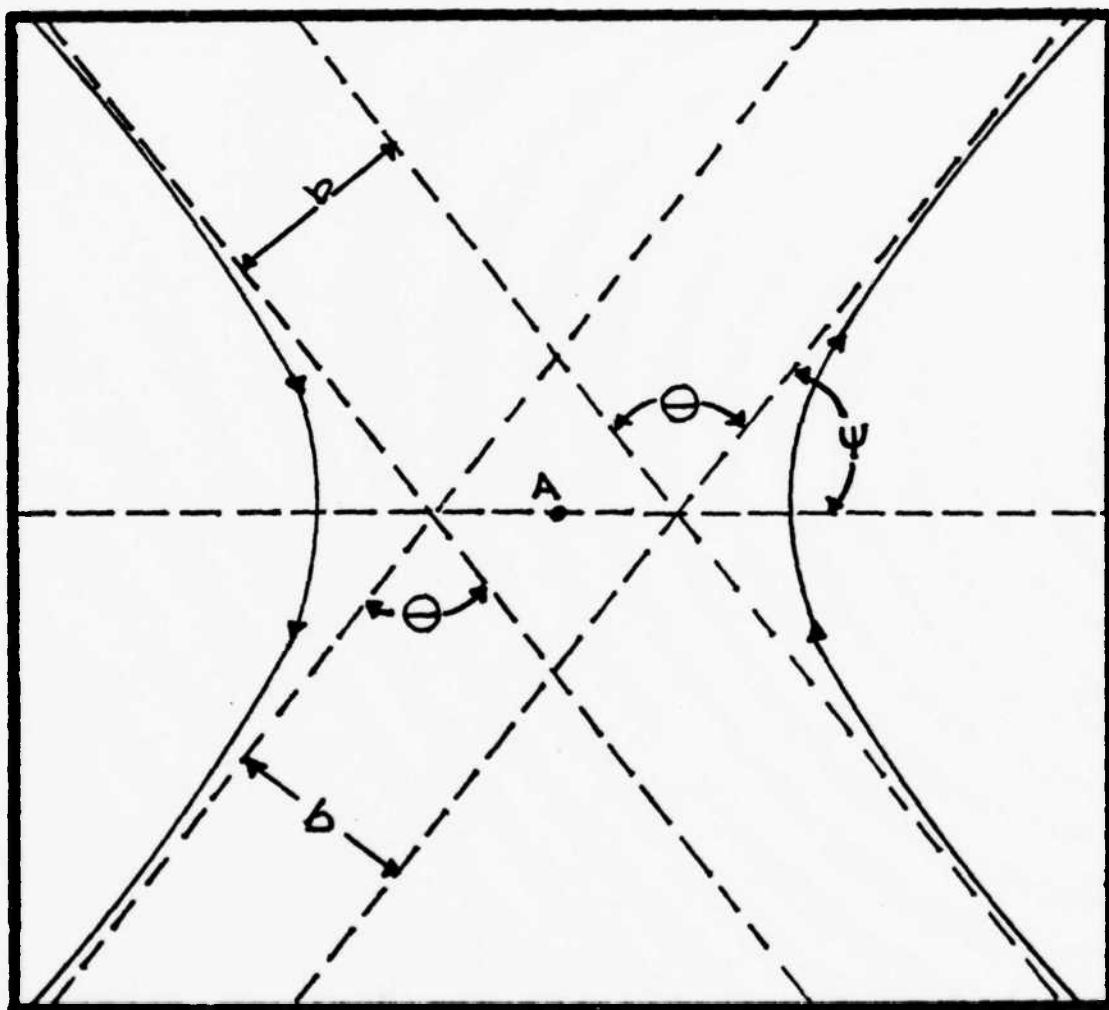
Figure 16. Hyperbolic Paths of Identical Particles in a Coulomb Encounter

The asymptotes are in dashed lines, the impact parameter b
is defined as the distance of closest approach in the absence
of other forces, the angular deflection Θ is defined as the
angle of deviation from the normal path, and the center of
mass is point A . The angle ψ is an angle of convenience
between the asymptote and the line through the actual distance of
closest approach. Note

$$\Theta = \pi - 2\psi \tag{C-1}$$

Extending to the case of nonidentical particles,

$$\tan \psi = \frac{M b v^2}{Z_1 Z_2 e^2} \tag{C-2}$$

where

    M is the reduced mass

    v is the relative velcoity between the particles
and Z_1 and Z_2 are the charge number of the two respective
particles (Ref 26:122).

    Of interest is the case where $\Theta = \pi/2$. From Eq (C-1)
it is apparent that $\Theta = \pi/2$ when $\psi = \pi/4$. This means
$\tan \psi = 1$ and therefore the impact parameter for a 90°
deflection, denoted b_o , is

$$b_o = \frac{Z_1 Z_2 e^2}{M v^2} \tag{C-3}$$

133

If one particle is very much larger, the heavier particle may
be taken as stationary and the relative velocity becomes the
velocity of incidence of the lighter particle. Denoting this
velocity v_1 and noting the reduced mass under the condition
$m_2 \gg m_1$ can be approximated by m_1 because

$$\frac{1}{m_1} + \frac{1}{m_2} \simeq m_1 \quad \text{WHEN} \quad m_2 \gg m_1 \tag{C-4}$$

In other words, $M \simeq m_1$. Thus, Eq (C-3) becomes

$$b_0 = \frac{Z_1 Z_2 e^2}{m_1 v_1^2} \tag{C-5}$$

The cross section for such a collision is then

$$\sigma_{c_{SR}} \simeq \pi b_0^2 \tag{C-6}$$

$$\sigma_{c_{SR}} \simeq \frac{\pi Z_1^2 Z_2^2 e^4}{m_1^2 v_1^4} \tag{C-7}$$

$$\sigma_{c_{SR}} \simeq \frac{\pi Z_1^2 Z_2^2 e^4}{4 E_1} \tag{8}$$

where E_1 is the energy of the less massive particle in the
rest frame of the more massive particle.

To arrive at a cross section for a long range collision,
consider Figure 17 illustrating a Coulomb collision in which
momentum transfer is small so that particle 1 is basically
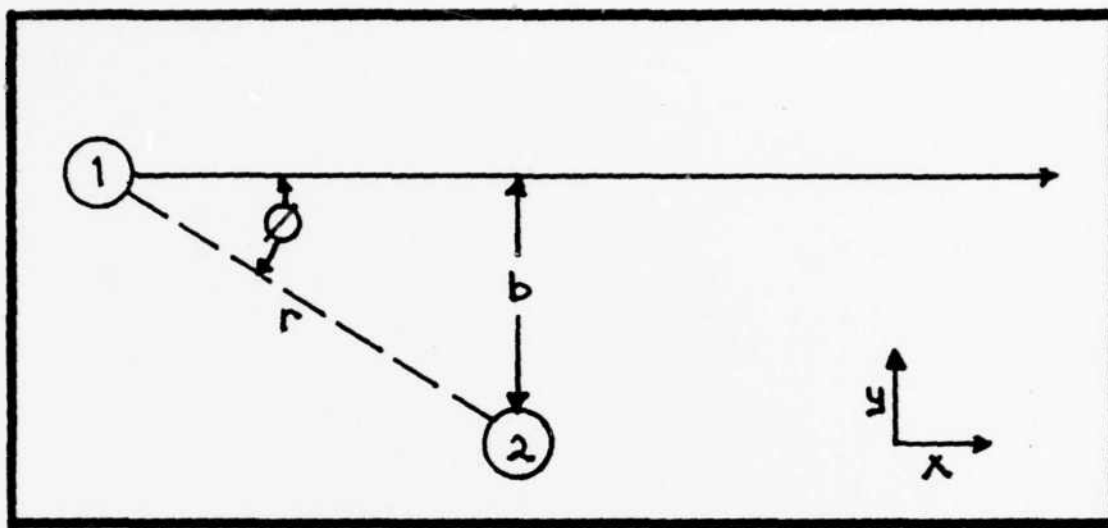
Figure 17.   Coulomb Collision Assuming Small
Momentum Transfer Between Interacting
Particles

undeflected from straight line motion.   This is essentially
the picture of an individual long range collision between
fast particles in the rest frame of particle 2.

Remember the long range encounter equivalent to a collective
scatter through an angle of 90° can be described as

$$\left(\widetilde{\Delta p}\right)^2 = p_{INITIAL}^2$$

(9)

The change in momentum for a single interaction, though, is

$$\Delta \underline{p} = \int_0^\infty \underline{F} \, dt \qquad \text{(C-8)}$$

Since particle 1 would apply an equal force in both the x
and -x directions when integrated over time, Eq (C-8) can
be reduced to

$$\Delta P_y = \int_0^\infty F_y \, dt \qquad \text{(C-9)}$$

The force is always along the ray r so that Eq (C-9) can be
written

$$\Delta P_y = \int_0^\infty F_r \sin \theta \, dt \qquad \text{(C-10)}$$

From Coulomb's law, this can be expressed

$$\Delta P_y = \int_0^\infty \frac{Z_1 Z_2 e^2}{r^2} \sin \theta \, dt \qquad \text{(C-11)}$$

Note from Figure 17 , $r = \dfrac{b}{\sin \theta}$, so this becomes

$$\Delta P_y = \frac{Z_1 Z_2 e^2}{b^2} \int_0^\infty \sin^2 \theta \, dt \qquad \text{(C-12)}$$

If $v = dx/dt$ is the velocity of particle 1, and noting that
$p = -x \tan \theta$, then

$$dt = \frac{b \csc^2 \theta \, d\theta}{v} \qquad \text{(C-13)}$$

136

Substituting this into Eq (C-12) results in

$$\Delta p_y = \frac{Z_1 Z_2 e^2}{v b} \int_0^\pi \sin\theta \, d\theta \qquad (C-14)$$

or

$$\Delta p_y = \frac{2 Z_1 Z_2 e^2}{v b} \qquad (C-15)$$

In a large collection of particles where N collisions occur, however, the total momentum charge will be

$$\Delta p_y = \sum_1^N (\Delta p_y)_i \qquad (C-16)$$

If the distribution of particles is isotropic, $\overline{\Delta p_y}$ will always be zero in a large collection of particles. The quantity $(\overline{\Delta p_y})_i^2$, however, will almost certainly be non-zero and

$$\left(\Delta p_y\right)^2 = \sum_1^N \left(\Delta p_y\right)_i^2 \qquad (C-17)$$

as all the cross terms will sum to zero. This can be expressed

$$\left(\overline{\Delta p_y}\right)^2 = N\left(\overline{\Delta p_y}\right)_i^2 \qquad (C-18)$$

for N collisions. Realizing that particles can be incident from any angle and not simply along the x axis, this can

137

be extended to

$$\left(\overline{\Delta p}\right)^2 = N\left(\overline{\Delta p}\right)_i^2 \tag{C-19}$$

so that

$$d\left(\overline{\Delta p}\right)^2 = \left(\overline{\Delta p}\right)_i^2 dN \tag{C-20}$$

and $(\Delta p)_i^2$ may be taken as $(\Delta p_y)^2$ as only magnitudes are being considered.

The number of encounters with an impact parameter between b and $b + dp$ per second depend on the number density of the interacting test particles and their average energy or velocity. This will be described by a cylindrical shell of length λ where λ is the distance traveled from one individual collision to the next individual collision or the mean free path or

$$dN = 2\pi n \lambda b \, db \tag{C-21}$$

Using this in Eq (C-20) results in

$$d\left(\overline{\Delta p}\right)^2 = \left(\overline{\Delta p}\right)_i^2 2\pi n \lambda b \, db \tag{C-22}$$

$$d\left(\overline{\Delta p}\right)^2 = \left(\frac{2 Z_1 Z_2 e^2}{v b}\right)^2 2\pi n \lambda b \, db \tag{C-23}$$

or

$$d\,(\overline{\Delta p})^2 = \frac{8\pi\,Z_1^2\,Z_2^2\,e^4}{\upsilon^2}\,n\,\lambda\,\frac{db}{b} \tag{C-24}$$

Therefore, integration yields

$$(\overline{\Delta p})^2 = \frac{8\pi\,Z_1^2\,Z_2^2\,e^4}{\upsilon^2}\,n\,\lambda\,\int_{b_{MIN}}^{\lambda_D}\frac{db}{b} \tag{C-25}$$

$$(\overline{\Delta p})^2 = \frac{8\pi\,Z_1^2\,Z_2^2\,e^4}{\upsilon^2}\,n\,\lambda\,\ln\Lambda \tag{C-26}$$

where $\Lambda = \lambda_D/b_{min}$.

Equation (C-26) describes the long range encounter equivalent to a 90° scatter when

$$(\overline{\Delta p})^2 = (m\upsilon)_{INITIAL}^2 \tag{C-27}$$

The mean free path is related to cross section by

$$\lambda = \frac{1}{n\,\sigma_{c_{LR}}} \tag{C-28}$$

or

$$\sigma_{c_{LR}} = \frac{1}{n\,\lambda} \tag{C-29}$$

139

Combining Eqs (C-27) and (C-29) with Eq (C-26) yields

$$(m_1 v_1)^2 = \frac{1}{\sigma_{c_{LR}}} \frac{8\pi Z_1^2 Z_2^2 e^4}{v^2} \ln \Lambda \qquad \text{(C-30)}$$

Noting $E_1 = \frac{1}{2} m_1 v_1^2$

$$\sigma_{c_{LR}} = \frac{2\pi Z_1^2 Z_2^2 e^4 \ln \Lambda}{E_1^2} \qquad \text{(10)}$$

140

APPENDIX D

Derivation of the Enhancement Factor for Bosons

A Bose particle is distinguished from a Fermi particle by the symmetry of its eigenfunction. A Fermi particle eigenfunction is asymmetric and a Bose particle eigenfunction is symmetric (Ref 7:411). As a result, if a Boson is introduced to a Bose distribution of similar particles, there is an enhanced probability the new Boson will be born into a quantum state already populated. In fact, this increased probability is highly dependent on the existing quantum state population so that the higher the state population, the higher the increased probability or enhancement factor.

The Bose distribution is given by Eisberg and Resnick (Ref 7:432) as

$$n(E_i) = \frac{1}{e^{E_i/kT} - 1} \tag{D-1}$$

where $n(E_i)$ is the state population

E_i is the energy corresponding to this state.

and T is the species temperature.

In a dynamic system $n(E_i)$ can be replaced by $\bar{n}(E_i)$ where $\bar{n}(E_i)$ is the average quantum state population or

$$\overline{n}(E_i) = \frac{1}{e^{E_i/kT} - 1} \tag{D-2}$$

Now

$$\overline{n}(E_i) = \frac{e^{-E_i/kT}}{1 - e^{-E_i/kT}} \tag{D-3}$$

Thus

$$\overline{n}(E_i) - \overline{n}(E_i) e^{-E_i/kT} = e^{-E_i/kT} \tag{D-4}$$

$$\overline{n}(E_i) = e^{-E_i/kT}\left(1 + \overline{n}(E_i)\right) \tag{D-5}$$

so at a given quantum state 1

$$\frac{\overline{n}_1(E_{1i})}{1 + \overline{n}_1(E_{1i})} e^{E_{1i}/kT} = 1 \tag{D-6}$$

At another given quantum state 2

$$\frac{\overline{n}_2(E_{2i})}{1 + \overline{n}_2(E_{2i})} e^{E_{2i}/kT} = 1 \tag{D-7}$$

Therefore

142

$$\frac{\bar{n}_1(E_{1i})}{1 + \bar{n}(E_{1i})} \, e^{E_{1i}/kT} = \frac{\bar{n}_2(E_{2i})}{1 + \bar{n}_2(E_{2i})} \, e^{E_{2i}/kT} \tag{D-8}$$

so that

$$\frac{e^{E_{1i}/kT}}{e^{E_{2i}/kT}} = \frac{\left[\dfrac{\bar{n}_2(E_{2i})}{1 + \bar{n}_2(E_{2i})}\right]}{\left[\dfrac{\bar{n}_1(E_{1i})}{1 + \bar{n}_1(E_{1i})}\right]} \tag{D-9}$$

therefore

$$e^{(E_{1i} - E_{2i})/kT} = \frac{\bar{n}_2(E_{2i})\left(1 + \bar{n}_1(E_{1i})\right)}{\bar{n}_1(E_{1i})\left(1 + \bar{n}_2(E_{2i})\right)} \tag{D-10}$$

or

$$e^{-(E_{1i} - E_{2i})/kT} = \frac{\bar{n}_1(E_{1i})\left(1 + \bar{n}_2(E_{2i})\right)}{\bar{n}_2(E_{2i})\left(1 + \bar{n}_1(E_{1i})\right)} \tag{D-11}$$

Ignoring degeneracies, this is the Boltzmann relation
(Ref 22:63). Recall the Boltzmann relation gives the ratio
of state populations for quantum states characterized by

143

different energies E_1 and E_2. Equation (D-11) shows that each state is enhanced by a factor of $1 + \bar{n}_j(E_{ji})$ where j is the energy state to which it is being compared. Given a situation near equilibrium then, the enhancement factor is $1 + \bar{n}_j(E_j)$. Referring to Eq (D-2), this can be expressed as

$$1 + \bar{n}(E_i) = \frac{1}{e^{E_i/kT} - 1} + 1 \tag{D-12}$$

or

$$1 + \bar{n}(E_i) = \frac{1}{e^{E_i/kT} - 1} + \frac{e^{E_i/kT} - 1}{e^{E_i/kT} - 1} \tag{D-13}$$

which is

$$1 + \bar{n}(E_i) = \frac{e^{E_i/kT}}{e^{E_i/kT} - 1} \tag{D-14}$$

or

$$1 + \bar{n}(E_i) = \frac{1}{1 - e^{-E_i/kT}} \tag{D-15}$$

Photons are Bose particles. The enhancement factor for photons born through bremsstrahlung or emitted during a Compton process can be written

$$1 + \bar{n}_v(E_v) = \frac{1}{1 - e^{-E_v/kT}} \tag{26}$$

144

where

E_ν is the photon energy in the quantum state

and T is the radiation temperature.

APPENDIX E

Derivation of Bremsstrahlung

and Inverse Bremsstrahlung Cross Sections

The bremsstrahlung cross section for a nonrelativistic
Coulomb collision is given by Jackson (Ref 15:513) as

$$\sigma_\beta (E_1, \hbar\omega) \simeq \frac{16}{3} \frac{Z_2^2 e^2}{\hbar c} \left(\frac{Z_1^2 e^2}{M c^2} \right)^2 \left(\frac{c}{v} \right)^2 \frac{1}{\hbar\omega} \ln \left(\frac{\sqrt{E_1} + \sqrt{E_1 - \hbar\omega}}{\sqrt{\hbar\omega}} \right)^2 \tag{20}$$

where

    Z_1 is the charge of the radiating particle

    Z_2 is the charge of the particle providing the
       accelerating force

    M is the mass of the radiating particle

    v is the velocity of the radiating particle.

Assuming the radiating particle is an electron so that
$E_1 = E_e$, $Z_1 = 1$, and $M = m_e$. Denoting the charge of the
particle providing the accelerating force as Z and the
photon energy as $\hbar\omega = E_\nu$, Eq (20) becomes

$$\sigma_\beta (E_e, E_\nu) \simeq \frac{16}{3} \frac{Z^2 e^2}{\hbar c} \left(\frac{e^2}{m_e c^2} \right)^2 \left(\frac{c}{v} \right)^2 \frac{1}{E_\nu} \ln \left(\frac{\sqrt{E_e} + \sqrt{E_e - E_\nu}}{\sqrt{E_\nu}} \right)^2 \tag{E-1}$$

Since the fine structure constant is $\alpha = e^2/\hbar c$, and the
classical electron radius $r_0 = e^2/m_e c^2$, Eq (E-1) can be

146

written

$$\sigma_\beta(E_e, E_\nu) \simeq \frac{16}{3} Z^2 \alpha\, r_o^2 \left(\frac{c^2}{v^2}\right) \frac{2}{E_\nu} \ln\left(\frac{\sqrt{E_e} + \sqrt{E_e - E_\nu}}{\sqrt{E_\nu}}\right) \tag{E-2}$$

Multiplying both numerator and denominator by m_e and recognizing

$$\frac{2}{m_e v^2} = \frac{1}{E_e} \tag{E-3}$$

Eq (E-2) becomes

$$\sigma_\beta(E_e, E_\nu) = \frac{16}{3} Z^2 \alpha\, r_o^2 \frac{m_e c^2}{E_e E_\nu} \ln\left(\frac{\sqrt{E_e} + \sqrt{E_e - E_\nu}}{\sqrt{E_\nu}}\right) \tag{31}$$

if treated as a strict equality which is the form of the
bremsstrahlung cross section used in the text.

The unenhanced bremsstrahlung reaction rate is then

$$RR_\beta = n_i\, n_e\, (E_e)\, v\, \sigma(E_e, E_\nu) \tag{22}$$

where

n_i is ion number density

n_e is electron number density

and   v   is their relative velocity or E_e in the
frame of the ion.

The inverse bremsstrahlung cross section may be derived

147

using this reaction rate and assuming local thermodynamic equilibrium. With this assumption, the principle of detailed balance requires the reaction rates of bremsstrahlung and inverse bremsstrahlung be equal or

$$RR_\beta = RR_{I\beta} \qquad (E-4)$$

The inverse bremsstrahlung reaction rate is

$$RR_{I\beta} = n_i n_\nu(E_\nu) n_e(E_e - E_\nu) c \; \sigma_{I\beta}(E_e - E_\nu, E_\nu) \qquad (E-5)$$

where

$n_\nu(E_\nu)$ is the photon number density

and $\sigma_{I\beta}(E_e - E_\nu, E_\nu)$ is the inverse bremsstrahlung reaction rate.

The ion number density is required as ions are required to conserve momentum in the inverse bremsstrahlung process. The relative velocity between a photon and an electron must be c . Also, as inverse bremsstrahlung adds E_ν to attain an electron at energy E_e , the electron number density of interest is $n_e(E_e - E_\nu)$. Equating RR_β and $RR_{I\beta}$,

$$n_i n_e(E_e) \nu(E_e) \sigma_\beta(E_e, E_\nu) = n_i n_\nu(E_\nu) n_e(E_e - E_\nu) c \; \sigma_{I\beta}(E_e - E_\nu, E_\nu) \qquad (E-6)$$

and including the enhancement factor

$$\sigma_{I\beta}(E_e - E_\nu, E_\nu) = \frac{n_e(E_e) \upsilon(E_e) \sigma_\beta(E_e, E_\nu)}{n_e(E_e - E_\nu) n_\nu(E_\nu) c \left(1 - e^{-E_\nu/kT_r}\right)} \tag{E-7}$$

For a higher given electron energy, this can be written

$$\sigma_{I\beta}(E_e, E_\nu) = \frac{n_e(E_e + E_\nu) \sigma_\beta(E_e + E_\nu, E_\nu) \upsilon(E_e + E_\nu)}{n_e(E_e) n_\nu(E_\nu) c \left(1 - e^{-E_\nu/kT_r}\right)} \tag{E-8}$$

The electron energies are in a Maxwellian distribution so that the radio of number densities can be expressed

$$\frac{n_e(E_e + E_\nu)}{n_e(E_\nu)} = \frac{\left(\frac{2}{\sqrt{\pi}}\right) \frac{N_e}{(kT_e)^{3/2}} \left(E_e + E_\nu\right)^{1/2} e^{-(E_e + E_\nu)/kT_e}}{\left(\frac{2}{\sqrt{\pi}}\right) \frac{N_e}{(kT_e)^{3/2}} E_e^{1/2} e^{-E_e/kT_e}} \tag{E-9}$$

$$\frac{n_e(E_e + E_\nu)}{n_e(E_\nu)} = \left(\frac{E_e + E_\nu}{E_e}\right)^{1/2} e^{-E_\nu/kT_e} \tag{E-10}$$

At the new given energy

$$\sigma_\beta(E_e + E_\nu, E_\nu) = \frac{16}{3} Z^2 \alpha r_0^2 \frac{m_e C^2}{(E_e + E_\nu) E_\nu} \ln\left(\frac{\sqrt{E_e + E_\nu} + \sqrt{E_e}}{\sqrt{E_\nu}}\right) \tag{E-11}$$

Substituting these into Eq (E-8)

$$\sigma_{I\beta}(E_e, E_\nu) = \frac{16}{3} Z^2 \alpha r_0^2 \left(\frac{2}{E_e m_e}\right)^K \frac{m_e C}{E_\nu n_\nu(E_\nu)} \left(\frac{e^{-E_\nu/kT_r}}{1 - e^{-E_\nu/kT_r}}\right) \ln\left(\frac{\sqrt{E_e + E_\nu} + \sqrt{E_e}}{\sqrt{E_\nu}}\right) \tag{23}$$

149

The bremsstrahlung and inverse bremsstrahlung add or substract to the electron number density at a given value of electron energy, E_e , in four ways. The number density can be increased by bremsstrahlung as an electron originally at a higher electron energy, $E_e + E_\nu$, loses energy E_ν to the radiation field. The number density can be increased by inverse bremsstrahlung as an electron originally at a lower electron energy, $E_e - E_\nu$, is boosted to energy E_e by a photon yielding energy E_ν .

The electron population at energy E_e can be decreased through both processes also. Bremsstrahlung occurring with an electron originally at energy E_e results in an electron now at energy $E_e - E_\nu$. Inverse bremsstrahlung occurring with an electron originally at energy E_e results in an electron now at $E_e + E_\nu$. The two processes are shown schematically adding and subtracting to the electron number density in a Maxwellian distribution at a given energy E_e in Figure 18.

In Figure 18 , processes I and II are inverse bremsstrahlung and processes III and IV are bremsstrahlung. In considering the additions or subtractions in the number density, the bremsstrahlung and inverse bremsstrahlung processes need only to be counted once, however, if the distribution function is integrated over the entire range of E_e .
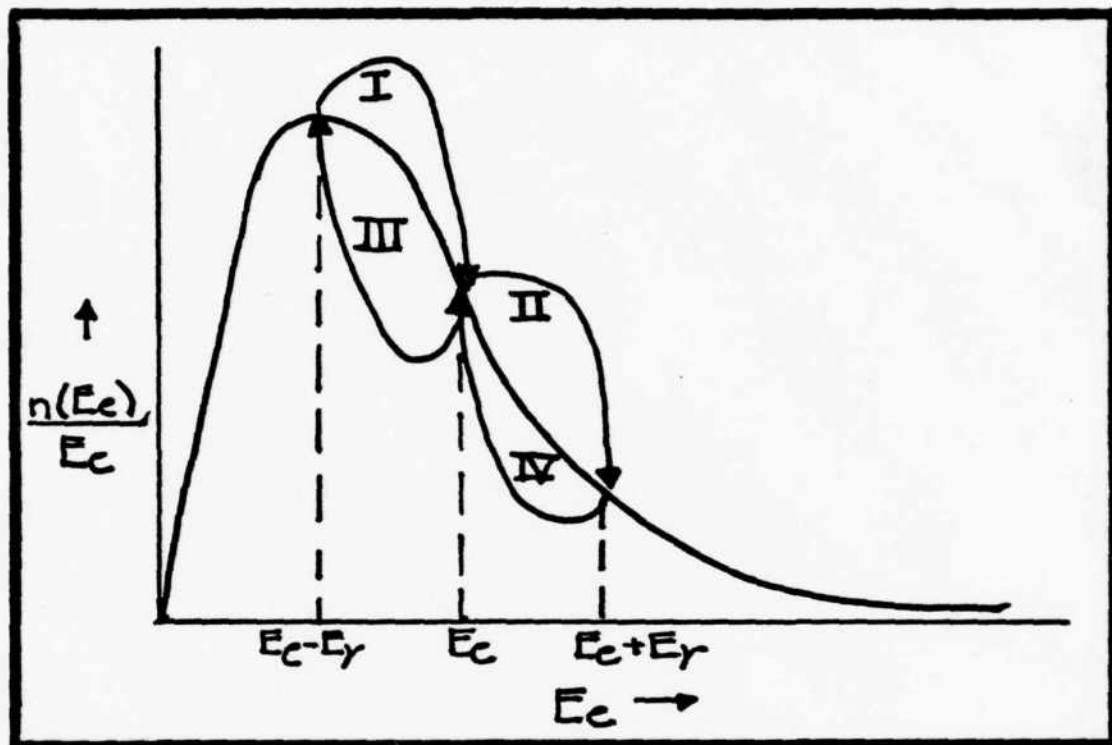
Figure 18 . Bremsstrahlung and Inverse Bremsstrahlung
Adding and Subtracting to the Electron
Number Density

151

APPENDIX F

Power Densities for Bremsstrahlung

and Inverse Bremsstrahlung with Gaunt Factors

The bremsstrahlung reaction rate denisty given in Chapter II is

$$RR_\beta = n_i n_e (E_e) v \, \sigma_A (E_e, E_v) \qquad (22)$$

The only bremsstrahlung process considered is an electron reacting to the Coulomb force of an ion. It also assumes the energy of the reaction is the energy of the electron relative to the ion.

To arrive at the reaction rate density for all energies, the electron number density and the bremsstrahlung cross section must be integrated over the entire range of energies. The electrons' energies are described by a Maxwellian distribution. The energy range of particles in a Maxwellian distribution is from 0 to infinity, which will be the limits of integration for the parameter E_e . The minimum of the resulting photon energy is 0 for corresponding to no energy being yielded to the radiation field. The maximum energy yielded to the radiation field is the entire energy of the electron or E_e . The limits of the photon energy E_v then, are 0 to E_e , which will be the limits of integration for the parameter E_v .

152

The electron velocity must be considered in the integration of the parameter E_e . This can be written

$$v = \left(\frac{2E_e}{m_e}\right)^{1/2}$$

(F-1)

Also, though, a photon is a Bose particle, so if $\bar{n}$ photons already exist in the radiation field, the bremsstrahlung process is enhanced by a factor of

$$1 + \bar{n}_v(E_v) = \frac{1}{1 - e^{-E_v/kT_r}}$$

(26)

Appendix D briefly investigates this enhancement factor.

With these considerations, Eq (22) becomes

$$RR_\beta = n_i \int_0^\infty n_e(E_e) \left(\frac{2E_e}{m_e}\right)^{1/2} dE_e \int_0^{E_e} \sigma_\beta(E_e, E_v) \frac{dE_v}{(1 - e^{-E_v/kT_r})}$$

(24)

The dimensions are inverse (volume-time).

The total energy yielded to the radiation field due to bremmstrahlung per unit volume per unit time can be attained by summing the total energy of each photon created. This can be done by multiplying the reaction rate density by photon energy and integrating over the range of possible photon energies or

$$P_\beta = n_i \int_0^\infty n_e(E_e) \left(\frac{2E_e}{m_e}\right)^{1/2} dE_e \int_0^{E_e} \sigma_\beta(E_e, E_v) E_v \frac{dE_v}{(1 - e^{-E_v/kT_r})}$$

(25)

153

Putting the explicit expressions for the Maxwellian electron distribution and the bremsstrahlung cross section into Eq (25) results in

$$P_\beta = n_i \int_0^\infty \frac{N_e}{V} \left(\frac{2}{\sqrt{\pi}}\right) \frac{1}{(kT_e)^{3/2}} E_e^{1/2} e^{-E_e/kT_e} E_e^{1/2} \left(\frac{2}{m_e}\right)^{1/2} dE_e$$

$$* \int_0^{E_e} \frac{16}{3} z^2 \alpha \, r_o^2 \frac{m_e c^2}{E_e E_\nu} \ln\left(\frac{\sqrt{E_o} + \sqrt{E_e - E_\nu}}{\sqrt{E_\nu}}\right) E_\nu \frac{dE_\nu}{(1 - e^{-E_\nu/kT_r})} \quad \text{(F-2)}$$

Multiplying and dividing twice by kTe , substituting for α and r_o , and reducing yields

$$P_\beta = n_i n_e \frac{32}{3} \left(\frac{2kT_e}{\pi m_e}\right)^{1/2} z^2 \alpha \, r_o^2 \, m_e c^2$$

$$* \int_0^\infty e^{-E_e/kT_e} \frac{dE_e}{kT_e} \int_0^{E_e} \ln\left(\sqrt{\frac{E_e}{E_\nu}} + \sqrt{\frac{E_e - E_\nu}{E_\nu}}\right) \left(\frac{1}{1 - e^{-E_\nu/kT_r}}\right) \frac{dE_\nu}{kT_e} \quad \text{(F-3)}$$

Useful simplifications can be made by defining

$$X = \frac{E_e}{E_\nu} \qquad\qquad (29)$$

$$\xi = \frac{E_\nu}{kT_e} \qquad\qquad (30)$$

$$\gamma = \frac{T_r}{T_e} \qquad\qquad (31)$$

154

Note that

$$X\xi = \frac{E_e}{kT_e}$$ (F-4)

$$\frac{\xi}{\gamma} = \frac{E_\nu}{kT_r}$$ (F-5)

By substituting these and further reducing, Eq (F-3) becomes

$$P_\beta = n_i n_e \frac{32}{3} \left(\frac{2}{\pi m_e}\right)^{1/2} Z^2 \alpha \, r_0^2 \, m_e \, c^2 \left(kT_e\right)^{1/2}$$

$$* \int_0^\infty e^{-X\xi} \frac{dE_e}{kT_e} \int_0^{E_e} \ln\left(\sqrt{x} + \sqrt{x-1}\right)\left(\frac{1}{1-e^{-\xi/\gamma}}\right) \frac{dE_\nu}{kT_e}$$ (F-6)

In preparation to change variables to x and ξ, note

$$dx = \frac{1}{\xi} d\left(\frac{E_e}{kT_e}\right)$$ (F-7)

$$d\xi = d\left(\frac{E_\nu}{kT_e}\right)$$ (F-8)

The new expression is

$$P_\beta = n_i n_e \frac{32}{3}\left(\frac{2}{\pi m_e}\right)^{1/2} Z^2 \alpha \, r_0^2 \left(kT_e\right)^{1/2}$$

$$* \int_1^\infty \int_0^\infty \xi \, e^{-X\xi} \ln\left(\sqrt{x} + \sqrt{x-1}\right)\left(\frac{1}{1-e^{-\xi/\gamma}}\right) d\xi \, dx$$ (F-9)

155

The upper limit of the inner integral is for the parameter ξ . The upper limit is established from the nature of the Maxwellian distribution. Remember $\xi = E_e/kTe$ so that a particle may have a very high energy for a given temperature so the upper limit is infinity. The lower limit of the variable x is illustrated in Figures 19 and 20, graphs of the $x = E_e/E_\nu$ versus the bremsstrahlung cross section, so that as $\sigma_\beta \to 0 \to x \to 1$ (Ref 14:512).

Reordering terms and substituting results in the form of the bremsstrahlung power density for a zero radiation temperature results in

$$P_\beta = n_i \, n_e \, \frac{32}{3} \left(\frac{2}{m_e \pi}\right)^{1/2} Z^2 \alpha \, r_o^2 \, m_e \, c^2 \left(kT_e\right)^{1/2}$$

$$* \int_0^\infty \xi \left(\frac{1}{1-e^{-1/\gamma}}\right) d\xi \int_1^\infty e^{-x\xi} \ln\left(\sqrt{x} + \sqrt{x-1}\right) dx \qquad (32)$$

The inverse bremsstrahlung reaction rate density is stated in Chapter II as

$$RR_{I\beta} = n_i \, c \int_0^\infty n_e\left(E_e\right) dE_e \int_0^\infty n_\nu\left(E_\nu\right) \sigma_{I\beta}\left(E_e, E_\nu\right) dE_\nu \qquad (27)$$

The energy limits on the second integral differ as the photons are free and are therefore in a Planckian distribution. The theoretical maximum energy is then infinity.
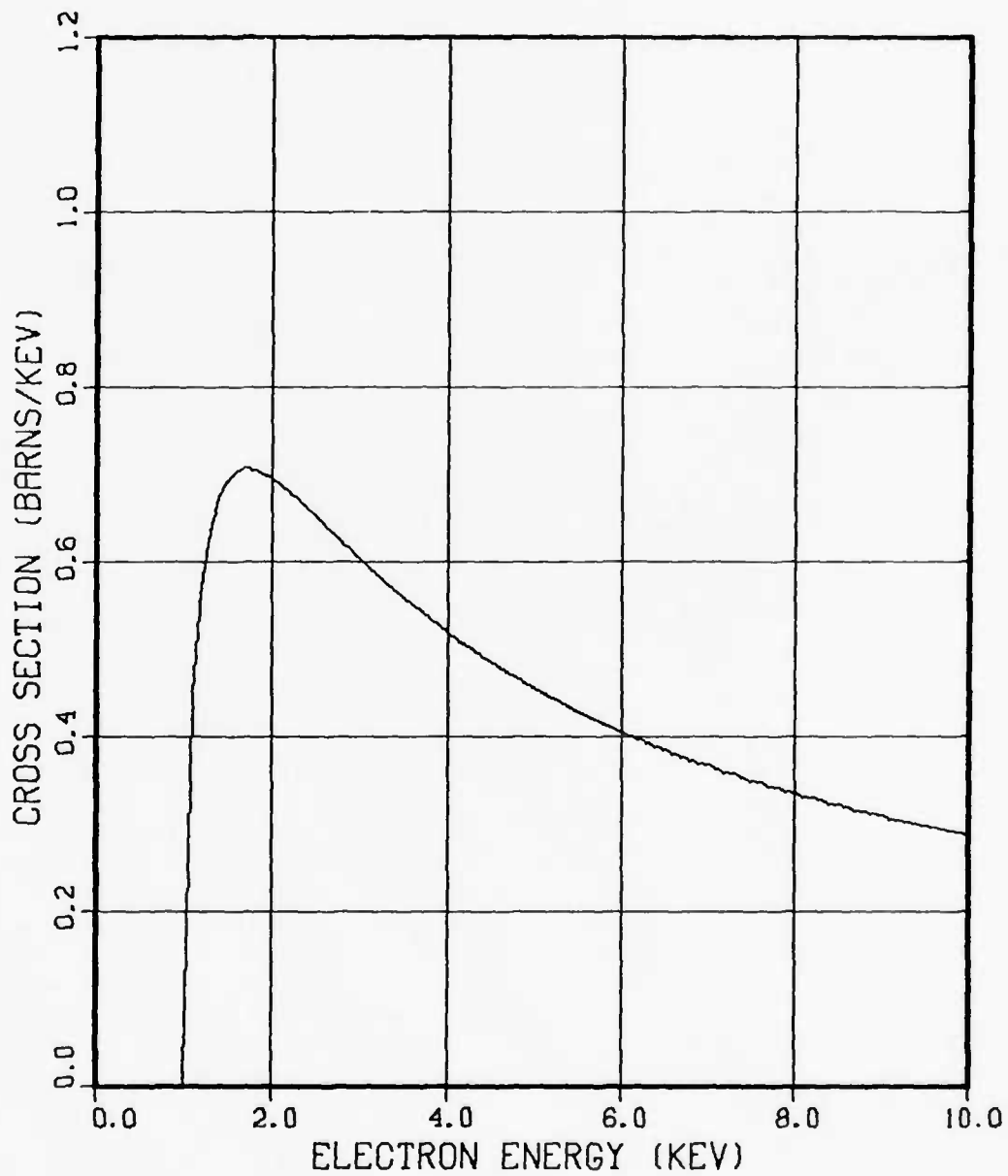
156

Figure 19 .   Bremsstrahlung Cross Section Versus
(Electron Energy)/(Photon Energy)
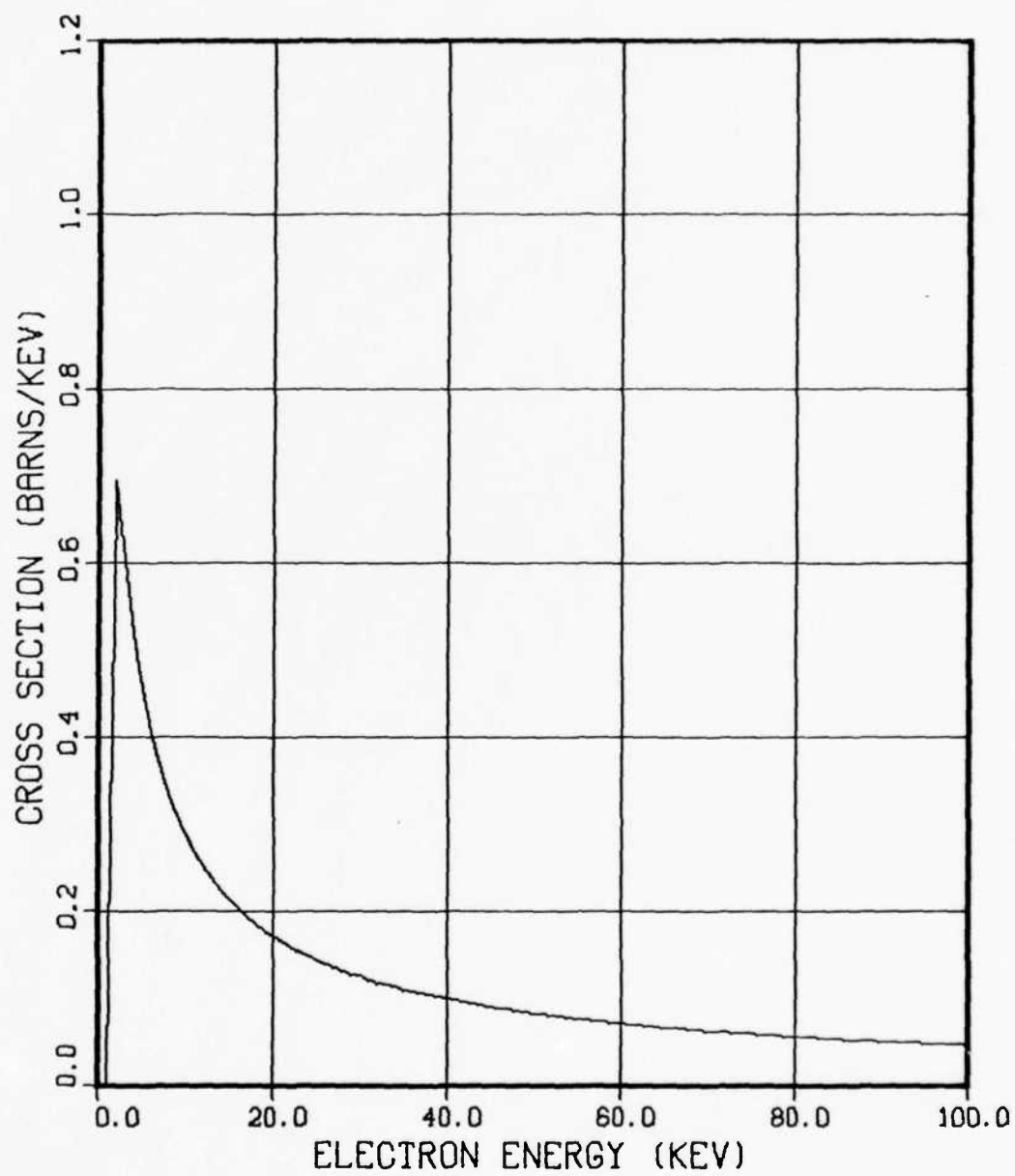
Figure 20.   Bremsstrahlung Cross Section Versus
(Electron Energy)/(Photon Energy)

158

Similar to the bremsstrahlung power density, the inverse bremsstrahlung power density can be written

$$P_{I\beta} = n_i c \int_0^\infty n_e(E_e)\, dE_e \int_0^\infty n_\nu(E_\nu)\, \sigma_{I\beta}(E_e, E_\nu) E_\nu\, dE_\nu \tag{28}$$

Substituting explicit expressions into this equation, it becomes

$$P_{I\beta} = n_i n_e \frac{32}{3}\left(\frac{2}{\pi m_e}\right)^{1/2}\left(\frac{1}{kT_e}\right)^{3/2} Z^2 \propto r_0^2 m_e c^2$$

$$* \int_0^\infty e^{-E_e/kT_e}\, dE_e \int_0^\infty \left(\frac{e^{-E_\nu/kT_r}}{1-e^{-E_\nu/kT_r}}\right) \ln\left(\frac{\sqrt{E_e+E_\nu}+\sqrt{E_e}}{\sqrt{E_\nu}}\right) dE_\nu \tag{F-10}$$

This becomes

$$P_{I\beta} = n_i n_e \frac{32}{3}\left(\frac{2}{\pi m_e}\right)^{1/2} Z^2 \propto r_0^2 m_e c^2 (kT_e)^{1/2}$$

$$* \int_0^\infty e^{-E_e/kT_e}\frac{E_e}{kT_e}\frac{dE_e}{kT_e} \int_0^\infty \left(\frac{e^{-E_\nu/kT_r}}{1-e^{-E_\nu/kT_r}}\right) \ln\left(\sqrt{\frac{E_e+E_\nu}{E_\nu}}+\sqrt{\frac{E_e}{E_\nu}}\right)\frac{dE_\nu}{E_e} \tag{F-11}$$

after multiplying numerator and denominator by $E_e(kTe)^2$. Using x, ξ, and γ from Eqs (29), (30), and (31), and noting

$$d\left(\frac{E_e}{kT_e}\right) = x\, d\xi \tag{F-12}$$

and

$$d\left(\frac{E\nu}{E_e}\right) = -\frac{1}{x^2}\, dx \tag{F-13}$$

$$P_{I\beta} = n_i\, n_e\, \frac{32}{3}\left(\frac{2}{m_e \pi}\right)^{1/2} Z^2 \propto r_0^2\, m_e\, c^2 \left(kT_e\right)^{1/2}$$

$$*\int_0^\infty e^{-x\xi} x^2 \xi\, d\xi \int_\infty^0 \left(\frac{e^{-\xi/\gamma}}{1 - e^{-\xi/\gamma}}\right) \ln\left(\sqrt{x+1} + \sqrt{x}\right) \frac{dx}{-x^2} \tag{F-14}$$

The limits of the integration over x can be seen as

$$\frac{E\nu}{E_e} = 0 \Rightarrow x = \infty \tag{F-15}$$

and

$$\frac{E\nu}{E_e} = \infty \Rightarrow x = 0 \tag{F-16}$$

Multiplying the second integral by -1 and reducing yields

$$P_{I\beta} = n_i\, n_e\, \frac{32}{3}\left(\frac{2}{m_e \pi}\right) Z^2 \propto r_0^2\, m_e\, c^2 \left(kT_e\right)^{1/2}$$

$$*\int_0^\infty e^{-x\xi} \xi\, d\xi \int_0^\infty \left(\frac{e^{-1/\gamma}}{1 - e^{-1/\gamma}}\right) \ln\left(\sqrt{x+1} + \sqrt{x}\right) dx \tag{F-17}$$

160

A transformation on the second integral may be performed by letting

$$x' = x + 1 \tag{F-18}$$

then

$$dx' = dx \tag{F-19}$$

The lower limit becomes

$$x = 0 \rightarrow x' = 1 \tag{F-20}$$

Now

$$P_{I\beta} = n_i \, n_e \, \frac{32}{3} \left(\frac{2}{m_e \pi}\right)^{1/2} Z^2 \alpha \, r_0^2 \, m_e \, c^2 \left(kT_e\right)^{1/2}$$

$$* \int_0^\infty \xi \, d\xi \int_1^\infty e^{-(x'-1)\xi} \left(\frac{e^{-\xi/\delta}}{1 - e^{-\xi/\delta}}\right) \ln\left(\sqrt{x'} + \sqrt{x'-1}\right) dx' \tag{F-21}$$

Realizing x' is simply a dummy variable of integration, Eq (F-21) can be written

161

$$P_{I\beta} = n_i\, n_e\, \frac{32}{3} \left(\frac{2}{m_e \pi}\right)^{1/2} Z^2 \alpha\, r_0^2\, m_e\, c^2 (kT_e)^{1/2}$$

$$* \int_0^\infty \xi \left(\frac{1}{1 - e^{-\xi/\gamma}}\right) d\xi \int_1^\infty e^{-\xi(x-1)}\, e^{-\xi/\gamma} \ln\left(\sqrt{x} + \sqrt{x-1}\right) dx \tag{33}$$

This is the form of inverse bremsstrahlung power density for a zero electron temperature. Note that Eqs (32) and (33) are integrated over all energies. The qualification concerning the addition or subtraction of electron numbers at a given electron energy is therefore satisfied.

Equations (32) and (33) can be expressed using a Gaunt factor $G(\gamma)_j$ where j denotes either pure bremsstrahlung or pure inverse bremsstrahlung. First, Eq (32) may be multiplied and divided by $(kT_e)^{1/2}/(kT_e - kT_r)$ yielding

$$P_\beta = n_i\, n_e\, \frac{32}{3} \left(\frac{2}{m_e \pi}\right)^{1/2} Z^2 \alpha\, r_0^2\, m_e\, c^2 \left(\frac{1}{kT_e}\right)^{1/2} \left(\frac{kT_e}{kT_e - kT_r}\right)(kT_e - kT_r)$$

$$* \int_0^\infty \xi \left(\frac{1}{1 - e^{-\xi/\gamma}}\right) d\xi \int_1^\infty e^{-x\xi} \ln\left(\sqrt{x} + \sqrt{x-1}\right) dx \tag{F-22}$$

Note that

$$\frac{kT_e}{kT_e - kT_r} = \frac{1}{1 - \gamma} \tag{F-23}$$

162

Therefore, the power density for bremsstrahlung only adding energy to the radiation field can be stated

$$P_\beta = n_i \, n_e \, \frac{32}{3} \left(\frac{2}{m_e \pi}\right)^{1/2} Z^2 \alpha \, r_0^2 \, m_e \, c^2 \left(\frac{1}{hT_e}\right)^{1/2} G(\gamma)_\beta \left(hT_e - hT_r\right) \tag{34}$$

where

$$G(\gamma)_\beta = \frac{1}{1-\gamma} \int_0^\infty \xi \left(\frac{1}{1 - e^{-\xi/\gamma}}\right) d\xi \int_1^\infty e^{-x\xi} \ln\left(\sqrt{x} + \sqrt{x-1}\right) dx \tag{35}$$

Similarly, the power density for inverse bremsstrahlung only taking energy from the radiation field

$$P_{I\beta} = n_i \, n_e \, \frac{32}{3} \left(\frac{2}{m_e \pi}\right)^{1/2} Z^2 \alpha \, r_0^2 \, m_e \, c^2 \left(\frac{1}{hT_e}\right)^{1/2} \left(\frac{kT_e}{kT_e - hT_r}\right)\left(kT_e - hT_r\right)$$

$$* \int_0^\infty \xi \left(\frac{1}{1 - e^{-\xi/\gamma}}\right) d\xi \int_1^\infty e^{-\xi(x-1)} e^{-\xi/\gamma} \ln\left(\sqrt{x} + \sqrt{x-1}\right) dx \tag{F-24}$$

or

$$P_{I\beta} = n_i \, n_e \, \frac{32}{3} \left(\frac{2}{m_e \pi}\right)^{1/2} Z^2 \alpha \, r_0^2 \, m_e \, c^2 \left(\frac{1}{hT_e}\right)^{1/2} G(\gamma)_{I\beta} \left(kT_e - kT_r\right) \tag{36}$$

163

where

$$G(\gamma)_{I\beta} = \frac{1}{1-\gamma} \int_0^\infty \xi \left(\frac{1}{1-e^{-\xi/\gamma}} \right) d\xi \int_1^\infty e^{-\xi(x-1)} e^{-\xi/\gamma} \ell_n \left(\sqrt{x} + \sqrt{x-1} \right) dx \quad (37)$$

For practical applications, the power density equations must be extended from the limiting cases of either pure bremsstrahlung or pure inverse bremsstrahlung to a combination of the competing processes. This may be done by simple subtraction. The net rate of energy flow into the radiation field is the energy that goes into this field minus the energy that leaves the field per unit time. This is

$$P_\beta - P_{I\beta} = n_i n_e \frac{32}{3} \left(\frac{2}{m_e \pi} \right)^{1/2} Z^2 \alpha r_0^2 m_e c^2 \left(\frac{1}{kT_e} \right)^{1/2} (kT_e - hT_r) G(\gamma)_\beta$$

$$- n_i n_e \frac{32}{3} \left(\frac{2}{m_e \pi} \right)^{1/2} Z^2 \alpha r_0^2 m_e c^2 \left(\frac{1}{kT_e} \right)^{1/2} (kT_e - hT_r) G(\gamma)_{I\beta}$$

$$(F-25)$$

Denoting the common coefficient by

$$A_{er}^\beta = n_i n_e \frac{32}{3} \left(\frac{2}{m_e \pi} \right)^{1/2} Z^2 \alpha r_0^2 m_e c^2 \left(\frac{1}{kT_e} \right)^{1/2}$$

$$(38)$$

164

Using explicit relationships for the fine structure constant, the classical electron radius and number densities, namely

$$\alpha = \frac{e^2}{\hbar c}$$

(F-26)

$$r_o^2 = \frac{e^2}{m_e c^2}$$

(F-27)

$$n_i = \frac{N_a}{A}\rho$$

(F-28)

and

$$n_e = Z n_i$$

(F-29)

the bremsstrahlung coupling coefficient can be expressed

$$A_{er}^{\beta} = \frac{32}{3}\left(\frac{2}{\pi m_e}\right)^{1/2}\frac{e^4 N_a^2}{\hbar c}k\left(\frac{Z^2}{A^2}\right)\frac{\rho^2 Z}{(kT_e)^{1/2}}r_o\, G(\gamma)$$

(39)

With this bremsstrahlung coupling coefficient, the power density due to bremsstrahlung processes is

$$P_\beta^{NET} = A_{er}^{\beta}\left(kT_e - kT_r\right)\left(G(\gamma)_\beta - G(\gamma)_{I\beta}\right)$$

(41)

Let

$$G(\gamma) = G(\gamma)_\beta - G(\gamma)_{I\beta}$$

(42)

165

Then referring to Eqs (35) and (37), this is

$$G(\gamma) = \frac{1}{1-\gamma} \int_0^\infty \xi \left(\frac{1}{1-e^{-\xi/\gamma}}\right) d\xi \int_1^\infty e^{-x\xi} \ln\left(\sqrt{x}+\sqrt{x-1}\right) dx$$

$$- \frac{1}{1-\gamma} \int_0^\infty \xi \left(\frac{1}{1-e^{-\xi/\gamma}}\right) d\xi \int_1^\infty e^{-x\xi} \ln\left(\sqrt{x}+\sqrt{x-1}\right) e^{-\xi\left(\frac{1}{\gamma}-1\right)} dx \quad (F-30)$$

or

$$G(\gamma) = \frac{1}{1-\gamma} \int_0^\infty \xi \left(\frac{1}{1-e^{-\xi/\gamma}}\right) d\xi \int_1^\infty e^{-x\xi} \ln\left(\sqrt{x}+\sqrt{x-1}\right)\left(1-e^{-\xi\left(\frac{1}{\gamma}-1\right)}\right) dx$$

$$(F-31)$$

Therefore

$$G(\gamma) = \frac{1}{1-\gamma} \int_0^\infty \xi \left(\frac{1-e^{-\xi\left(\frac{1}{\gamma}-1\right)}}{1-e^{-\xi/\gamma}}\right) d\xi \int_1^\infty e^{-x\xi} \ln\left(\sqrt{x}+\sqrt{x-1}\right) dx$$

$$(44)$$

This may be written

$$G(\gamma) = \int_0^\infty \frac{\xi\, d\xi\, f(\xi)\left(1-e^{-\xi\left(\frac{1}{\gamma}-1\right)}\right)}{(1-\gamma)\left(1-e^{-\xi/\gamma}\right)}$$

$$(45)$$

where

166

$$f(\xi) = \int_1^\infty \ln\left(\sqrt{x} + \sqrt{x-1}\right) e^{-\xi x} dx \tag{46}$$

so that

$$P_\beta^{NET} = A_{ec}^\beta \left(kT_e - kT_r\right) G(\gamma) \tag{43}$$

167

APPENDIX G

Evaluation of Limiting Values

of the Bremsstrahlung Gaunt Factor with Model Discussion

The Gaunt factor for bremsstrahlung may be stated

$$G(\gamma) = \frac{1}{1-\gamma} \int_0^\infty \xi \left(\frac{1 - e^{-\xi(\frac{1}{\gamma}-1)}}{1 - e^{-\xi/\gamma}} \right) d\xi \int_1^\infty e^{-\xi x} \ln \left(\sqrt{x} + \sqrt{x-1} \right) dx \tag{44}$$

At the limiting value of $\gamma = 0$, this becomes

$$G(0) = \int_0^\infty \xi \, d\xi \int_1^\infty e^{-\xi x} \ln \left(\sqrt{x} + \sqrt{x-1} \right) dx \tag{G-1}$$

which can be written

$$G(0) = \int_1^\infty \ln \left(\sqrt{x} + \sqrt{x-1} \right) dx \int_0^\infty \xi \, e^{-\xi x} d\xi \tag{G-2}$$

Now

$$\int_0^\infty \xi \, e^{-\xi x} d\xi = \frac{1}{x^2} \tag{G-3}$$

(Ref 11:310). Therefore,

$$G(0) = \int_1^\infty \frac{1}{x^2} \ln \left(\sqrt{x} + \sqrt{x-1} \right) dx \tag{G-4}$$

168

Integrating by parts yields

$$G(0) = \frac{1}{2} \int_1^\infty \frac{1}{x^{3/2}\sqrt{x-1}} \, dx \tag{G-5}$$

Letting $y^2 = x$, this becomes

$$G(0) = \int_1^\infty \frac{1}{y^2\sqrt{y^2-1}} \, dy \tag{G-6}$$

Another substitution using $Z = \frac{1}{y}$ results in

$$G(0) = \int_0^1 \frac{z}{\sqrt{1-z^2}} \, dz \tag{G-7}$$

Finally, letting $\sin\theta = x$ yields

$$G(0) = \int_0^{\pi/2} \frac{\sin\theta\cos\theta}{\sqrt{1-\sin^2\theta}} \, d\theta \tag{G-8}$$

$$G(0) = \int_0^{\pi/2} \sin\theta \, d\theta \tag{G-9}$$

so

$$G(0) = 1 \tag{47}$$

At the limiting value of $\gamma = \infty$, the bremsstrahlung Gaunt factor is

$$G(\infty) = \lim_{\gamma \to \infty} \int_0^\infty \xi \, d\xi \int_1^\infty \frac{\ln(\sqrt{x} + \sqrt{x-1}) e^{-x\xi}}{(1-\gamma)(1 - e^{-\xi/\gamma})} \left(1 - e^{-\xi(\frac{1}{\gamma} - 1)}\right) dx$$

(G-10)

or

$$G(\infty) = \int_0^\infty \xi \, d\xi \int_1^\infty \ln(\sqrt{x} + \sqrt{x-1}) e^{-x\xi} \lim_{\gamma \to \infty} \frac{(1 - e^{-\xi(\frac{1}{\gamma} - 1)})}{(1-\gamma)(1 - e^{-\xi/\gamma})} dx$$

(G-11)

Ignoring all but the first two terms of the series expansion for e , this can be written

$$G(\infty) = \int_0^\infty \xi \, d\xi \int_1^\infty \ln(\sqrt{x} + \sqrt{x-1}) e^{-x\xi} \lim_{\gamma \to \infty} \frac{\left[1 - e^{\xi(1 - \xi/\gamma)}\right]}{(1-\gamma)(1 - 1 + \xi/\gamma)} dx$$

(G-12)

Cancelling the factor ξ and applying L'Hospital's rule to evaluate the limit, this becomes

$$G(\infty) = -\int_0^\infty d\xi \int_1^\infty \ln(\sqrt{x} + \sqrt{x-1}) e^{-x\xi} (1 - e^\xi) \, dx$$

(G-13)

The integration of ξ can then be done so

$$G(\infty) = \int_1^\infty \frac{\ln(\sqrt{x} + \sqrt{x-1})}{x(x-1)} dx$$

(G-14)

170

Integrating by parts and inverting the argument of the logarithm to get a positive sign yields

$$G(\infty) = \frac{1}{2} \int_1^\infty \ln\left(\frac{x}{x-1}\right) \frac{1}{\sqrt{x}\sqrt{x-1}} \, dx \qquad \text{(G-15)}$$

Letting $e^y = \left(\frac{x}{x-1}\right)$ reduces this to

$$G(\infty) = \frac{1}{2} \int_0^\infty \frac{y}{e^{y/2} - e^{-y/2}} \, dy \qquad \text{(G-16)}$$

A further transformation letting $Z = e^{-y/2}$ gives

$$G(\infty) = -2 \int_0^1 \frac{\ln Z}{1 - Z^2} \, dZ \qquad \text{(G-17)}$$

Reference 11 from 4.231.13 has

$$\int_0^1 \frac{\ln Z}{1 - Z^2} \, dZ = -\frac{\pi^2}{8} \qquad \text{(G-18)}$$

Therefore

$$G(\infty) = \frac{\pi^2}{4} \qquad \text{(48)}$$

The bremsstrahlung Gaunt factor varies, then, between the values of 1 and $\pi^2/4$. A numerical integration of $G(\gamma)$ was performed using a two dimensional trapezoidal scheme described in Reference 13. This data was fit with the function

171

$$G(\gamma) = \frac{\pi^2}{4} - \left(\frac{\pi}{4} - 1\right) e^{-(0.2\gamma)}$$

<div align="right">(126)</div>

Figure 21 is a graph of this function.

The function $G(\gamma)$ presented in Eq (44) was integrated using a two dimensional trapezoidal integration scheme. Figure 22 is a graph of the results of this integration.

The integration was designed to attain a minimal grid size at the areas of larget $G(\gamma)$ values. As a result, areas where $G(\gamma)$ values were very small were neglected. Since the integral upper limits are both ∞ , it is felt the neglect of the aforementioned areas account for the low values of $G(\gamma)$ computed. The shape is felt to be revealing, however, and it is this shape that was duplicated using the analytic limits previously discussed.
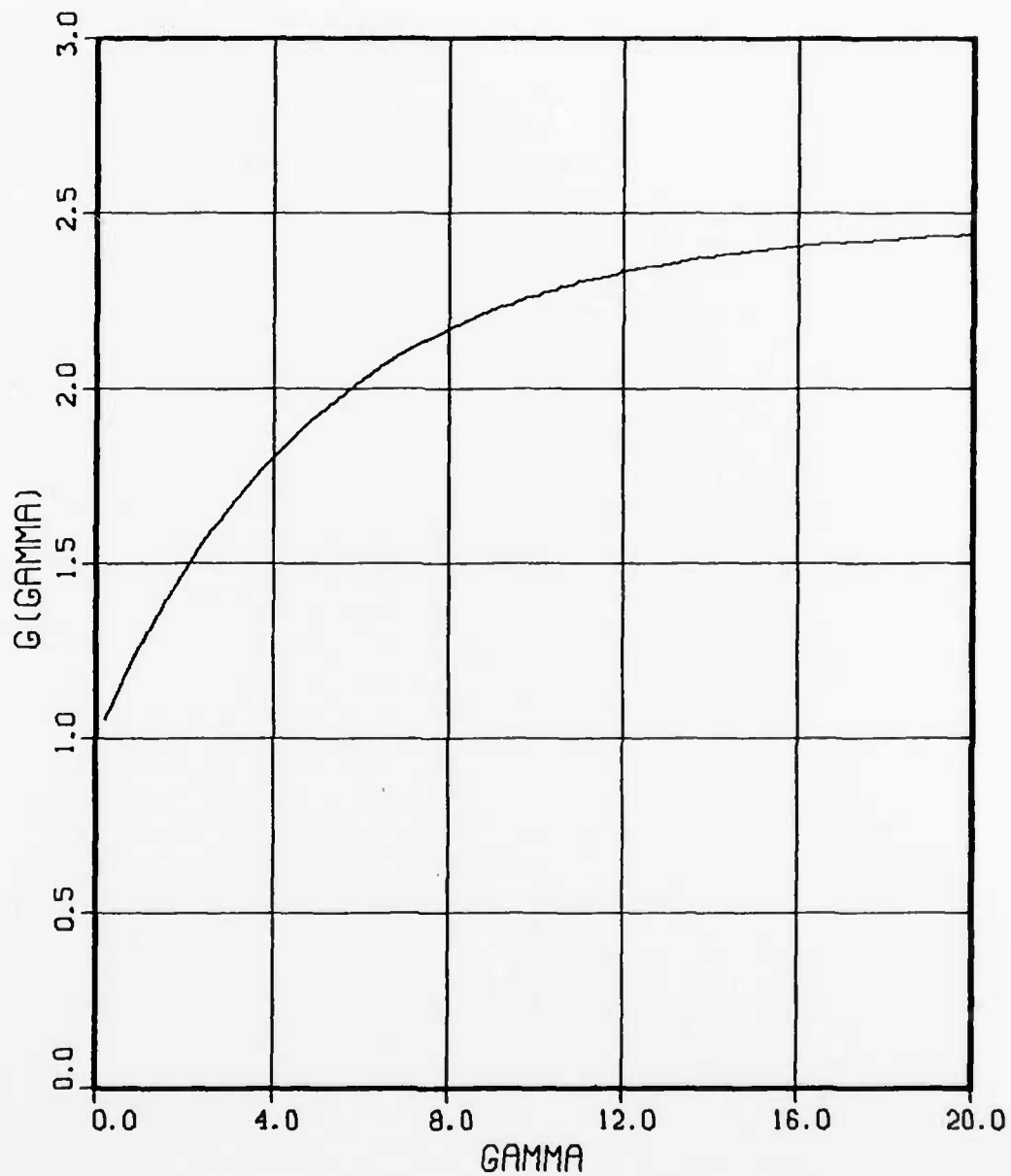
Figure 21.   Bremsstrahlung Gaunt Factor Model versus γ

173

COMPUTED CURVE FOR G(GAMMA)
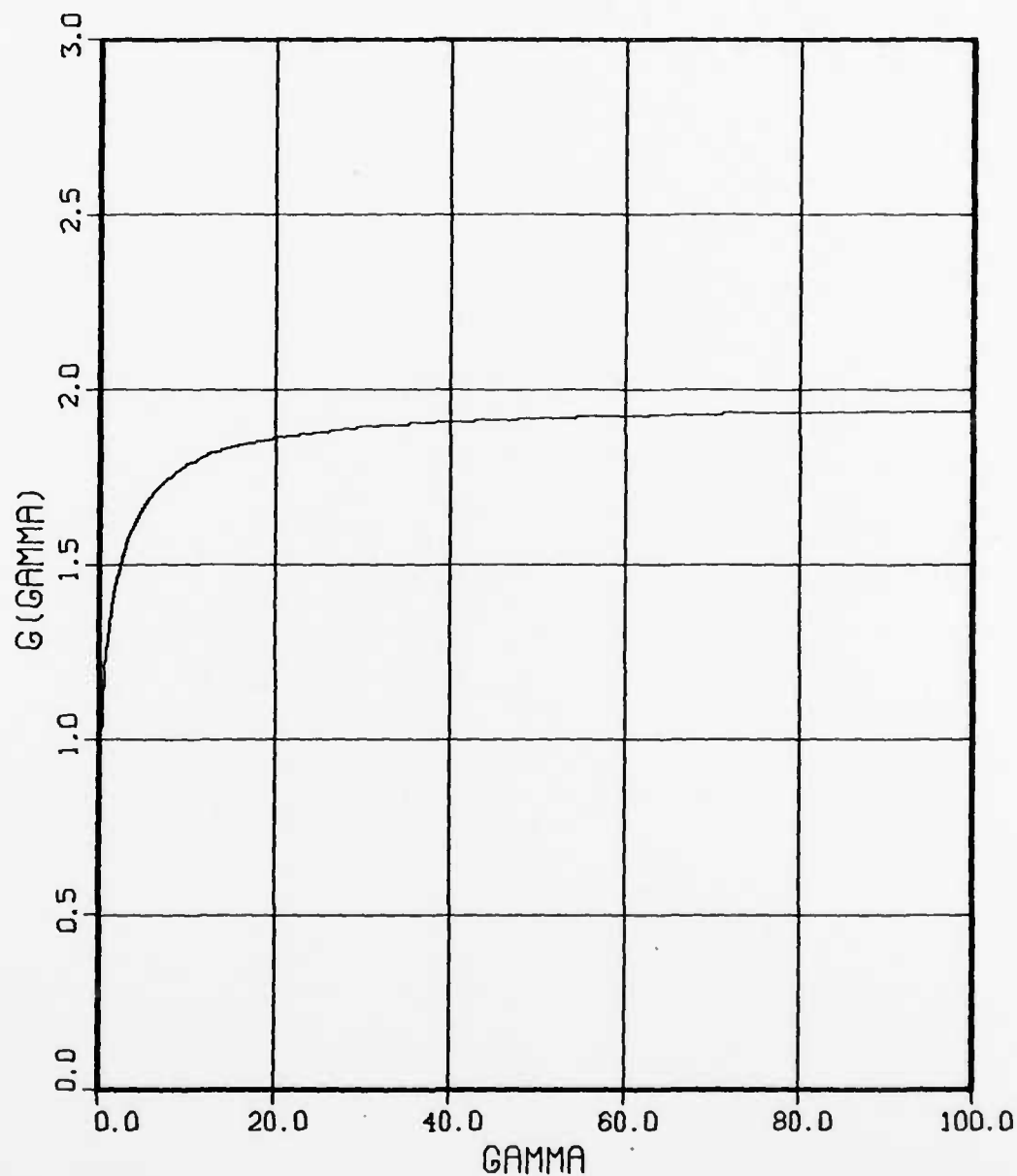
Figure 22 .   Integration Results for
the Bremsstrahlung Gaunt
Factor

174

APPENDIX H

Derivation of the Average Energy

Exchange During a Compton Collision

The average energy loss of a photon E_o in a collision with an electron may be more easily approached by first noting Figure 23, with the electron initially at rest.
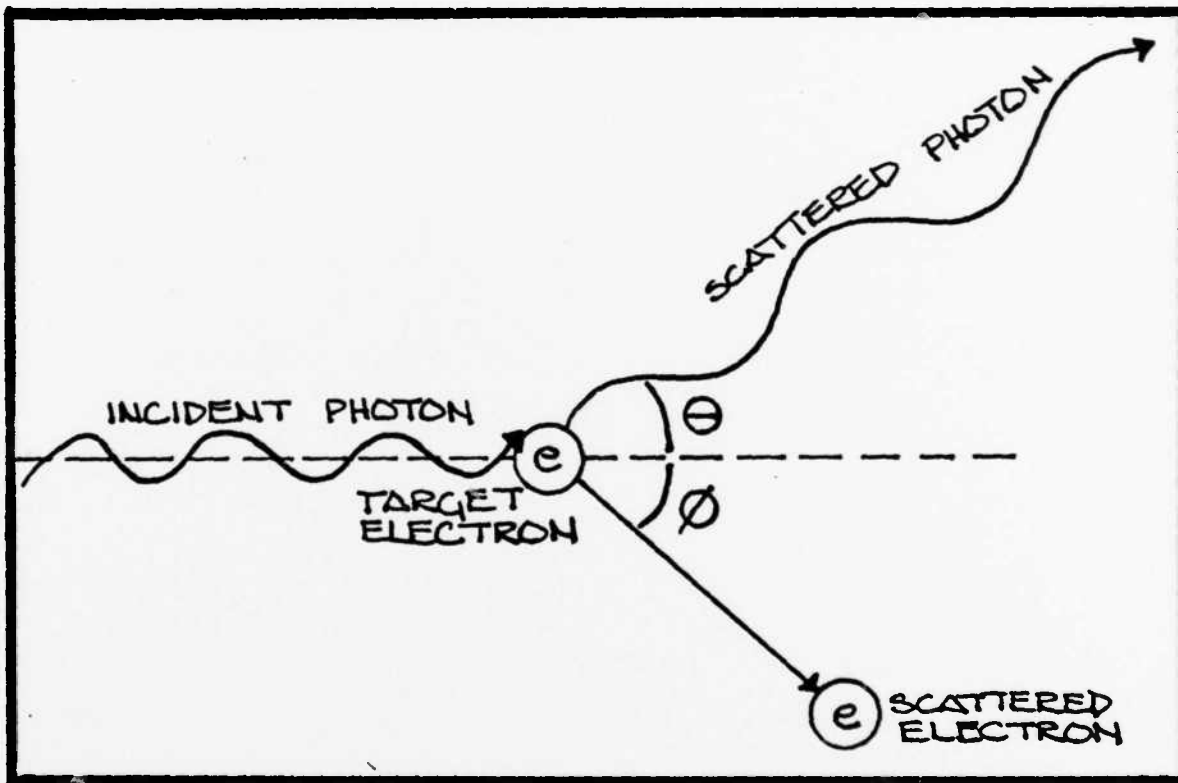
Figure 23. Symbolic Illustration of Compton Scatter with Parameters

Since energy must be conserved

$$E_\nu = E_\nu' + \frac{p^2}{2m_e}$$

(H-1)

175

and since momentum must be conserved

$$\frac{E_\nu'}{c} \sin\theta = p \sin\phi$$

(H-2)

and

$$\frac{E_\nu}{c} = \frac{E_\nu'}{c} \cos\theta + p \cos\phi$$

(H-3)

Multiplying Eqs (H-2) and (H-3) by c results in

$$E_\nu' \sin\theta = pc \sin\phi$$

(H-4)

and

$$E_\nu = E_\nu' \cos\theta + pc \cos\phi$$

(H-5)

Squaring these equations and then adding yields

$$p^2 c^2 = E_\nu^2 - 2E_\nu E_\nu' \cos\theta + E_\nu'^2$$

(H-6)

Equating the two expressions for total energy gives

$$E_e + m_e c^2 = \left(m_e^2 c^4 + p^2 c^2 \right)^{1/2}$$

(H-7)

By squaring the two sides and solving for $p^2 c^2$, it can be written

A
806
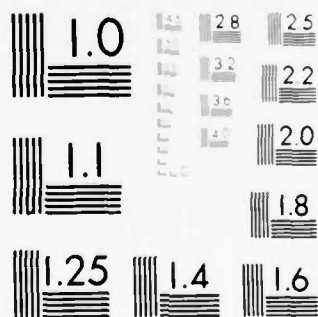
MICROCOPY RESOLUTION TEST CHART
NATIONAL BUREAU OF STANDARDS-1963-A

$$P^2c^2 = E_e^2 + 2E_e m_e c^2$$

(H-8)

Since $E_e = E_\nu - E_\nu'$ this can be stated

$$P^2c^2 = E_\nu^2 - 2E_\nu E_\nu' + E_\nu'^2 + 2m_e c^2(E_\nu - E_\nu')$$

(H-9)

Equating this to Eq (H-6),

$$2m_e c^2(E_\nu - E_\nu') = 2E_\nu E_\nu'(1-\cos\theta)$$

(H-10)

Now $\delta E = E_\nu - E_\nu'$ so that

$$\delta E = \frac{E_\nu E_\nu'}{m_e c^2}(1-\cos\theta)$$

(H-11)

This can be expressed

$$\delta E = \frac{E_\nu(E_\nu - \delta E)}{m_e c^2}(1-\cos\theta)$$

(H-12)

This can be approximated if δE is small by

$$\delta E = \frac{E_\nu^2}{m_e c^2}(1-\cos\theta)$$

(H-13)

This approximation gives values that are somewhat high as illustrated by Table 17.

177

Table 17

Values of δE Computed

Using Equations (H-12) and (H-13)

E_ν (kev)	δE from Eq 13 (kev)	δE from Eq 12 (kev)	% Error
1	8.6264×10^{-4}	8.6189×10^{-4}	0.09 %
5	2.0862×10^{-2}	2.0776×10^{-2}	0.53 %
10	8.0668×10^{-2}	8.0023×10^{-2}	0.81 %
20	3.1169×10^{-1}	3.0000×10^{-1}	3.90 %

The electron energies used to compute Table 17 are average electron energies corresponding to average scattering angles. Average scattering angles are taken from a graph in Evans (Ref 8:691).

Typical radiation temperatures in a thermonuclear plasma can be expected to be on the order of 1 kev (Ref 9:475). The error introduced by Eq (H-13) should not then be significant.

Equation (H-13) gives the energy gain by an electron at a given angle. The average energy gain may be found by integrating over angles. The Thomson cross section has an angular dependence of $(1 + \cos^2\Theta)$ so this factor must be included in the integration. This is stated

$$\langle \delta E \rangle = \frac{\bar{E}_\nu^2}{m_e c^2} \frac{\int_0^\pi (1-\cos\theta)(1+\cos^2\theta) 2\pi \sin\theta \, d\theta}{\int_0^\pi (1+\cos^2\theta) 2\pi \sin\theta \, d\theta}$$

(H-14)

or

$$\langle \delta E \rangle = \frac{\bar{E}_\nu^2}{m_e c^2} \frac{\int_0^\pi (1-\cos\theta)(1+\cos^2\theta) \sin\theta \, d\theta}{\int_0^\pi (1+\cos^2\theta) \sin\theta \, d\theta}$$

(H-15)

The upper limit of integration is the maximum angle of scatter. Letting $\cos\theta = x$

$$\langle \delta E \rangle = \frac{\bar{E}_\nu^2}{m_e c^2} \frac{\int_{-1}^1 (1-x)(1+x^2) dx}{\int_{-1}^1 (1+x^2) dx}$$

(H-16)

$$\langle \delta E \rangle = \frac{\bar{E}_\nu^2}{m_e c^2} \frac{\int_{-1}^1 (1-x+x^2-x^3) dx}{\int_{-1}^1 (1+x^2) dx}$$

(H-17)

179

$$\langle \delta E \rangle = \frac{E_\nu^2}{m_e c^2} \frac{(8/3)}{(8/3)}$$

<div align="right">(H-18)</div>

Therefore

$$\langle \delta E \rangle = \frac{E_\nu^2}{m_e c^2}$$

<div align="right">(54)</div>

APPENDIX I

Derivation of the

Compton Coupling Coefficient

The reaction rate density from Chapter II for Compton collisions assuming electrons at rest and photon energies such that $E_\nu \ll m_e c^2$ is

$$RR_c = n_e \, n_\nu(E_\nu) \, \sigma_T \, c \, \frac{1}{1 - e^{-E_\nu/hT_r}} \tag{53}$$

Using the average energy lost to the electrons from the photon during a Compton collision (Appendix H) is

$$\langle \delta E \rangle = \frac{E_\nu^2}{m_e c^2} \tag{54}$$

The power going to electrons from photons per unit volume is then

$$P_c = n_e \int_0^\infty n_\nu(E_\nu) \, \sigma_T \, c \left(\frac{E_\nu^2}{m_e c^2}\right) \frac{1}{1 - e^{-E_\nu/hT_r}} \, dE_\nu \tag{55}$$

No integration is done over electron energy as the electrons are assumed to be at rest. The Planckian photon energy distribution is

181

$$n_\nu(E_\nu) = \frac{8\pi E_\nu^2}{h^3 c^3} \frac{1}{e^{E_\nu/kT_r} - 1} \tag{I-1}$$

and the Thomson cross section is

$$\sigma_T = \frac{8}{3} \pi r_0^2 \tag{50}$$

With these, the Compton power density is

$$P_c = n_e \int_0^\infty \frac{8\pi E_\nu^2}{h^3 c^3} \frac{1}{e^{E_\nu/kT_r} - 1} \frac{8}{3} \pi r_0^2 c \frac{E_\nu^2}{m_e c^2} \frac{dE_\nu}{1 - e^{-E_\nu/kT_r}} \tag{I-2}$$

so

$$P_c = \frac{64}{3} \pi^2 \left(\frac{1}{hc}\right)^3 \frac{c n_e}{m_e c^2} r_0^2 \int_0^\infty \frac{E_\nu^2 e^{E_\nu/kT_r}}{\left(e^{E_\nu/kT_r} - 1\right)^2} dE_\nu \tag{I-3}$$

Multiplying and dividing by $(kT_r)^5$ and noting $\hbar = 2\pi h$

$$P_c = \frac{8}{3} \frac{1}{\pi} \left(\frac{1}{\hbar c}\right)^3 \frac{c n_e}{m_e c^2} r_0^2 \int_0^\infty \frac{\left(E_\nu/kT_r\right)^4 e^{E_\nu/kT_r}}{\left(e^{E_\nu/kT_r} - 1\right)^2} \left(\frac{dE_\nu}{kT_r}\right) \tag{I-4}$$

Letting $y = E_\nu/kT_r$, then

$$P_c = \frac{8}{3} \frac{1}{\pi} \left(\frac{1}{\hbar c}\right)^3 \frac{c n_e}{m_e c^2} r_0^2 \left(kT_r\right)^5 \int_0^\infty \frac{y^4 e^y}{\left(e^y - 1\right)^2} dy \tag{57}$$

182

The integral

$$\int_0^\infty \frac{y^4 e^y}{(e^y - 1)^2} dy = \int_0^\infty \frac{y^4 e^{-y}}{(1 - e^{-y})^2} dy \tag{I-5}$$

Now

$$\frac{1}{1 - e^{-y}} = \sum_{J=0}^\infty e^{-Jy} \tag{I-6}$$

so

$$\left(\frac{1}{1 - e^{-y}}\right)^2 = \left(\sum_{J=0}^\infty e^{-Jy}\right)^2 \tag{I-7}$$

which is

$$\left(\frac{1}{1 - e^{-y}}\right)^2 = \sum_{J=0}^\infty (J+1) e^{-Jy} \tag{I-8}$$

The integral then is

$$\int_0^\infty y^4 e^{-y} dy \sum_{J=0}^\infty (J+1) e^{-Jy} = \int_0^\infty \sum_{J=0}^\infty (J+1) e^{-(J+1)y} y^4 dy \tag{I-9}$$

Denoting the integral I

$$I = \sum_{J=0}^\infty (J+1) \int_0^\infty e^{-(J+1)y} y^4 dy \tag{I-10}$$

183

$$I = \sum_{J=0}^{\infty} \left[\frac{J+1}{(J+1)^5} \right] \int_0^{\infty} e^{-(J+1)y} \left[(J+1)y \right]^4 d\left[(J+1)y \right]$$

(I-11)

This is equivalent to

$$\sum_{J=1}^{\infty} \frac{1}{J^4} \int_0^{\infty} e^{-Jy} (Jy)^4 d(Jy) = \sum_{J=1}^{\infty} \frac{1}{J^4} \int_0^{\infty} e^{-z} z^4 dz$$

(I-12)

Now

$$\sum_{J=1}^{\infty} \frac{1}{J^4} = \frac{\pi^4}{90}$$

(I-13)

(Ref 1:807), and

$$\int_0^{\infty} e^{-z} z^4 dz = 4!$$

(I-14)

(Ref 11:310).   Therefore the integral is

$$4! \frac{\pi^4}{90} = \frac{4}{15} \pi^4$$

(I-15)

Integrals similar to this are discussed in Reference 23, Appendix A-11.

The Compton power density reduces to

184

$$P_c = \frac{32}{45} \pi^3 \left(\frac{1}{\hbar c}\right)^3 \frac{c\, n_e}{m_e c^2}\, r_o^2 \left(kT_r\right)^5 \tag{58}$$

This refers again to electrons at rest or pure Compton scatter.

The calculation for inverse Compton scatter interactions will not be included in this report. Inverse Compton requires that the electron have non-zero kinetic energy prior to incidence with the photon. The calculation first requires a transformation to the rest frame of the electron. The energies of the incident and emerging photons are also transformed in the electron rest frame. Rates are calculated in this reference frame and transformation back to the original frame is required. The result is (Ref 20)

$$P_{Ic} = \frac{32}{45} \pi^3 \left(\frac{1}{\hbar c}\right)^3 \frac{c\, n_e}{m_e c^2}\, r_o^2 \left(kT_r\right)^4 \left(kT_e\right) \tag{59}$$

This equation represents pure inverse Compton scatter.

The net flow of energy from electrons to radiation can be found by subtracting the power from radiation to electrons due to Compton scatter from the power from electrons to radiation due to inverse Compton scatter or

$$P_c^{NET} = P_{Ic} - P_c \tag{60}$$

Inserting Eqs (58) and (59) for P_{Ic} and P_C

$$P_c^{NET} = \frac{32}{45} \pi^3 \left(\frac{1}{\hbar c}\right)^3 \frac{c\, n_e}{m_e c^2} r_0^2 \left(kT_r\right)^4 \left(kT_e - kT_r\right) \tag{61}$$

The coupling coefficient for Compton scatter then can be written

$$A_{er}^c = \frac{32}{45} \pi^3 \left(\frac{1}{\hbar c}\right)^3 \frac{c\, n_e}{m_e c^2} r_0^2 \left(kT_r\right)^4 \tag{62}$$

By multiplying and dividing by the Stephan-Boltzmann constant, namely

$$\sigma = \frac{2\pi^5}{15} \frac{k^4}{h^3 c^2} \tag{I-16}$$

the Compton coupling coefficient can be written

$$A_{er}^c = \frac{128}{3} \pi \sigma \frac{n_e}{m_e c^2} r_0^2 T_r^4 \tag{I-17}$$

Using the relations

$$n_e = Z n_i \tag{I-18}$$

$$n_i = \frac{N_a}{A} \rho \tag{I-19}$$

186

and

$$r_0 = \frac{e^2}{m_e c^2} \qquad (I\text{-}20)$$

the Compton coupling coefficient may be expressed

$$A_{er}^c = \frac{128}{3} \pi \sigma \frac{e^2}{(m_e c^2)^2} N_a \left(\frac{Z}{A}\right) r_0 \rho T_r^4$$

$$(63)$$

APPENDIX J

Derivation of the Lagrangian Energy Equation Form

Used in the MOXNEX Code with Source Term and Specific Heat Comments

Reference 12 gives the Lagrangian form of the mass, momentum, and energy equations as

$$\frac{D\rho}{Dt} + \rho \frac{\partial v}{\partial r} = 0 \qquad (J-1)$$

$$\frac{Dv}{Dt} + \frac{1}{\rho} \frac{\partial P}{\partial r} = 0 \qquad (J-2)$$

$$\frac{DE_m}{Dt} + \frac{1}{\rho} \frac{\partial (Pv)}{\partial r} = 0 \qquad (J-3)$$

where

$$\frac{D}{Dt} = \frac{\partial}{\partial t} + v \frac{\partial}{\partial r} \qquad (J-4)$$

and

    ρ is mass per unit volume

    v is species velocity

    t is time

    r is length

    P is pressure

    E_M is total species energy per unit mass.

Multiplying the momentum equation by v yields

188

$$\upsilon \frac{\partial \upsilon}{\partial t} + \upsilon^2 \frac{\partial \upsilon}{\partial r} + \frac{\upsilon}{\rho} \frac{\partial P}{\partial r} = 0 \qquad \text{(J-5)}$$

Expanding the last derivative in the energy equation and subtracting Eq (J-5) results in

$$\frac{\partial E_m}{\partial t} + \upsilon \frac{\partial E_m}{\partial r} - \upsilon^2 \frac{\partial \upsilon}{\partial r} - \upsilon \frac{\partial \upsilon}{\partial t} + \frac{P}{\rho} \frac{\partial \upsilon}{\partial r} = 0 \qquad \text{(J-6)}$$

The total energy per unit mass can be written

$$E_m = I + \frac{1}{2} \upsilon^2 \qquad \text{(J-7)}$$

where I is the random thermal or heat energy. Note that

$$\frac{\partial E_m}{\partial t} = \frac{\partial \left(I + \frac{1}{2} \upsilon^2 \right)}{\partial t} \qquad \text{(J-8)}$$

or

$$\frac{\partial E_m}{\partial t} = \frac{\partial I}{\partial t} + \upsilon \frac{\partial \upsilon}{\partial t} \qquad \text{(J-9)}$$

and that

$$\upsilon \frac{\partial E_m}{\partial r} = \upsilon \frac{\partial \left(I + \frac{1}{2} \upsilon^2 \right)}{\partial r} \qquad \text{(J-10)}$$

so

189

$$v \frac{\partial Em}{\partial r} = v \frac{\partial I}{\partial r} + v^2 \frac{\partial v}{\partial r} \qquad (J-11)$$

Substituting these terms into Eq (J-6) yields

$$\frac{\partial I}{\partial t} + v \frac{\partial I}{\partial r} + \frac{P}{\rho} \frac{\partial v}{\partial r} = 0 \qquad (J-12)$$

If viscosity is included

$$\frac{\partial I}{\partial t} + v \frac{\partial I}{\partial r} = - \frac{P+q}{\rho} \frac{\partial v}{\partial r} \qquad (J-13)$$

Multiplying the mass conservation equation by $\frac{P+q}{\rho^2}$ and subtracting gives

$$\frac{\partial I}{\partial t} + v \frac{\partial I}{\partial r} = \left(\frac{P+q}{\rho^2} \right) \frac{\partial \rho}{\partial t} + \left(\frac{P+q}{\rho^2} \right) v \frac{\partial \rho}{\partial t} \qquad (J-14)$$

Noting that

$$v = \frac{\partial r}{\partial t} \qquad (J-15)$$

this equation becomes

$$\frac{\partial I}{\partial t} + \frac{\partial r}{\partial t} \frac{\partial I}{\partial r} = \left(\frac{P+q}{\rho^2} \right) \frac{\partial \rho}{\partial t} + \left(\frac{P+q}{\rho^2} \right) \frac{\partial r}{\partial t} \frac{\partial \rho}{\partial t} \qquad (J-16)$$

190

Now

$$\frac{\partial I}{\partial t} = \frac{P+q}{\rho^2} \frac{\partial \rho}{\partial t}$$

(J-17)

$$\frac{\partial I}{\partial t} = -(P+q)\frac{\partial}{\partial t}\left(\frac{1}{\rho}\right)$$

(J-18)

$$\frac{\partial I}{\partial t} = -(P+q)\frac{\partial V}{\partial t}$$

(J-19)

since $\rho = 1/v$. Noting

$$C_v = \frac{\partial I}{\partial T}$$

(J-20)

and

$$\frac{\partial I}{\partial t} = \frac{\partial I}{\partial T}\frac{\partial T}{\partial t} + \frac{\partial I}{\partial v}\frac{\partial v}{\partial t}$$

(J-21)

Eq (J-16) may be expressed

$$C_v \frac{\partial T}{\partial t} + \frac{\partial I}{\partial v}\frac{\partial v}{\partial t} = -(P+q)\frac{\partial V}{\partial t}$$

(J-22)

or

$$\frac{\partial T}{\partial t} = \frac{1}{C_v}\left[-\left(P+q+\frac{\partial I}{\partial V}\right)\frac{\partial V}{\partial t}\right]$$

(J-23)

191

But

$$\left(\frac{\partial I}{\partial V}\right)_T = 0 \tag{J-24}$$

for an ideal gas, so Eq (J-23) may be written

$$\frac{\partial T}{\partial t} = \frac{1}{C_v}\left[-(P+q)\frac{\partial V}{\partial t}\right] \tag{101}$$

A source term S may be added so that

$$\frac{\partial T}{\partial t} = \frac{1}{C_v}\left[\frac{\partial S}{\partial t} - (P+q)\frac{\partial V}{\partial t}\right] \tag{J-25}$$

This source term could be input from a laser, a particle
beam, or another source of energy.

   Also note that for an ideal gas

$$C_\nu = 12.47 \text{ Joules/deg-mole} \tag{J-26}$$

(Ref 23:158). This can be expressed

$$C_\nu = \frac{3}{2}/\text{part} \tag{J-27}$$

192

APPENDIX L

Derivation of Equivalent Fermi Temperature Equation

for Deuterium-Tritium Solid in the Limit of Full Degeneracy

$(T_e \rightarrow 0)$

The mean kinetic electron energy in the full limit of degeneracy is

$$\frac{3}{2} T_{e(effective)} = \frac{3}{5} \epsilon_f \tag{K-1}$$

where

T_e is the kinetic electron temperature in kev

and ϵ_f is the Fermi energy in the limit of full

degeneracy given by Zel'dovich and Raizer

(Ref 28:220) as

$$\epsilon_f = \frac{1}{8} \left(\frac{3}{\pi}\right)^{2/3} \frac{h^2}{m_e k} n_e^{2/3} \tag{K-2}$$

h   is Planck's constant in erg-sec

k   is Boltzmann's constant in erg per kev

m_e is the electron mass in grams

n_e is the elctron per cubic centimeter.

Then

$$T_{e(effective} = \frac{2}{5}\left(\frac{1}{8}\right)\left(\frac{3}{\pi}\right)^{2/3}\frac{h^2}{m_e k} n_e^{2/3} \tag{K-3}$$

193

or

$$Te_{(effective)} = 1.46 \times 10^{-18} n_e^{2/3} \qquad (K-4)$$

Now

$$n_e = \rho \frac{Z}{A} N_a \qquad (K-5)$$

since for a mix of hydrogen 50% deuterium and 50% tritium
A = 2.5 and Z = 1 . Therefore

$$Te_{(effective)} = (1.46 \times 10^{-18})(3.87 \times 10^{15}) \rho^{2/3} \qquad (K-6)$$

which is

$$Te_{(effective)} = 5.65 \times 10^{-3} \rho^{2/3} \qquad (102)$$

which is the form used in subroutine HYDRO. This temperature
represents the minimum temperature attainable for a given
density.

APPENDIX L

Derivation of the Adiabatic
Update Equation for Radiation Temperature

Adiabatic compression or expansion is described by

$$P_1 V_1^\gamma = P_2 V_2^\gamma \tag{L-1}$$

For an ideal gas, an equation of state can be written

$$PV = (\gamma - 1) I \tag{L-2}$$

where I is internal energy. If $\gamma = 4/3$ for photons, the adiabatic gas law can be stated

$$P_1 V_1 V_1^{1/3} = P_2 V_2 V_2^{1/3} \tag{L-3}$$

and the equation of state is

$$PV = \frac{1}{3} I \tag{L-4}$$

Combining these

$$I_1 V_1^{1/3} = I_2 V_2^{1/3} \tag{L-5}$$

or

$$I_2 = I_1 \left(\frac{V_1}{V_2} \right)^{1/3} \tag{L-6}$$

If $V_2 = V_1 + \Delta V$, this becomes

$$I_2 = I_1 \left(\frac{V_1}{V_1 + \Delta V} \right)^{1/3} \tag{L-7}$$

so that

$$I_2 = I_1 \left(\frac{1}{1 + \frac{\Delta V}{V_1}} \right)^{1/3} \tag{L-8}$$

Long division can then be used to evaluate the quotient, and if $\Delta V \ll 1$, the internal energy can be expressed

$$I_2 = I_1 \left(1 - \frac{\Delta V}{V_1} \right)^{1/3} \tag{L-9}$$

Again with the condition $\Delta V \ll 1$, the binomial theorem can be applied resulting in

$$I_2 = I_1 \left(1 - \frac{\Delta V}{3 V_1} \right) \tag{L-10}$$

The internal energy is related to the radiation temperature by

$$I_r = \frac{4 \sigma}{3 c} T_r^4 V \tag{L-11}$$

196

so Eq (L-10) can be written

$$T_{r_2}^4 V_2 = T_{r_1}^4 V_1 \left(1 - \frac{\Delta V}{3 V_1} \right)$$

(L-12)

or

$$T_{r_2}^4 = T_{r_1}^4 \left[\frac{\left(V_1 - \frac{\Delta V}{3} \right)}{V_2} \right]$$

(L-13)

which is equivalent to

$$T_{r_2} = T_{r_1} \left[\frac{\left(V_1 - \Delta V/3 \right)}{V_2} \right]^{1/4}$$

(L-14)

and can be expressed

$$T_r^{(n+1)} = T_r^{(n)} \left[\frac{\left(V^{(n)} - \Delta V/3 \right)}{V^{(n+1)}} \right]^{1/4}$$

(106)

for use in an iterative scheme where n denotes iteration
number.

APPENDIX M

Geometry Models for

Geometry Subroutines of Subprogram ALPHA1

The purpose of subroutines XYT3 thorugh XYT9 and
GETA through GETC in subprogram ALPHA1 is to find the distance
an alpha particle travels within a zone. Knowing this dis-
tance, energy deposition modelling for the zone is done by
subroutines FINDDS and ELOSS. This Appendix will briefly
discuss and illustrate geometry used in subprogram ALPHA1
(Ref 16).

The alpha particles born in a zone are assumed to be
born at zone center. The angular paths they can take are
illustrated in Figure 24. The angular paths are most finely
divided near $\pi/2$.

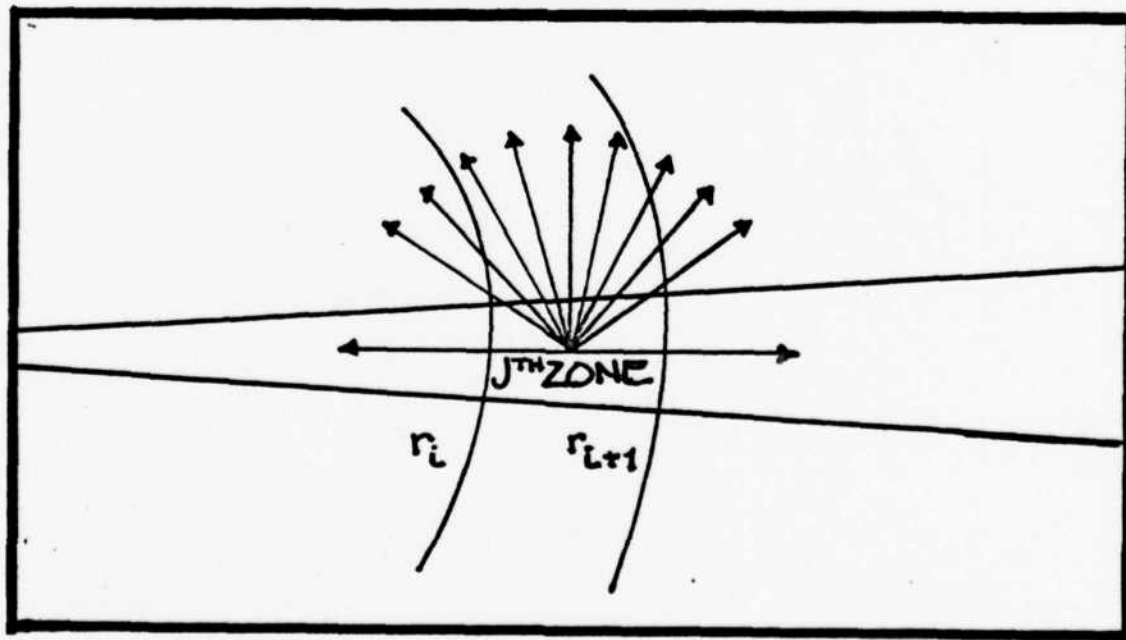Figure 24.   Angular Directions for Alpha Particles
Leaving the jth Zone

198

Two coordinate systems are used. One is for motion from the center of the zone and one is for motion from a zone boundary as it crosses the boundary.

If the angle Θ is $\pi/2$, subroutine XYT3 is called. The parameter DIST is returned as the distance traveled in the zone.
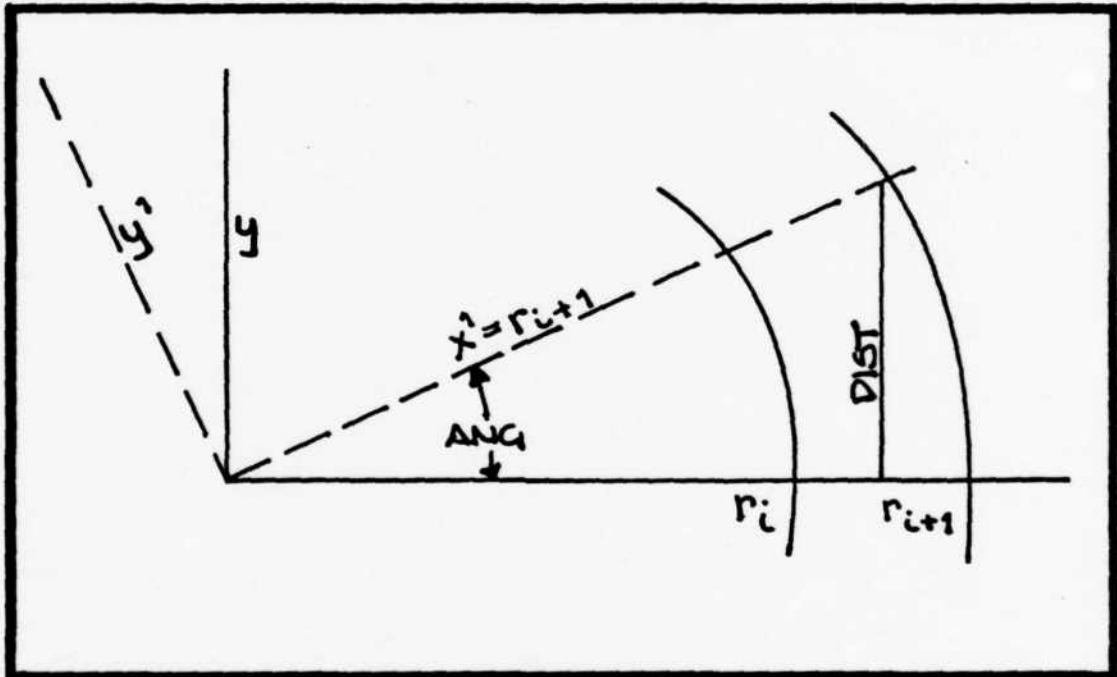
Figure 25. Geometry for Subroutine XYT3

If the angle θ is greater than $\pi/2$ but not π, subroutine XYT4 is called. Here the alpha particle may either intercept the next inner zone or the next outer zone. The decision is made on the value of the discriminant of the solution of the equation of the line of travel with the circle representing the next inner zone. Subroutines GETA, GETB, and GETC are called to compute this discriminant. If the particle path intercepts the next inner zone wall, subroutine XYT4A is called.
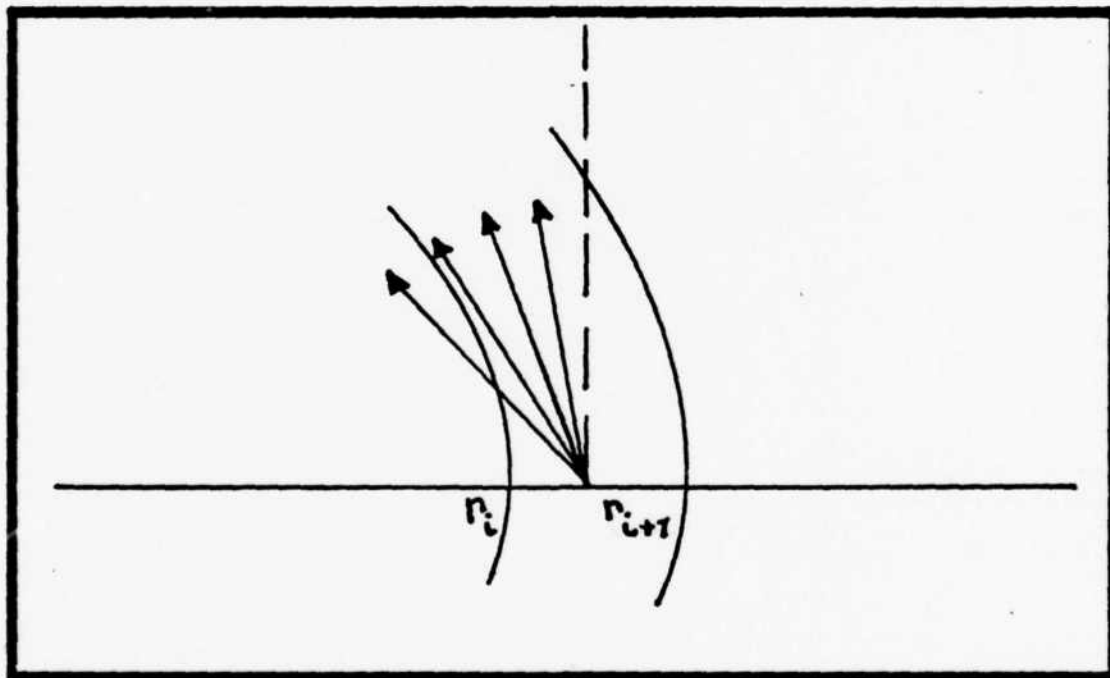
Figure 26. Geometry for Subroutine XYT4
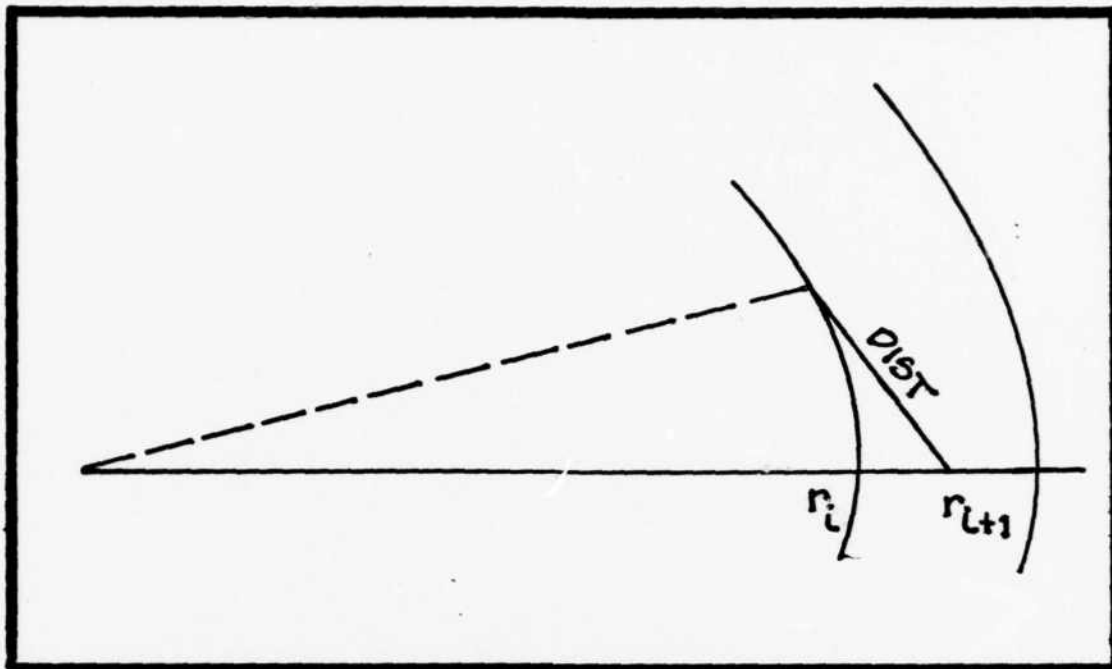
Figure 27.   Geometry for Subroutine XYT4A

If the next outer zone wall is intersected, subroutine XYT4B is called.   In both cases, DIST is returned as the distance traveled in the zone.

Subroutine XYT5 is used if angle θ is π.   If the center of the microsphere is intercepted, the direction of the alpha particle path is reversed and the alpha particle begins to travel outward.   Again, DIST is the distance traveled in the zone.

201
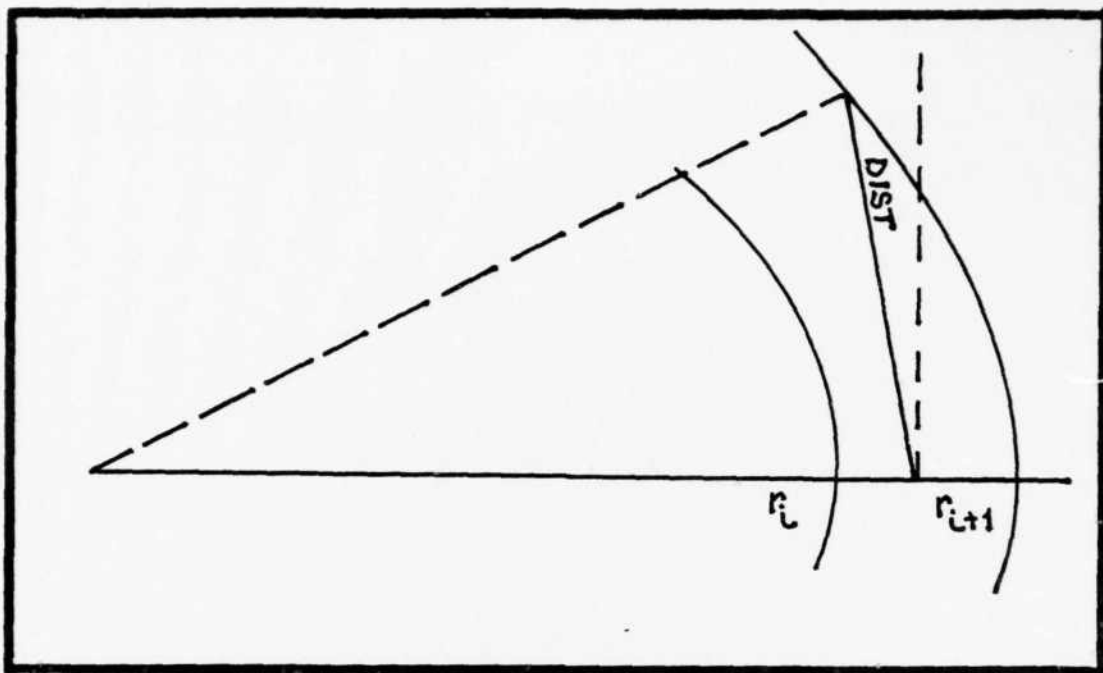
Figure 28. Geometry for Subroutine XYT4B
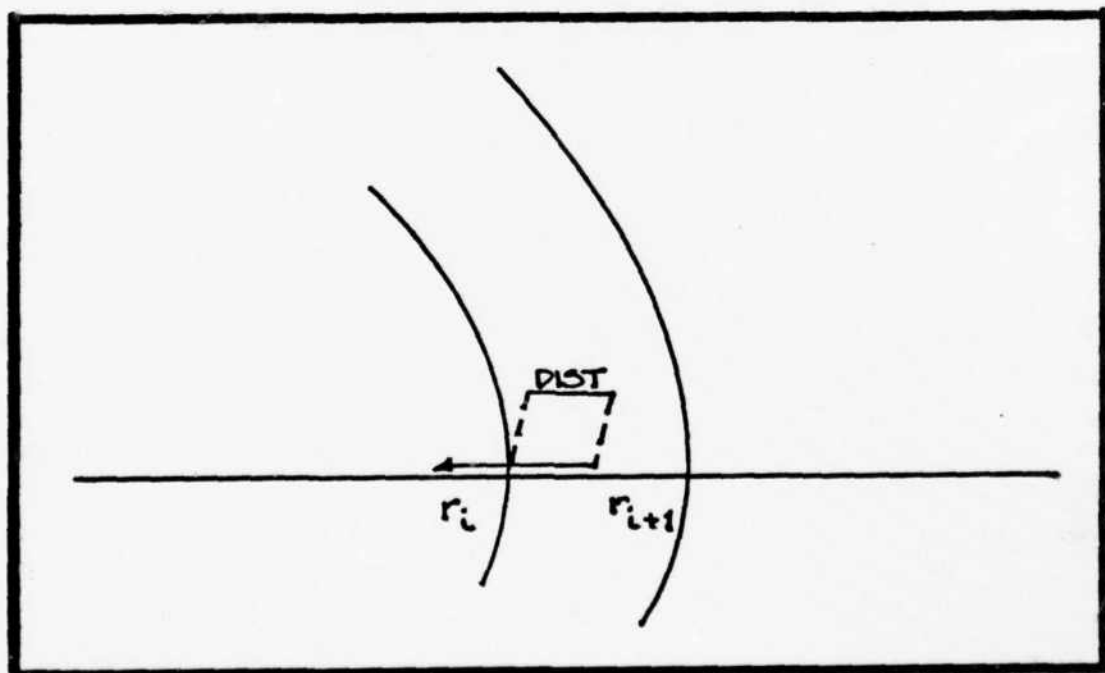
Figure 29. Geometry for Subroutine XYT5

Subroutine XYT6 is called if angle Θ is 0 . The parameter DIST is seen from Figure 30.
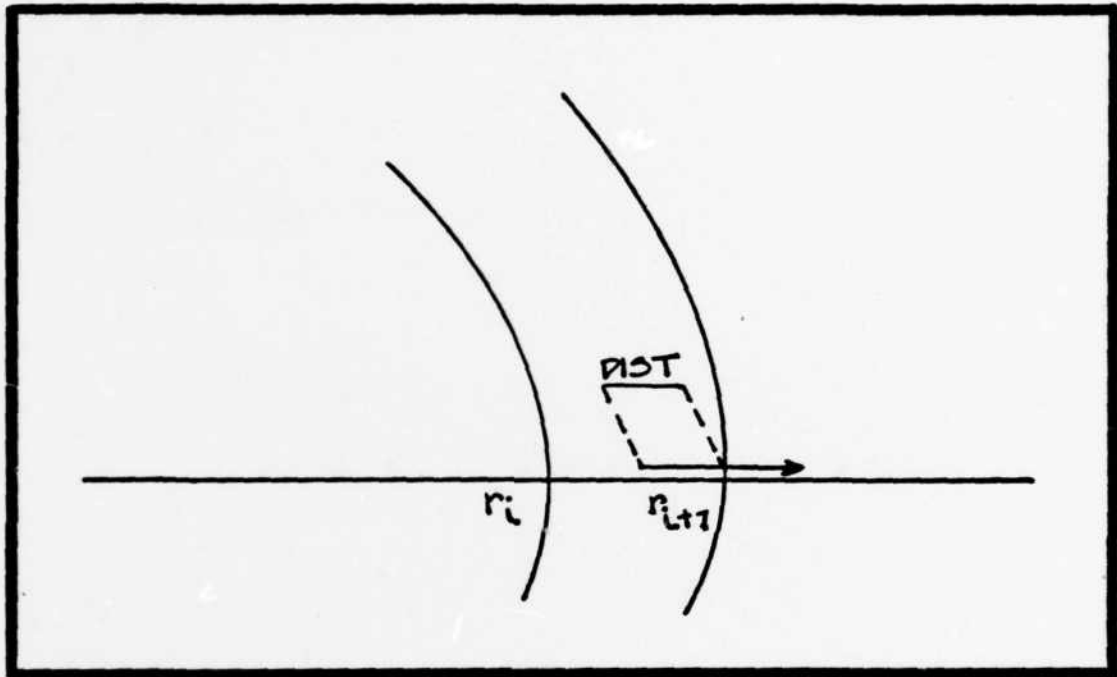
Figure 30. Geometry for Subroutine XYT6

If angle Θ is greater than 0 but less than π/2 , subroutine XYT7 is used. The only possibility for the path of the particle is to intercept the wall of the next outer zone. The discriminants of the solution of the equation of the line of travel with the circle representing the next outer zone are required to compute DIST. Sub-routines GETA, GETB, and GETC provide these.

203
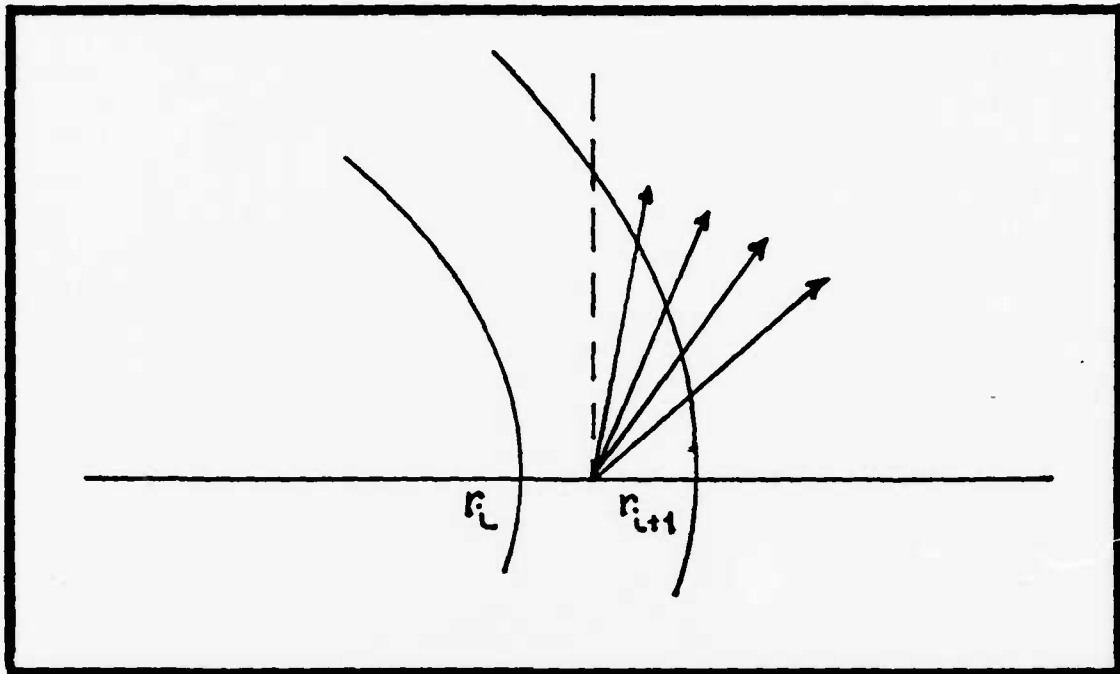
Figure 31.   Geometry for Subroutine XYT7

Subroutine XYT8 is similar in function to subroutine
XYT4 but is written for the case where subsequent motion of
the particle is located on a zone boundary instead of a
cell center.   In the instance the alpha particle is travel-
ing inward, it may intersect the next inner zone or the
next outer zone.   Therefore, subroutines XYT4A and XYT4B
are used.   Subroutine XYT8 is used only for angles between
0 and π .

If subsequent motion from a cell boundary is at the
angle π , subroutine XYT9 is used.   As with subroutine
XYT5, if the microsphere center is reached the path of the
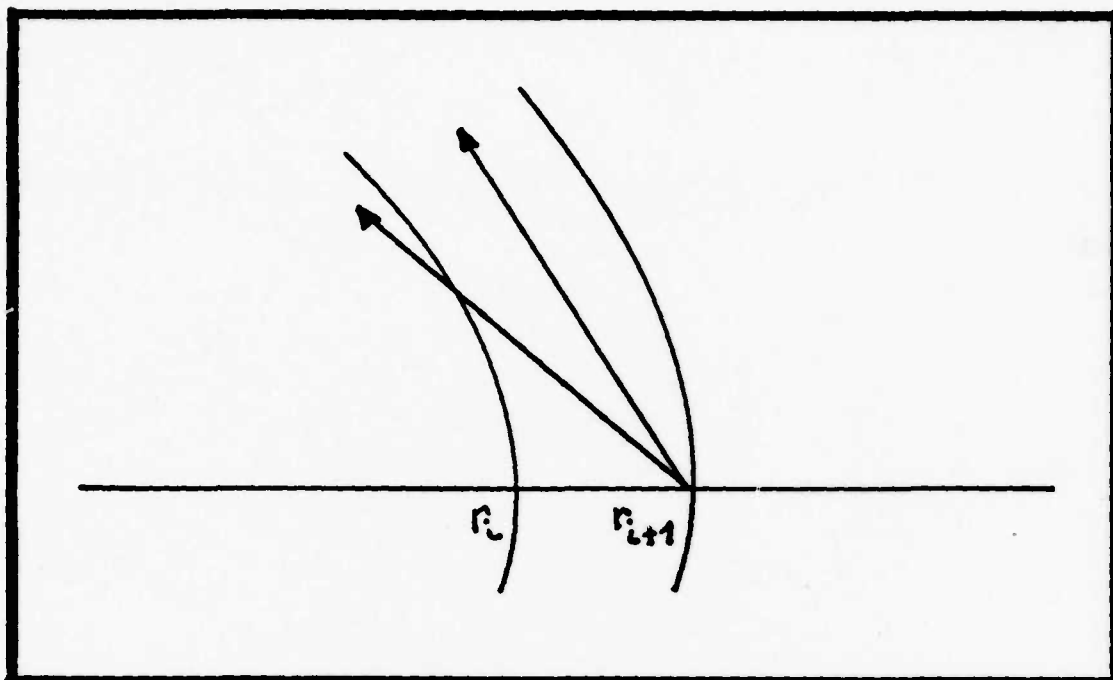
Figure 32. Geometry for Subroutine XYT8
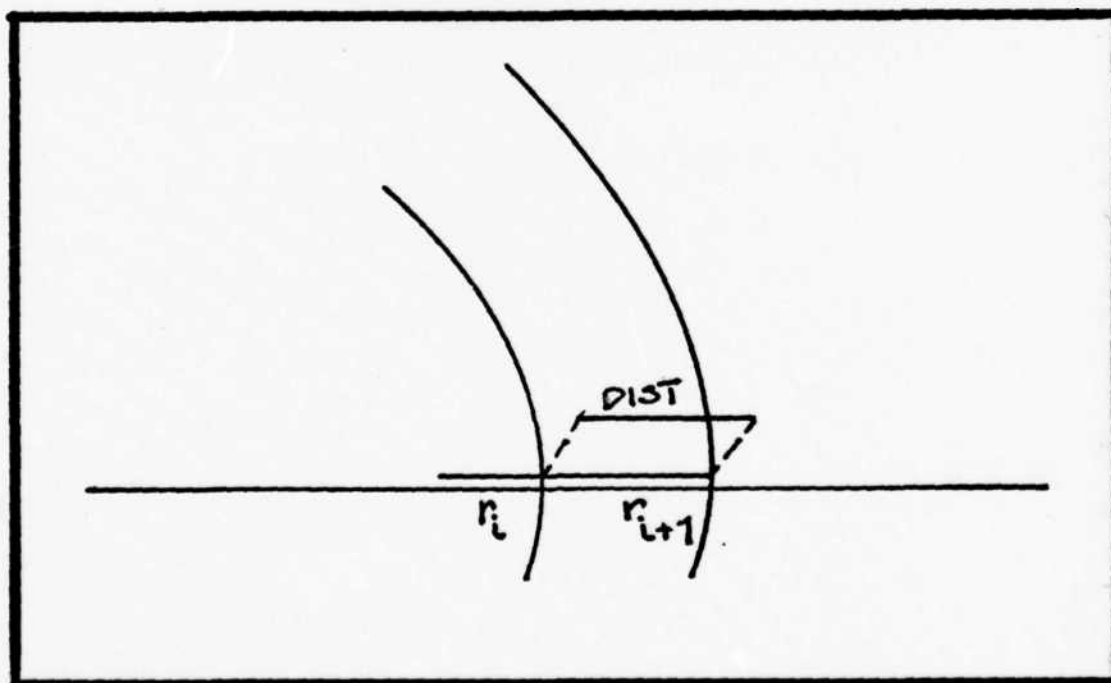
Figure 33. Geometry for Subroutine XYT9

particle is reversed and the particle begins to travel outward. If the angle Θ is 0 , subroutine XYT6 returns the distance in the zone.

The subroutines GETA, GETB and GETC return the coefficients a , b , and c from the quadratic equation

$$a x^2 + bx + c = 0$$

(M-1)

These coefficients are

$$a = 1 + \frac{1}{\tan^2 \Theta}$$

(M-2)

$$b = \frac{-2 (x_0) \tan (\pi - \Theta)}{\tan^2 \Theta}$$

(M-3)

and

$$c = -r_j^2 + \frac{x_0 \tan^2 (\pi - \Theta)}{\tan^2 \Theta}$$

(M-4)

where

r_j is the radius of zone r_i or r_{i+1}

x_0 is the original position of the alpha particle.

206

APPENDIX N

Derivation of the

Electron Temperature Update Equations

The random thermal energy possessed by electrons is

$$E_{rte} = \frac{3}{2} N_e k T_e \tag{N-1}$$

or

$$E_{rte} = \frac{3}{2} n_e k T_e V \tag{N-2}$$

In a spherical volume, this may be expressed

$$E_{rte} = \frac{4}{3} \pi \left(r_+^3 - r_-^3 \right) \frac{3}{2} n_e k T_e \tag{N-3}$$

where

r_+ is the outside annulus radius

r_- is the inside annulus radius.

The energy may be calculated knowing the radii of the volume element, the electron number in that volume, and the electron species temperature. In a non-equilibrium situation, an updated temperature may be calculated using the conservation of energy expressed in a flux conservative scheme. In a spherical volume, this can be written

$$\frac{4}{3}\pi\left(r_+^3 - r_-^3\right)\frac{3}{2}n_e k T_e^{n+1} = \frac{4}{3}\pi\left(r_+^3 - r_-^3\right)\frac{3}{2}n_e k T_e^n$$

$$+ 4\pi r_-^2 F_- \Delta t - 4\pi r_+^2 F_+ \Delta t$$

(N-3)

where

F_+ is the outward energy flux

F_- is the inward energy flux

Δt is the time increment.

Flux is in energy/area/time. Figure 34 illustrates the flux entering and leaving a spherical volume element.
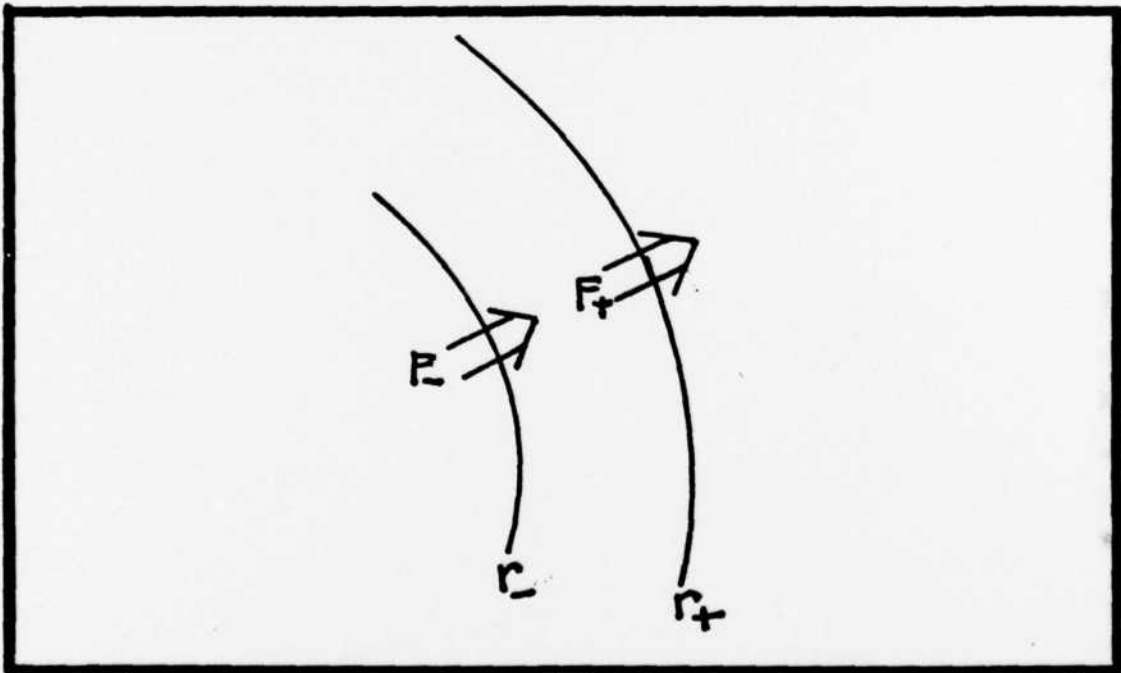
Figure 34. Flux Entering and Leaving A
Spherical Volume Element

Fick's law models flux across a gradient using a diffusion coefficient K_e and may be stated in one dimension as

$$F = -K_e \left(\frac{dT_e}{dr} \right) \tag{N-4}$$

so

$$F \simeq -K_e \left(\frac{\Delta T_e}{\Delta r} \right) \tag{N-5}$$

Using this, Eq (N-3) becomes

$$\frac{4}{3} \pi \left(r_+^3 - r_-^3 \right) \frac{3}{2} n_e k T_e^{n+1} = \frac{4}{3} \pi \left(r_+^3 - r_-^3 \right) \frac{3}{2} n_e k T_e^n$$

$$+ 4\pi \left(r_+^2 K_e \left. \frac{\Delta T_e}{\Delta r} \right|_{r_+} - r_-^2 K_e \left. \frac{\Delta T_e}{\Delta r} \right|_{r_-} \right) \Delta t \tag{N-6}$$

This can be simplified to

$$\frac{3}{2} n_e k \left(T_e^{n+1} - T_e^n \right) = \frac{3}{r_+^3 - r_-^3} \left(r_+^2 K_e \left. \frac{\Delta T_e}{\Delta r} \right|_{r_+} - r_- K_e \left. \frac{\Delta T_e}{\Delta r} \right|_{r_-} \right) \Delta t \tag{N-7}$$

If

$$r_+ = r_- + dr \tag{N-8}$$

$$r_+^3 - r_-^3 = 3 r_-^2 dr \tag{N-9}$$

$$r_+^3 - r_-^3 \simeq 3r^2 \Delta r \tag{N-10}$$

Substituting this with further manipulations into Eq (N-7), the result is

$$T_e^{n+1} = T_e^n + \frac{2}{3r_- \Delta r n_e k}\left(r_+^2 K_e \frac{\Delta T_e}{\Delta r}\bigg|_{r_+} - r_-^2 K_e \frac{\Delta T_e}{\Delta r}\bigg|_{r_-}\right)\Delta t \tag{N-11}$$

Defining

$$FLUXP = r_+^2 K_e \frac{\Delta T_e}{\Delta r}\bigg|_{r_+} \tag{N-12}$$

and

$$FLUXM = r_-^2 K_e \frac{\Delta T_e}{\Delta r}\bigg|_{r_-} \tag{N-13}$$

this becomes

$$T_e^{n+1} = T_e^n + \frac{2}{3r_-^2 \Delta r n_e k}\left(FLUXP - FLUXM\right)\Delta t \tag{N-14}$$

The term n_e is in spherical coordinates

$$n_e = \frac{N_e}{V} \tag{N-15}$$

210

which is

$$n_e = \frac{N_e}{4\pi(r_+^3 - r_-^3)} \qquad \text{(N-16)}$$

or

$$n_e = \frac{N_e}{(4\pi)3r_-^2\Delta r} \qquad \text{(N-17)}$$

Using this result, Eq (N-14) becomes

$$T_e^{n+1} = T_e^n + \frac{8\pi}{k N_e}\left(FLUXP - FLUXM\right)\Delta t \qquad \text{(N-18)}$$

This is the equation used to model electron heat conduction in subroutine HTFLX of the MOXNEX program.

Equipartition of energy between the electrons and ions is also computed in subroutine HTFLX. Spitzer describes the equipartition of energy between two groups of particles in Reference 26, assuming both particle groups have Maxwellian velocity distributions, as

$$\frac{dT_e}{dt} = \frac{T_i - T_e}{t_{eq}} \qquad \text{(N-19)}$$

where t_{eq} is the time of equipartition. This may be written in finite difference form as

211

$$T_e^{n+1} = T_e^n + \frac{(T_i^n - T_e^n)\Delta t}{t_{eq}} \qquad \text{(N-20)}$$

Spitzer gives the time of equipartition in Reference 26 as

$$t_{eq} = \frac{3 m_e m_i k^{3/2}}{8 (2\pi)^{1/2} n_i Z_e^2 Z_i^2 e^4 \ln \Lambda_{ei}} \left(\frac{T_e}{m_e} + \frac{T_i}{m_i}\right)^{3/2} \qquad \text{(N-21)}$$

where

m_e is the electron mass

m_i is the average ion mass

n_i is the ion number density

Z_e is the charge on the electron

Z_i is the average charge on the ion

e   is the unit of electric charge

Λ_{ei} is the ratio

T_e is the average electron temperature

T_i is the average ion temperature.

Since $m_e \ll m_i$ and assuming T_e is not $\ll T_i$, the term T_i/m_i will contribute insignificantly to the time of equipartition and may be disregarded. Using a frequency representation $\nu_{eq} = 1/t_{eq}$, Eq (N-21) becomes

$$\nu_{eq} = \frac{8(2\pi)^{1/2} m_e^{1/2} n_i Z_e^2 Z_i^2 e^4 \ln \Lambda_{ei}}{3 m_i (kT_e)^{3/2}}$$

(N-22)

Noting the two relations

$$n_i = \frac{\rho N_a}{A}$$

(N-23)

and

$$m_i = \frac{A}{N_a}$$

(N-24)

where

ρ is the density

N_a is Avagadro's number

A is the ion mass number

and also that $Z_e = 1$, Eq (N-22) may be written

$$\nu_{eq} = \frac{8(2\pi)^{1/2} e^4 N_a^2 Z^2 \rho \ln \Lambda_{ei}}{3 A^2 (kT_e)^{3/2}}$$

(82)

Equation (N-20) can be written

$$T_e^{n+1} = T_e^n + \nu_{eq} (T_i^n - T_e^n) \Delta t$$

(N-25)

This is the equation used to model equipartition of energy between electrons and ions in subroutine HTFLX of the MOXNEX code.

213

APPENDIX O

Derivation of the Radiation Temperature Update Equations

The energy in a radiation field is

$$E_{rf} = \frac{4\sigma}{c} T_r^4 V \qquad (O-1)$$

where

   σ is the Stephan-Boltzmann constant

   c is the speed of light

   T_r is the radiation temperature

   V is the containing volume.

The quantity $4\sigma/c$ is often denoted as the constant a or

$$E_{rf} = a T_r^4 V \qquad (O-2)$$

In spherical coordinates, this may be expressed

$$E_{rf} = \frac{4}{3}\pi \left(r_+^3 - r_-^3\right) a T_r^4 \qquad (O-3)$$

where

   r_+ is the outside annulus radius

   r_- is the inside annulus radius.

The energy may be calculated knowing the radii of the volume
element and the radiation temperature in the volume. In a

214

non-equilibrium situation, an updated temperature may be calculated using the conservation of energy in a flux conservative scheme. For a spherical volume, this can be written

$$\frac{4}{3} \pi (r_+^3 - r_-^3) a \, T_r^{4\,(n+1)} = \frac{4}{3} \pi (r_+^3 - r_-^3) a \, T_r^{4\,(n+1)}$$

$$+ \, 4\pi r_-^2 \, F_- \, \Delta t \; - \; 4\pi r_+^2 \, F_+ \, \Delta t$$

(0-4)

where

 F_+ is the outward energy flux at r_+ in energy/area/time

 F_- is the negative of the outward energy flux at r_- in energy/area/time

 Δt is the time increment = total time^{n+1} - total time^{n}

Figure 35 illustrates the flux entering and leaving a spherical volume.

Fick's law models flux across a gradient using a diffusion coefficient K_r and may be stated in one dimension as

$$F = - K_r \left(\frac{dT_r}{dr} \right)$$

(0-5)

or
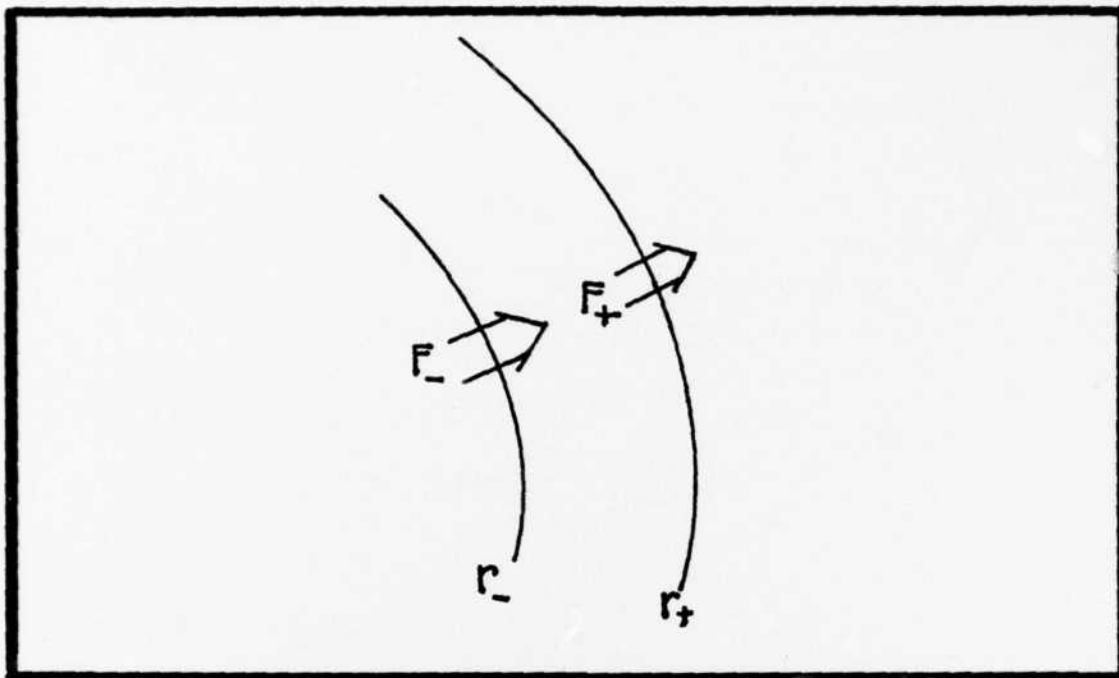
Figure 35. Flux Entering and Leaving A
Spherical Volume Element

$$F \simeq - K_r \left(\frac{\Delta T_r}{\Delta r} \right)$$

(0-6)

Using this equation (0-4) becomes

$$\frac{4}{3} \pi \left(r_+^3 - r_-^3 \right) a \, T_r^{+(n+1)} = \frac{4}{3} \pi \left(r_+^3 - r_-^3 \right) a \, T_r^{(n)}$$

$$+ 4 \pi \left(r_+^2 \, K_r \left. \frac{\Delta T_r}{\Delta r} \right|_{r_+} - r_-^2 \, K_r \left. \frac{\Delta T_r}{\Delta r} \right|_{r_-} \right) \Delta t$$

(0-7)

Between each radius increment, the volume is

216

$$V_i = \frac{4}{3}\pi\left(r_+^3 - r_-^3\right) \tag{0-8}$$

Substituting this with further manipulations into Eq (0-7), the result is

$$T_r^{4\,(n+1)} = T_r^{4\,(n)} + \frac{4\pi}{9\,V_i}\left(r_+^2 K_r \left.\frac{\Delta T_r}{\Delta r}\right|_{r_+} - r_-^2 K_r \left.\frac{\Delta T_r}{\Delta r}\right|_{r_-}\right)\Delta t \tag{0-9}$$

Defining

$$RFLUXP = r_+^2 K_r \left.\frac{\Delta T_r}{\Delta r}\right|_{r_+} \tag{0-10}$$

and

$$RFLUXM = r_-^2 K_r \left.\frac{\Delta T_r}{\Delta r}\right|_{r_-} \tag{0-11}$$

this becomes

$$T_r^{4\,(n+1)} = T_r^{4\,(n)} + \frac{4\pi}{9\,V_i}\left(RFLUXP - RFLUXM\right)\Delta t \tag{0-12}$$

If

$$T_r^{n+1} = T_r^n + \Delta T_r \qquad (0-13)$$

or

$$\Delta T_r = T_r^{n+1} - T_r^n \qquad (0-14)$$

then

$$T_r^{4(n+1)} \simeq T_r^{4(n)} + 4 T_r^{3(n)} \Delta T_r \qquad (0-15)$$

or

$$T_r^{4(n+1)} - T_r^{4(n)} = 4 T_r^{3(n)} \left(T_r^{(n+1)} - T_r^{(n)} \right) \qquad (0-16)$$

Substituting this into Eq (0-12),

$$4 T_r^{3(n)} \left(T_r^{(n+1)} - T_r^{(n)} \right) = \frac{4\pi}{a V_i} \left(RFLUXP - RFLUXM \right) \Delta t \qquad (0-17)$$

or

$$T_r^{(n+1)} = T_r^{(n)} + \frac{4\pi}{4 a T_r^{3(n)} V_i} \left(RFLUXP - RFLUXM \right) \Delta t \qquad (0-18)$$

Since

$$C_{\nu r} = \frac{4a}{\rho} T_r^3 \qquad (0-19)$$

218

$$4aT_r^3 = \rho \, C_{yr}$$

(O-20)

Then Eq (O-18) becomes

$$T_r^{n+1} = T_r^n + \frac{4\pi}{\rho \, C_{yr} V_i} \left(RFLUXP - RFLUXM \right) \Delta t$$

(O-21)

This is the radiation diffusion term of the radiation temperature update equation.

Now since

$$A_{er} = A_{er}^{\beta} + A_{er}^{c}$$

(85)

and

$$\frac{dT_r}{dt} = \frac{A_{er}}{C_{yr}} \left(T_e - T_r \right)$$

(O-22)

the electron-radiation energy transfer portion of the radiation temperature update equation can be written

$$T_r^{n+1} = T_r^n + \frac{A_{er}}{C_{yr}} \left(T_e^n - T_r^n \right) \Delta t$$

(O-23)

219

Vita

David A. DeBruyne was born on 18 January 1951 in Olympia, Washington. He graduated from Tumwater High School in 1969 and enrolled in Washington State University where he completed a Bachelor of Science degree in Physics in 1973. He was commissioned in the United States Marine Corps in 1974 and was winged as a Naval Flight Officer in 1975. After completing type training in the F-4 Phantom in 1976, he was assigned to VMFA-323 based in El Toro, California. Included in his tour with VMFA-323 was a West Pac cruise aboard the U.S.S. Coral Sea. He was assigned to the Nuclear Engineering Program at the Air Force Institute of Technology in August 1980. He is an active member in the American Nuclear Society.

<div style="text-align: right">

Permanent Address: 1611 88th Avenue, S.W.
Olympia, Washington 98501

</div>

REPORT DOCUMENTATION PAGE		READ INSTRUCTIONS BEFORE COMPLETING FORM
1. REPORT NUMBER GNE/PH/82-5	2. GOVT ACCESSION NO. AD-A118065	3. RECIPIENT'S CATALOG NUMBER
4. TITLE (and Subtitle) One Dimensional Analysis of Inertially Confined Plasma		5. TYPE OF REPORT & PERIOD COVERED MS Thesis
		6. PERFORMING ORG. REPORT NUMBER
7. AUTHOR(s) David A. DeBruyne Captain USMC		8. CONTRACT OR GRANT NUMBER(s)
9. PERFORMING ORGANIZATION NAME AND ADDRESS Air Force Institute of Technology (AFIT/EN) Wright Patterson AFB, Ohio 45433		10. PROGRAM ELEMENT, PROJECT, TASK AREA & WORK UNIT NUMBERS
11. CONTROLLING OFFICE NAME AND ADDRESS		12. REPORT DATE March 1982
		13. NUMBER OF PAGES 220
14. MONITORING AGENCY NAME & ADDRESS(if different from Controlling Office)		15. SECURITY CLASS. (of this report) unclassified
		15a. DECLASSIFICATION/DOWNGRADING SCHEDULE

16. DISTRIBUTION STATEMENT (of this Report)

Approved for Public Release; Distribution Unlimited.

17. DISTRIBUTION STATEMENT (of the abstract entered in Block 20, if different from Report)

18. SUPPLEMENTARY NOTES

19. KEY WORDS (Continue on reverse side if necessary and identify by block number)

Fusion
Inertial Confinement
Compton Scatter
Bremsstrahlung
Plasma
Thermonuclear Plasma

20. ABSTRACT (Continue on reverse side if necessary and identify by block number)

Energy transfer processes in a thermonuclear plasma including Coulombic phenomena, bremsstrahlung, and Compton scatter are critically reviewed. These processes are incorporated in a three temperature, inertially confined fusion computer simulation which uses a one dimensional, spherical, Lagrangian hydrodynamics scheme. The computer code, still in the validation phase, uses separate subroutines to model hydrodynamics, thermonuclear burn, neutron heating, alpha particle heating, and energy transfer processes in CGS units.

DD FORM 1473 1 JAN 73 EDITION OF 1 NOV 65 IS OBSOLETE